CAPITAL UNIVERSITY OF SCIENCE AND TECHNOLOGY, ISLAMABAD

Micropolar Flow of EMHD Nanofluid Flow over a Convectively Heated Sheet with Cattaneo-Christov Double Diffusion

by

Hina Gul

A thesis submitted in partial fulfillment for the degree of Master of Philosophy

in the

Faculty of Computing
Department of Mathematics

2022

*I dedicate my dissertation work to my **family** and dignified **teachers**. A special feeling of gratitude to my loving parents who have supported me in my studies.*

CERTIFICATE OF APPROVAL

Micropolar Flow of EMHD Nanofluid Flow over a Convectively Heated Sheet with Cattaneo-Christov Double Diffusion

by

Hina Gul

(MMT203024)

THESIS EXAMINING COMMITTEE

(a) External Examiner	Dr. Rashid Mahmood	Air University, Islamabad
(b) Internal Examiner	Dr. Muhammad Afzal	CUST, Islamabad
(c) Supervisor	Dr. Muhammad Sagheer	CUST, Islamabad

Dr. Muhammad Sagheer
Thesis Supervisor
November, 2022

Dr. Muhammad Sagheer
Head
Dept. of Mathematics
November, 2022

Dr. M. Abdul Qadir
Dean
Faculty of Computing
November, 2022

Author's Declaration

I, **Hina Gul**, hereby state that my MPhil thesis titled "**Micropolar Flow of EMHD Nanofluid Flow over a Convectively Heated Sheet with Cattaneo-Christov Double Diffusion**" is my own work and has not been submitted previously by me for taking any degree from Capital University of Science and Technology, Islamabad or anywhere else in the country/abroad.

At any time if my statement is found to be incorrect even after my graduation, the University has the right to withdraw my MPhil Degree.

(Hina Gul)
Registration No: MMT203024

Plagiarism Undertaking

I solemnly declare that research work presented in this thesis titled "**Micropolar Flow of EMHD Nanofluid Flow over a Convectively Heated Sheet with Cattaneo-Christov Double Diffusion**" is solely my research work with no significant contribution from any other person. Small contribution/help wherever taken has been dully acknowledged and that complete thesis has been written by me.

I understand the zero tolerance policy of the HEC and Capital University of Science and Technology towards plagiarism. Therefore, I as an author of the above titled thesis declare that no portion of my thesis has been plagiarized and any material used as reference is properly referred/cited.

I undertake that if I am found guilty of any formal plagiarism in the above titled thesis even after award of MPhil Degree, the University reserves the right to withdraw/revoke my MPhil degree and that HEC and the University have the right to publish my name on the HEC/University website on which names of students are placed who submitted plagiarized work.

(Hina Gul)

Registration No: MMT203024

Acknowledgement

I got no words to articulate my cordial sense of gratitude to **Almighty Allah** who is the most merciful and most beneficent to his creation.

I also express my gratitude to the last Prophet of **Almighty Allah, Prophet Muhammad (PBUH)** the supreme reformer of the world and knowledge for human being.

I would like to be thankful to all those who provided support and encouraged me during this work.

I would like to be grateful to my thesis supervisor **Dr. Muhammad Sagheer**, the Head of the Department of Mathematics, for guiding and encouraging towards writing this thesis. It would have remained incomplete without his endeavours. Due to his efforts I was able to write and complete this assertation.

I would like to pay great tribute to my **parents**, for their prayers, moral support, encouragment and appreciation.

Last but not the least, I want to express my gratitude to my **friends** who helped me throughout in my MPhil degree.

(Hina Gul)

Abstract

A mathematical model has been presented for analyzing the flow of micropolar nanofluid above a convectively heated permeable stretching sheet with Cattaneo-Christov double diffusion. The similarity transformation is utilized to change the governing partial differential equations (PDEs) to a system of nonlinear ordinary differential equations (ODEs). The resulting system of ODEs is sorted out mathematically by utilizing the shooting method. Graphical results are exploited to view the behavior of emerging parameters on velocity, temperature and concentration of nanofluid. The effects of non-dimensional parameters on velocity, temperature and concentration have been discussed with the help of graphs for both suction and injection cases. Moreover, for comprehension, the physical presentation of the embedded parameters, such as unsteady squeezing parameter, thermal radiation parameter, thermophoresis parameter, Levis number and Prandtl number are plotted and discussed graphically. Numerical computations are performed for the local Sherwood and Nusselt number and skin friction coefficient and discussed in this work. Extend the flow analysis by considering the additional effects of Cattaneo Christov double diffusion model with the assumptions of laminar, steady, incompressible, two dimensional, porous stretching sheet, viscous dissipation, nonlinear thermal radiation, Joule heating with convective boundary condition. It is observed that the electric field is dominant over the magnetic field. The behavior of velocity profile is reserved in the absence of the electric field. Further, the nonlinear thermal radiation aggregates the temperature profile.

Contents

Author's Declaration iv

Plagiarism Undertaking v

Acknowledgement vi

Abstract vii

List of Figures x

List of Tables xii

Abbreviations xiii

Symbols xiv

1 Introduction 1
- 1.1 Thesis Contributions . . . 4
- 1.2 Thesis outlines . . . 4

2 Preliminaries 6
- 2.1 Some Basic Terminologies . . . 6
- 2.2 Types of Flow . . . 8
- 2.3 Types of Fluid . . . 9
- 2.4 Modes of Heat Transfer . . . 10
- 2.5 Dimensionless Number . . . 11
- 2.6 Governing Laws . . . 13
- 2.7 Shooting Method . . . 15

3 Magneto-micropolar nanofluid flow over a convectively heated sheet with non-linear radiation and viscous dissipation 18
- 3.1 Introduction . . . 18
- 3.2 Problem Formulation . . . 19
- 3.3 Conversion of the Model . . . 20
- 3.4 Solution Methodology . . . 38

3.5 Results and Discussion 43

4 The Cattaneo-Christov double diffusion model analysis of EMHD micropolar fluid flow using nonlinear thermal radiation 58

4.1 Introduction 58
4.2 Problem Formulation 59
4.3 Conversion of the Model 59
4.4 Solution Methodology 64
4.5 Results and Discussion 67

5 Conclusion 80

Bibliography 82

List of Figures

3.1 Geometry of the problem. 18
3.2 Influence of α on $f'(\zeta)$. 47
3.3 Influence of f_w on $f'(\zeta)$. 47
3.4 Influence of K on $f'(\zeta)$. 48
3.5 Influence of K on $h(\zeta)$. 48
3.6 Influence of M on $f'(\zeta)$. 49
3.7 Influence of M on $\theta(\zeta)$. 49
3.8 Influence of γ_1 on $\theta(\zeta)$. 50
3.9 Influence of Ec on $\theta(\zeta)$. 50
3.10 Influence of θ_w on $\theta(\zeta)$. 51
3.11 Influence of P_r on $\theta(\zeta)$. 51
3.12 Influence of Nt on $\theta(\zeta)$. 52
3.13 Influence of R on $\theta(\zeta)$. 52
3.14 Influence of L_e on $\phi(\zeta)$. 53
3.15 Influence of Nt on $\phi(\zeta)$. 53
3.16 Influence of P_r on $\phi(\zeta)$. 54
3.17 Influence of Nb on $\phi(\zeta)$. 54
3.18 Influence of γ_2 on $\phi(\zeta)$. 55
3.19 Influence of Nt *and* Nb on $Nu_x Re_x{}^{-\frac{1}{2}}$. 55
3.20 Influence of Nt *and* Nb on the $Sh_x Re_x{}^{-\frac{1}{2}}$. 56

4.1 Impact of α on $\theta(\zeta)$. 70
4.2 Impact of f_w on $\theta(\zeta)$. 70
4.3 Impact of K on $\theta(\zeta)$. 71
4.4 Impact of M on $\theta(\zeta)$. 71
4.5 Impact of λ_t on $\theta(\zeta)$. 72
4.6 Impact of Nt on $\theta(\zeta)$. 72
4.7 Impact of Pr on $\theta(\zeta)$. 73
4.8 Impact of Nb on $\theta(\zeta)$. 73
4.9 Impact of γ_1 on $\theta(\zeta)$. 74
4.10 Impact of Le on $\phi(\zeta)$. 74
4.11 Impact of Nt on $\phi(\zeta)$. 75
4.12 Impact of Ec on $\phi(\zeta)$. 75
4.13 Impact of λ_c on $\phi(\zeta)$. 76
4.14 Impact of Pr on $\phi(\zeta)$. 76

4.15 Impact of Nb on $\phi(\zeta)$. 77
4.16 Impact of γ_2 on $\phi(\zeta)$. 77

List of Tables

3.1 Results of $(Re_x)^{\frac{1}{2}}\frac{1}{2}C_f$ for various parameters 44

3.2 Results of $Nu(Re_x)^{-\frac{1}{2}}$ *and* $Sh(Re_x)^{-\frac{1}{2}}$ when $K = 0.2$, $E = 0.2$, $f_w = 0.1$, $\alpha = 1.4$, $n = 0.5$, $N_t = 0.2$, $L_e = 1.2$, $\gamma_1 = \gamma_2 = 0.1$ 45

3.3 Results of $Nu(Re_x)^{-\frac{1}{2}}$ *and* $Sh(Re_x)^{-\frac{1}{2}}$ when $K = 0.2$, $E = 0.2$, $f_w = 0.1$, $\alpha = 1.4$, $n = 0.5$, $N_b = 0.2$, $P_r = 1.6$, $E_c = 0.1$ 46

4.1 Results of $Nu(Re_x)^{-\frac{1}{2}}$ *and* $Sh(Re_x)^{-\frac{1}{2}}$ when $K = 0.2$, $E = 0.2$, $M = 0.1$, $f_w = 0.1$, $\alpha = 1.4$, $n = 0.5$, $N_t = 0.2$, $L_e = 1.2$, $\gamma_1 = \gamma_2 = 0.1$ 68

4.2 Results of $Nu(Re_x)^{-\frac{1}{2}}$ *and* $Sh(Re_x)^{-\frac{1}{2}}$ when $K = 0.2$, $E = 0.2$, $f_w = 0.1$, $\alpha = 1.4$, $n = 0.5$, $N_b = 0.2$, $P_r = 1.6$, $E_c = 0.1$ 69

Abbreviations

IVP	Initial value problem
BVP	Boundary value problem
MHD	Magnetohydrodynamics
ODEs	Ordinary differential equations
PDEs	Partial differential equations
RK	Runge-Kutta

Symbols

ρ	Density
τ	Stress tensor
k	Thermal conductivity
α	Thermal diffisuitivity
σ	Electrical conductivity
u	x-component of fluid velocity
v	y-component of fluid velocity
B_0	Magnetic field constant
T_w	Temperature of the wall
T_∞	Ambient temperature of the nanofluid
T	Temperature
ρ_f	Density of the fluid
μ_f	Viscosity of the fluid
ρ_{nf}	Density of the nanofluid
μ_{nf}	Viscosity of the nanofluid
q_r	Radiative heat flux
q	Heat generation constant
q_w	Heat flux
q_m	Mass flux
σ^*	Stefan Boltzmann constant
k^*	Absorption coefficient
C_f	Skin friction coefficient
Nu_x	Local Nusselt number

Sh_x	Local Sherwood number
ϕ	Nanoparticle volume fraction
R	Thermal radiation parameter
n	Stretching parameter
M	Magnetic parameter
K	material parameter
Ec	Eckert number
Pr	Prandtl number
γ_1	Relaxation time parameter
Nb	Brownain motion parameter
Nt	Thermophoresis parameter
γ_2	Chemical reaction parameter
L_e	Lewis number
μ_f	Viscosity of the base fluid
$(\rho C_p)_f$	Heat capacitance of base fluid
$(\rho C_p)_s$	Heat capacitance of nanoparticle
σ_f	Electrical conductivity of the base fluid
σ_s	Electrical conductivity of the nanoparticle
k_f	Thermal conductivity of the base fluid
k_s	Thermal conductivity of the nanoparticle
f	Dimensionless velocity
θ	Dimensionless temperature
h	Dimensionless concentration
C_∞	Ambient concentration
C	Concentration
C_w	Nanoparticles concentration at the stretching surface

Chapter 1

Introduction

Micropolar fluid is a viscous fluid that suspends stiff tiny particles that are randomly oriented and rotate and spin slightly about their own axes. Examples of micropolar fluids include animal blood, anisotropic fluids, lubricating fluids, intricate biological structures, and specific polymer solutions. Magnetohydrodynamics is the name of the science that examines how a magnetic field affects the movement of a highly conducting fluid (MHD).

There are countless applications in engineering and business of Newtonian and non-Newtonian flows in the presence of magnetic fields. The preparation of food products, oil industry, microelectronic devices, geothermal energy extraction of metals, accelerators, atomic reactors, liquid beads and sprays, and MHD power generators are a few of the noteworthy applications of MHD. The theory of the micropolar fluid was first put forth by [1].

In Eringen's theory, a new constitutive equation and a new micro-rotation material independent vector field are added to the Navier Stokes equation. Eringen [2] expanded his findings by developing a generalised theory of thermomicropolar fluids.

Shu and Lee [3] computed several fundamental solutions for unbounded steady Oseen, Stokes, Stokeslet, Stokes couplet, Oseenlet, and Oseen couplet flow in three and two dimensions. Rashad et al [4] investigated the boundary layer flow of micropolar fluid f or c oupled heat a nd m ass t ransfer across a s tratified medium

and isothermal vertical surface, as well as chemical reaction and mixed convection. Mabood et al. [5] published an investigation of two-dimensional micropolar fluid flow in a non Darcian with temperature dependent thermal conductivity and thermal radiation. They also studied viscous-Ohmic dissipation, Soret effects, and non-uniform heat sources for flow, heat, and mass transport. To solve the governing differential equation, the shooting technique is used with the Runge-Kutta-Fhelberg method.

Mirzaaghaian and Ganji [6] investigate the flow of a micropolar fluid in a permeable tube for temperature and velocity distribution. The differential transformation method is used to address the problem. They concluded that decreasing the Reynolds number increases the value of the stream function. Micropolar fluids have micro-constituents that can rotate, the appearance of which can alter the hydrodynamics of the stream, making it plainly non-Newtonian. In everyday life, non-ideal fluids such as macromolecules, animal blood, and shampoo can be found.

Turkyilmazoglu [7] investigated the MHD micropolar fluid over a deformable heated/cooled porous plate, including heat generation and absorption effects. The flow, temperature, and concentration characteristics are precisely solved analytically. Bilal et al. [8] have attempted to investigate the Hall and ion-slip effects on magneto-micropolar nanofluid flow via a porous medium. They employed varying thermal physical parameters to numerically study heat transmission over the permeable sheet. More about the micropolar fluid with different aspects can be found in [9]-[13].

Nanofluids are regular fluids with nanoscale metal or metallic oxide particles added to improve the thermal conductivity of the working liquids. Researchers have generally acknowledged Choi's contribution to the modelling and thorough investigation of nanofluids [14].

He conducted an experiment to demonstrate that adding nanofluids to base fluids can improve their thermal properties. For the first time, Buongiorno established two component slip mechanism models for the mass and energy transport

in nanofluids, namely Brownian motion and thermophoresis of nanofluid.

Ramzan and Bilal [16] investigate the series solution of an un-steady second-grade nanofluid caused by a porous perpendicular sheet in the presence of mixed convection, heat radiation, and magnetohydrodynamics. Pal et al. [17] developed numerical solutions for MHD Casson nanofluid boundary layer flow across a vertical non-linear porous surface with Ohmic dissipation and heat radiation.

Khan et al. [18] investigated the unsteady Flakner-Skan wedge flow of Carreau nanofluid across a stretched sheet using the zero mass flux and melting heat condition at the boundary. They investigated the impact of nanofluids using Brownian motion and thermophoresis methods. Hayat et al. [19] adopted an analytical approach lately focused on evenly applied magnetic field and heat generation/absorption over three dimensional electrically conducting Oldroyd-B nanofluid flow generated by stretching surface. They used the convective boundary for temperature and the zero mass flux criterion for nanoparticle mass diffusion. The numerical approach was utilised by Bilal et al. [20] to solve the problem of three-dimensional upper convected Maxwell nanofluid with nonlinear thermal radiation and magnetohydrodynamics over a bidirectional plate. Some other nominated articles featuring the importance of nanofluid are highlighted as [21]-[23].

The use of nanofluid technology may also be seen in bubble electrospinning [24], which used bubbles to create nanomaterials such as porous nanoscale materials, nanoparticles, two-dimensional nanomaterials, and nanofibers. Bubbfil and blown bubblespinning are the most often utilised industrial nanofiber production methods [25]-[26].

The concept of fractional calculus or fractal calculus is applied when working with nanomaterials or nanofibers. Some information is lost when a higher-dimensional (3D) problem is reduced to a lower-dimensional (2D or 1D)problem. The two scale approach is typically used to reveal missing information. A two-scale transformation converts fractional calculus [27]-[29] into traditional partner to make two-scale thermodynamics practical. Thermal radiation is the term describing the

phenomenon of heat transmission by electromagnetic waves. It happens as a result of a significant temperature difference between the two media. The majority of technical activities take place at respectable temperatures.

1.1 Thesis Contributions

In this thesis, we provide a review study of Hussain [30] and extend the flow analysis by considering the additional effects of Cattaneo-Christov double diffusion model with the assumptions of laminar, steady, incompressible, two dimensional, porous stretching sheet, viscous dissipation, nonlinear thermal radiation, Joule heating with convective boundary condition. The obtained system of PDEs is transformed into a system of nonlinear and coupled ODEs by using a suitable similarity transformation. A numerical solution of the system of ODEs is obtained by employing the shooting method. The mathematical inferences are discussed for different physical parameters appearing in the solution influencing the flow and heat transform.

1.2 Thesis outlines

Chapter 2 demonstrates some important definitions, laws and concepts which are useful in understanding the upcoming work.

Chapter 3 contains a comprehensive numerical review of [30]. A numerical study of micropolar nanofluid through a horizontal sheet with convective boundary conditions is analyzed. The constitutive flow model expression are sorted out numerically and the impact of physical parameters concerning the flow model on dimensionless energy, velocity, and microrotation are presented through graphs and tables.

Chapter 4 extends the flow model discussed in Chapter 3 by including the impacts of Cattaneo-Christov double diffusion. The reduced system of ODEs after applying a proper similarity transform is solved numerically. Graphs and tables

describe the behavior of physical quantities such as, Pr, Nb, Nt, Ec, Le, M, and R etc. Numerical values of skin friction coefficient, Nusselt number and Sherwood number have also been computed and discussed in this Chapter.

Chapter 5 summarizes overall analysis performed in this dissertation.

Chapter 2

Preliminaries

In this chapter, certain fundamental definitions, governing laws and dimensional quantities are presented that will be useful in the subsequent chapters.

2.1 Some Basic Terminologies

Definition 2.1.1 (Fluid)

"A fluid is a substance that deforms continuously under the application of a shear (Tangential) stress no matter how small the shear stress may be." [31]

Definition 2.1.2 (Fluid Mechanics)

"Fluid mechanics is that branch of science which deals with the behavior of the fluids (liquids or gases) at rest as well as in motion." [32]

Definition 2.1.3 (Fluid Dynamics)

The study of fluid if the pressure forces are also considered for the fluids in motion, that branch of science is called fluid dynamics. [32]

Definition 2.1.4 (Fluid Statics)

"The study of fluids at rest is called fluid statics." [32]

Definition 2.1.5 (Viscosity)

"Viscosity is defined as the property of a fluid which offers resistance to the

movement of one layer of fluid over another adjacent layer of the fluid. The top layer causes a shear stress on the adjacent lower layer while the lower layer causes a shear stress on the adjacent top layer. This shear stress is proportional to the rate of change of velocity with respect to y. It is denoted by symbol τ. Mathematically,

$$\tau \propto \frac{du}{dy}$$
$$\tau = \mu \frac{du}{dy}$$
$$\mu = \frac{\tau}{\frac{\partial u}{\partial y}},$$

where μ (called **mu**) is the constant of proportionality and is known as the coefficient of dynamic viscosity or only viscosity. $\frac{du}{dy}$ represents the rate of shear strain or velocity gradient." [32]

Definition 2.1.6 (Kinematic Viscosity)

"It is defined as the ratio between the dynamic viscosity and density of the fluid. It is denoted by symbol ν called **nu**. Mathematically,

$$\nu = \frac{\mu}{\rho}." \text{ [32]}$$

Definition 2.1.7 (Thermal Conductivity)

"The Fourier heat conduction law states that the heat flow is proportional to the Temperature gradient. The coefficient of proportionality is a material parameter known as the thermal conductivity, which may be a function of several variables." [33]

Definition 2.1.8 (Thermal Diffusivity)

"The rate at which heat diffuses by conducting through a material depends on the Thermal diffusivity. It can be defined as

$$\alpha = \frac{k}{\rho C_p},$$

where α is the thermal diffusivity, k is the thermal conductivity, ρ is the density

and C_p is the specifc heat at constant pressure." [33]

2.2 Types of Flow

Definition 2.2.1 (Rotational Flow)

"Rotational flow is that type of flow in which the fluid particles, while flowing along stream-lines, also rotate about their own axis." [32]

Definition 2.2.2 (Irrotational Flow)

"Is the fluid particles while flowing along stream-lines, do not rotate about their own axis then this type of flow is called Irrotational flow." [32]

Definition 2.2.3 (Compressible Flow)

Compressible flow is that type of flow in which the density of the fluid changes from point to point or in other words the density (ρ) is not constant for the fluid, Mathematically,

$$\rho \neq Constant \text{ [32]}$$

Definition 2.2.4 (Incompressible Flow)

Incompressible flow is that type of flow in which the density is constant for the fluid. Liquids are generally incompressible while gases are compressible. Mathematically,

$$\rho = Constant. \text{ [32]}$$

Definition 2 .2.5 (Internal Flow)

"Flows completely bounded by a solid surfaces are called internal or duct flows." [31]

Definition 2 .2.6 (External Flow)

"Flows over bodies immersed in an unbounded fluid a re s aid t o b e a n external flow." [31]

2.3 Types of Fluid

Definition 2.3.1 (Ideal Fluid)

"A fluid, which is incompressible and has no viscosity, is an ideal fluid. Ideal fluid is only an imaginary fluid as all the fluids, which exist, have some viscosity." [32]

Definition 2.3.2 (Real Fluid)

"A fluid, which possesses viscosity, is known as a real fluid. In actual practice, all the fluids are real fluids." [32]

Definition 2.3.3 (Newtonian Fluid)

"A real fluid, in which the shear stress is directly proportional to the rate of shear strain (or velocity gradient), is known as a Newtonian fluid."

$$\tau \propto \left(\frac{du}{dy}\right),$$
$$\tau = \mu\left(\frac{du}{dy}\right)." \text{ [32]}$$

Definition 2.3.4 (Non-Newtonian Fluid)

"A real fluid in which the shear stress is not directly proportional to the rate of shear strain (or velocity gradient), is known as a non-Newtonian fluid.

$$\tau \propto \left(\frac{du}{dy}\right)^m, \qquad m \neq 1$$
$$\tau = \mu\left(\frac{du}{dy}\right)^m." \text{ [32]}$$

Definition 2.3.5 (Ideal Plastic Fluid)

"A fluid, in which shear stress is more than the yield value and shear stress is proportional to the rate of shear strain or (velocity gradient), is known as a ideal plastic fluid." [32]

Definition 2.3.6 (Magnetohydrodynamics)

"Magnetohydrodynamics(MHD) is concerned with the mutual interaction of fluid flow and magnetic fields. The fluids in question must be electrically conducting

and non-magnetic, which limits us to liquid metals, hot ionised gases (plasmas) and strong electrolytes." [34]

2.4 Modes of Heat Transfer

Definition 2.4.1 (Heat Transfer)

"Heat transfer is a branch of engineering that deals with the transfer of thermal energy from one point to another within a medium or from one medium to another due to the occurrence of a temperature difference." [33]

Definition 2.4.2 (Conduction)

"The transfer of heat within a medium due to a diffusion process is called conduction." [33]

Definition 2.4.3 (Convection)

"Convection heat transfer is usually defined as energy transport effected by the motion of a fluid. Newtons law of cooling governs the convection heat transfer between two different media." [33]

Definition 2 .4.4 (Thermal Radiation)

"Thermal radiation is defined as r adiant (electromagnetic) e nergy e mitted b y a medium and is sole to the temperature of the medium. Sometimes radiant energy is taken to be transported by electromagnetic waves while at other times it is supposed to be transported by particle like photons." [33]

2.5 Dimensionless Number

Definition 2.5.1 (Eckert Number)

"It is the dimensionless number used in continuum mechanics. It describes the relation between flows and the boundary layer enthalpy difference and is used to

characterized heat dissipation. Mathematically,

$$Ec = \frac{u^2}{C_p \nabla T}$$

where C_p denotes the specific heat." [31]

Definition 2.5.2 (Prandtl Number)

"It is the ratio between the momentum diffusivity ν and thermal diffusivity α. Mathematically, it can be defined as

$$Pr = \frac{\nu}{\alpha} = \frac{\frac{\mu}{\rho}}{\frac{k}{C_p \rho}} = \frac{\mu C_p}{k}$$

where μ represents the dynamic viscosity, Cp denotes the specific heat and k stands for thermal conductivity. The Prandtl number controls the relatives thickness of thermal and momentum boundary layer. For small Pr, heat distributed rapidly corresponds to the momentum." [31]

Definition 2.5.3 (Skin Friction Coefficient)

"The steady flow of an incompressible gas or liquid in a long pipe of internal D. The mean velocity is denoted by u_w. The skin friction coefficient can be defined as

$$C_f = \frac{2\tau_0}{\rho u_w^2}$$

where τ_0 denotes the wall shear stress and ρ is the density." [35]

Definition 2.5.4 (Nusselt Number)

"The hot surface is cooled by a cold fluid stream. The heat from the hot surface, which is maintained at a constant temperature, is diffused through a boundary layer and convected away by the cold stream. Mathematically,

$$Nu = \frac{qL}{k}$$

where q stands for the convection heat transfer, L for the characteristic length and k stands for thermal conductivity." [36]

Definition 2.5.5 (Sherwood Number)

"It is the non-dimensional quantity that shows the ratio of the mass transport by convection to the transfer of mass by diffusion. Mathematically:

$$Sh = \frac{kL}{D}$$

here L is characteristics length, D is the mass diffusivity and k is the mass transfer coefficient." [37]

Definition 2.5.6 (Lewis Number)

"The Lewis number can be defined as the ratio of thermal diffusivity to molecular diffusivity. I t c haracterizes the m utual r elation o f h eat and m ass t ransfers in various materials. Mathematically

$$Le = \frac{\lambda}{\rho\ D_m C_p}$$

where λ is the thermal conductivity, Dm the molecular diffusivity, and C_p the specific heat capacity at constant pressure." [31]

2.6 Governing Laws

Definition 2.6.1 (Continuity Equation)

"The principle of conservation of mass can be stated as the time rate of change of mass in a fixed volume is equal to the net rate of flow of mass across the surface. The mathematical statement of the principle results in the following equation, known as the continuity (of mass) equation

$$\frac{\partial \rho}{\partial t} + \nabla.(\rho \mathbf{v}) = 0.$$

where ρ is the density (kg/m^3) of the medium, v the velocity vector (m/s), and ∇ is the nabla or del operator. For steady-state conditions, the continuity equation

(2.1) becomes

$$\nabla.(\rho\mathbf{v}) = 0. \tag{2.1}$$

When the density changes following a fluid particle are negligible, the continuum is termed incompressible. The continuity equation (2.2) becomes

$$\nabla.\mathbf{v} = 0. \tag{2.2}$$

which is often referred to as the incompressibility condition or incompressibility constraint." [33]

Definition 2.6.2 (Momentum Equation)

The principle of conservation of linear momentum (or Newton's Second Law of motion) states that the time rate of change of linear momentum of a given set of particles is equal to the vector sum of all the external forces acting on the particles of the set, provided Newton's Third Law of action and reaction governs the internal forces. Newton's Second Law can be written as

$$\frac{\partial}{\partial t}(\rho\mathbf{v}) + \nabla.[(\rho\mathbf{v})\mathbf{v}] = \nabla.\sigma + \rho\mathbf{f}. \tag{2.3}$$

Where is the tensor (or dyadic) product of two vectors, σ is the Cauchy stress tensor (N/m^2) and f is the body force vector, measured per unit mass and normally taken to be the gravity vector.

Equation (2.1) describes the motion of a continuous medium, and in fluid mechanics they are also known as the Navier equations. The form of the momentum equation shown in (2.4) is the conservation (divergence) form that is most often utilized for compressible flows. This equation may be simplified to a form more commonly used with incompressible flows. Expanding the first two derivatives and collecting terms

$$\rho\left(\frac{\partial\mathbf{v}}{\partial t} + \mathbf{v}\nabla.\mathbf{v}\right) + \mathbf{v}\left(\frac{\partial\rho}{\partial t} + \nabla.\rho\mathbf{v}\right) = \nabla.\sigma + \sigma\mathbf{f}. \tag{2.4}$$

The second term in parentheses is the continuity equation (2.1 and neglecting this

term allows (2.5) to reduce to the non-conservation (advective) form

$$\rho\left(\frac{\partial \mathbf{v}}{\partial t} + \mathbf{v}\nabla.\mathbf{v}\right) = \nabla.\sigma + \rho\mathbf{f}. \text{ [33]} \tag{2.5}$$

Definition 2.6.3 (Energy Equation)

"The law of conservation of energy (or the First Law of Thermodynamics) states that the time rate of change of the total energy is equal to the sum of the rate of work done by applied forces and the change of heat content per unit time.

In the general case, the First Law of Thermodynamics can be expressed in conservation form as

$$\frac{\partial \rho\ e^t}{\partial t} + \nabla.\rho\mathbf{v}e^t = -\nabla.\mathbf{q} + \nabla.(\sigma.\mathbf{v}) + Q + \sigma\mathbf{f}.\mathbf{v} \tag{2.6}$$

where $e^t = e + 1/2\mathbf{v}.\mathbf{v}$ is the total energy (J/m^3), e is the internal energy, q is the heat flux vector (W/m^2) and Q is the internal heat generation (W/m^3).

The total energy equation (2.7) is useful for high speed compressible flows where the kinetic energy is significant.

For incompressible flows, an internal energy equation is more appropriate and can be derived from (2.7) with use of the momentum equation (2.4).

Taking the dot product of the velocity vector with the momentum equation produces an equation for the kinetic energy; this equation is subtracted from the total energy equation (2.7) to produce the conservation (divergence) form of the internal energy equation

$$\frac{\partial \rho\ e}{\partial t} + \nabla.\rho\mathbf{v}e = -\nabla.q + Q + \phi \tag{2.7}$$

where ϕ is the dissipation function that is defined by

$$\phi = \sigma : \nabla : \nabla\mathbf{v} \tag{2.8}$$

In Eq.(2.9) $\nabla\mathbf{v}$ is the velocity gradient tensor. [33]

2.7 Shooting Method

To elaborate the shooting method, consider the following nonlinear BVP.

$$\left.\begin{aligned} N''(x) &= N(x)N'(x) + 2N^2(x) \\ N(0) &= 0, \qquad N(H) = G. \end{aligned}\right\} \tag{2.9}$$

To reduce the order of the above boundary value problem, introduce the following notations.

$$N = X_1 \qquad N' = X_1' = X_2 \qquad N'' = X_2'. \tag{2.10}$$

As a result,

$$X_1' = X_2, \qquad X_1(0) = 0, \tag{2.11}$$

$$X_2' = X_1X_2 + 2X_1^2 \qquad X_2(0) = k \tag{2.12}$$

where k is the missing initial condition. The missing condition k is to be chosen such that

$$X_1(H, k) = G. \tag{2.13}$$

Now onward $X_1(H, k)$ will be denoted by $X_1(k)$. Let us further denote $X_1(k) - G$ by $M(k)$, so that

$$M(k) = 0. \tag{2.14}$$

The above equation can be solved by using Newton's method with the following iterative formula

$$\begin{aligned} k_{n+1} &= k_n - \frac{Mk_n}{\frac{\partial Mk_n}{\partial k}}, \\ k_{n+1} &= k_n - \frac{X_1k_n - G}{\frac{\partial X_1k_n}{\partial k}}. \end{aligned} \tag{2.15}$$

To find $\frac{\partial X_1 k_n}{\partial k}$, introduce the following notations

$$\frac{\partial X_1}{\partial k} = X_3, \quad \frac{\partial X_2}{\partial k} = X_4. \tag{2.16}$$

As a result of these new notations, the Newton's iterative scheme, will then get the form

$$k_{n+1} = k_n - \frac{X_1 k_n - G}{X_3 k_n}. \tag{2.17}$$

Now differentiating the system of two first order ODEs (2.11)-(2.12) with respect to k, we get another system of ODEs, as follows

$$X_3' = X_4, \qquad X_3(0) = 0, \tag{2.18}$$

$$X_4' = X_3 X_2 + X_1 X_4 + 4 X_1 X_3. \qquad X_4(0) = 1. \tag{2.19}$$

Writing all the four ODEs (2.11), (2.12), (2.18) and (2.19) together, we have the following initial value problem

$$\begin{aligned} X_1' &= X_2, & X_1(0) &= 0, \\ X_2' &= X_1 X_2 + 2X_1^2, & X_2(0) &= k, \\ X_3' &= X_4, & X_3(0) &= 0, \\ X_4' &= X_3 X_2 + X_1 X_4 + 4 X_1 X_3. & X_4(0) &= 1. \end{aligned}$$

The above system together will be numerically solved by Runge-Kutta technique of order four. The stopping criteria for the Newton's technique is set as,

$$\mid X_1(k) - G \mid < \epsilon.$$

Here $\epsilon > 0$ is small positive real number.

Chapter 3

Magneto-micropolar Nanofluid Flow over a convectively heated sheet with non-linear radiation and viscous dissipation

3.1 Introduction

The review study of Hussain [30] is provided in this chapter. To convert the boundary layer equations into nonlinear and coupled ordinary differential equations, an appropriate similarity transformation is used.

The shooting method is used to sort out these ODEs numerically. Graphical representations are also provided to explain the effect of evolving parameters. Tables and graphs are used to investigate the numerical results produced.

3.2 Problem Formulation

Figure 3.1 depicts the shape of the flow model.

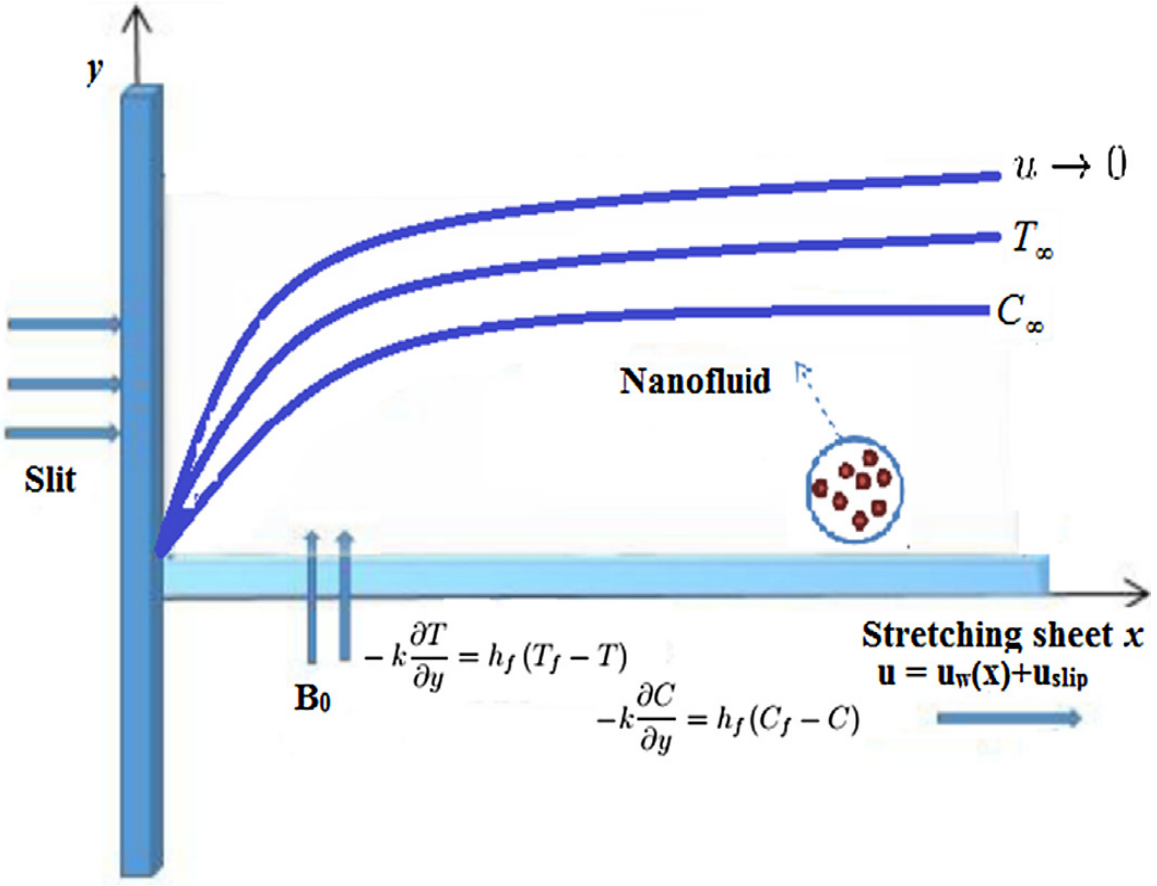

FIGURE 3.1: Geometry of the problem.

The set of equations describing the flow is as follows

$$\frac{\partial u}{\partial x} + \frac{\partial v}{\partial y} = 0, \tag{3.1}$$

$$u\frac{\partial u}{\partial x} + v\frac{\partial u}{\partial y} = \left(\frac{\mu + k}{\rho}\right)\frac{\partial^2 u}{\partial^2 y} + \frac{k}{\rho}\frac{\partial G}{\partial y} + \frac{\sigma}{\rho}\left(E_0 B_0 - B_0^2 u\right), \tag{3.2}$$

$$u\frac{\partial G}{\partial x} + v\frac{\partial G}{\partial y} = \frac{\gamma^*}{\rho j}\frac{\partial^2 G}{\partial^2 y} - \frac{k}{\rho j}\left(2G + \frac{\partial u}{\partial y}\right), \tag{3.3}$$

$$\begin{aligned} u\frac{\partial T}{\partial x} + v\frac{\partial T}{\partial y} = {} & \frac{k}{\rho C_p}\left(\frac{\partial^2 T}{\partial^2 y}\right) + \frac{\left(uB_0 - E_0\right)^2 \sigma}{\rho C_p} - \frac{1}{\rho C_p}\frac{\partial q_r}{\partial y}, \\ & + \left(\frac{\mu + k}{\rho C_p}\right)\left(\frac{\partial u}{\partial y}\right)^2 + \tau\left[D_B\frac{\partial T}{\partial y}\frac{\partial C}{\partial y} + \frac{D_T}{T_\infty}\left(\frac{\partial T}{\partial y}\right)^2\right], \end{aligned} \tag{3.4}$$

$$u\frac{\partial C}{\partial x} + v\frac{\partial C}{\partial y} = D_B\frac{\partial^2 C}{\partial^2 y} + \frac{D_T}{T_\infty}\frac{\partial^2 T}{\partial^2 y}. \tag{3.5}$$

The aforementioned set of equations' corresponding boundary conditions are:

$$\left.\begin{aligned} &u = ax + \alpha^*\left[(\mu + k)\frac{\partial u}{\partial y} + kG\right], \quad v = v_w, \\ &G = -n\frac{\partial u}{\partial y}, \quad -k\left(\frac{\partial T}{\partial y}\right) = h_{ft}\left(T_f - T\right), \\ &-D_B\frac{\partial C}{\partial y} = h_{fc}\left(C_f - C\right) \qquad at \quad y = 0, \\ &u \to 0,\ G \to 0,\ T \to T_\infty,\ C \to C_\infty\ as\ y \to \infty. \end{aligned}\right\} \tag{3.6}$$

3.3 Conversion of the Model

In this section, we convert the system of equations (3.1)-(3.5) along with the boundary conditions (3.6) into a unitless form. The following similarity transformation is employed

$$\left.\begin{aligned} &\zeta = \sqrt{\frac{a}{v}}y, \quad G = ax\sqrt{\frac{a}{v}}h(\zeta), \quad u = axf'(\zeta), \quad v = -\sqrt{av}f(\zeta), \\ &\theta(\zeta) = \frac{T - T_\infty}{T_f - T_\infty}, \quad \phi(\zeta) = \frac{C - C_\infty}{C_f - C_\infty}. \end{aligned}\right\} \tag{3.7}$$

In the above discussions K, M, f_w, P_r, α, E, R, E_c, N_t, N_b and L_e are the material parameter, Hartman number, suction/injection parameter, Prandtl number, slip parameter, electric parameter, radiation parameter, Eckert number, thermophoresis parameter, Brownian motion parameter and Lewis number respectively. These quantities are written as follows:

$$\left.\begin{aligned} &K = \frac{k}{\mu}, \quad M^2 = \frac{\sigma B_0^2}{\rho a}, \quad f_w = -(av)^{\frac{-1}{2}}v_w, \quad P_r = \frac{\mu C_p}{k}, \\ &\alpha = \alpha^*\mu\sqrt{\frac{a}{v}}, \quad E = \frac{E_0}{\mu_w B_0}, \quad R = \frac{4\sigma^* T_\infty^3}{k^* k_1}, \quad E_c = \frac{u_w^2}{C_p\left(T_f - T_\infty\right)}, \\ &N_t = \frac{\tau D_T}{vT_\infty}\left(T_f - T_\infty\right), \quad N_b = \frac{\tau}{v}D_B\left(C_f - C_\infty\right), \quad L_e = \frac{\alpha}{D_B}, \\ &\gamma_2 = \frac{h_{fc}}{D_B}\sqrt{\frac{v}{a}}, \quad \gamma_1 = \frac{h_{ft}}{k}\sqrt{\frac{v}{a}}, \quad Re_x^2 = \frac{ax}{v}, \quad \theta_w = \frac{T_f}{T_\infty}. \end{aligned}\right\}$$

The entire procedure for converting (3.1)-(3.5) into the dimensionless form is discussed below:

$$\begin{aligned} u &= axf'(\zeta) \\ \frac{\partial u}{\partial x} &= \frac{\partial}{\partial x}\left(axf'(\zeta)\right) \\ &= af'(\zeta). \end{aligned} \tag{3.8}$$

$$\begin{aligned} v &= -\sqrt{av}f(\zeta). \\ \frac{\partial v}{\partial x} &= -\frac{\partial}{\partial x}\left(\sqrt{av}f(\zeta)\right) \\ &= -\sqrt{av}f'\left(\sqrt{\frac{a}{v}}y\right)\left(\sqrt{\frac{a}{v}}\right) \\ &= -af'(\zeta). \end{aligned} \tag{3.9}$$

Using (3.8) and (3.9) in (3.1)

$$\frac{\partial u}{\partial x} + \frac{\partial v}{\partial y} = af'(\zeta) - af'(\zeta) = 0.$$

Procedure for the conversion of (3.2) into the dimensionless form is as follow

$$\frac{\partial u}{\partial y} = ax\frac{\partial}{\partial y}f'\left(\sqrt{\frac{a}{v}}y\right) = axf''\left(\sqrt{\frac{a}{v}}y\right)\frac{\partial}{\partial y}\left(\sqrt{\frac{a}{v}}y\right) = \frac{a^{\frac{3}{2}}xf''(\zeta)}{\sqrt{v}}.$$

$$u\frac{\partial u}{\partial x} = \left(axf'(\zeta)\right)\left(af'(\zeta)\right) = a^2x\left(f'(\zeta)\right)^2. \tag{3.10}$$

$$v\frac{\partial u}{\partial y} = -\sqrt{av}f(\zeta)\frac{a^{\frac{3}{2}}xf''(\zeta)}{\sqrt{v}} = -a^2xf(\zeta)f''(\zeta). \tag{3.11}$$

Using (3.10) and (3.11), the left side of (3.2) becomes:

$$\begin{aligned} u\frac{\partial u}{\partial x} + v\frac{\partial u}{\partial y} &= a^2x\left(f'(\zeta)\right)^2 - a^2xf(\zeta)f''(\zeta) \\ &= a^2x\left[\left(f'(\zeta)\right)^2 - f(\zeta)f''(\zeta)\right]. \end{aligned}$$

The following approach has been used to transform the right side of (3.2) into a dimensionless form

$$\frac{\partial u}{\partial y} = ax\frac{\partial}{\partial y}f'\left(\sqrt{\frac{a}{v}}y\right) = axf''\left(\sqrt{\frac{a}{v}}y\right)\frac{\partial}{\partial y}\left(\sqrt{\frac{a}{v}}y\right) = \frac{a^{\frac{3}{2}}xf''(\zeta)}{\sqrt{v}}.$$

$$\frac{\partial^2 u}{\partial^2 y} = \frac{a^{\frac{3}{2}}x}{\sqrt{v}}f'''\left(\sqrt{\frac{a}{v}}y\right)\frac{\partial}{\partial y}\left(\sqrt{\frac{a}{v}}y\right) = \frac{a^2xf'''(\zeta)}{v}. \tag{3.12}$$

$$\frac{\partial G}{\partial y} = ax\sqrt{\frac{a}{v}}\frac{\partial}{\partial y}h(\zeta) = ax\sqrt{\frac{a}{v}}h'(\zeta)\frac{\partial}{\partial y}\left(\sqrt{\frac{a}{v}}y\right) = \frac{a^2x}{v}h'(\zeta). \tag{3.13}$$

$$\begin{aligned}\left(\frac{\mu+k}{\rho}\right)\frac{\partial^2 u}{\partial^2 y} &= \left(\frac{\mu+k}{\rho}\right)\frac{a^2x}{v}f'''(\zeta)\\ &= a^2x\left[\left(\frac{\mu+k}{\rho\ v}\right)f'''(\zeta)\right]\\ &= a^2x\left[\left(\frac{\mu+k}{\mu}\right)f'''(\zeta)\right]\\ &= a^2x\left[\left(\frac{\mu}{\mu}+\frac{k}{\mu}\right)f'''(\zeta)\right]\\ &= a^2x\,(1+K)\,f'''(\zeta). \qquad (3.14)\\ &\qquad\qquad \left(\because \quad K=\frac{k}{\mu}\right)\end{aligned}$$

$$\begin{aligned}\frac{k}{\rho}\frac{\partial G}{\partial y} &= \frac{k}{\rho}\frac{a^2\ x}{v}h'(\zeta) = a^2x\left[\frac{k}{\rho\ v}h'(\zeta)\right] = a^2x\left[\frac{k}{\mu}h'(\zeta)\right]\\ &= a^2\ Kxh'(\zeta). \qquad (3.15)\end{aligned}$$

$$\begin{aligned}\frac{\sigma}{\rho}\left(E_0B_0 - B_0^2\mu\right) &= \frac{\sigma}{\rho}\left(E_0B_0 - B_0^2axf'(\zeta)\right)\\ &= a^2x\left[\frac{\sigma\ E_0B_0}{\rho\ a^2\ x} - \frac{\sigma\ B_0^2}{\rho\ a}f'(\zeta)\right]\\ &= a^2x\left[\left(\frac{B_0^2\sigma}{a\rho}\right)\left(\frac{E_0}{axB_0}\right) - \left(\frac{\sigma\ B_0^2}{a\rho}\right)f'(\zeta)\right]\\ &= a^2x\left[M^2E - M^2f'(\zeta)\right]. \qquad (3.16)\\ &\qquad \left(\because \quad M^2=\frac{\sigma\ B_0^2}{\rho\ a}, E=\frac{E_0}{axB_0}\right)\end{aligned}$$

Using (3.12)-(3.16) in the right side of (3.2), we get

$$\begin{aligned}&\left(\frac{\mu+k}{\rho}\right)\frac{\partial^2 u}{\partial^2 y} + \frac{k}{\rho}\frac{\partial G}{\partial y} + \frac{\sigma}{\rho}\left(E_0B_0 - B_0^2\mu\right)\\ &\qquad = a^2x\left[(1+K)\,f'''(\zeta)\right] + a^2x\left[Kh'(\zeta)\right] + a^2x\left[M^2E - M^2f'(\zeta)\right].\end{aligned}$$

Hence the dimensionless form of (3.2) becomes:

$$\begin{aligned} a^2x\left[(f'(\zeta))^2 - f(\zeta)f''(\zeta)\right] &= a^2x\left[(1+K)\,f'''(\zeta)\right] + a^2x\left[Kh'(\zeta)\right] + a^2x\left[M^2E\right. \\ &\quad \left. - M^2f'(\zeta).\right. \\ \Rightarrow \left[(f'(\zeta))^2 - f(\zeta)f''(\zeta)\right] &= \left[(1+K)\,f'''(\zeta)\right] + \left[Kh'(\zeta)\right] + \left[M^2E - M^2f'(\zeta)\right]. \\ \Rightarrow (1+K)\,f''' + ff'' - f'^2 - M^2f' + Kh' + M^2E &= 0. \end{aligned} \tag{3.17}$$

Procedure for the conversion of (3.3) into the dimensionless form is as follows:

$$\begin{aligned} \frac{\partial G}{\partial x} &= a\sqrt{\frac{a}{v}}\frac{\partial}{\partial x}\left(xh(\sqrt{\frac{a}{v}})\right) = \frac{a^{\frac{3}{2}}h(\zeta)}{\sqrt{v}}. \\ u\frac{\partial G}{\partial x} &= axf'(\zeta) \times \frac{a^{\frac{3}{2}}h(\zeta)}{\sqrt{v}} = \frac{a^{\frac{5}{2}}xf'h(\zeta)}{\sqrt{v}}. \end{aligned} \tag{3.18}$$

$$\begin{aligned} \frac{\partial G}{\partial y} &= ax\sqrt{\frac{a}{v}}h'(\sqrt{\frac{a}{v}}y)\sqrt{\frac{a}{v}}. \\ v\frac{\partial G}{\partial y} &= \left(-\sqrt{av}f(\zeta)\right)\frac{a^2x}{v}h'(\zeta) \\ &= -\frac{a^{\frac{5}{2}}x}{\sqrt{v}}f(\zeta)h'(\zeta). \end{aligned} \tag{3.19}$$

Using (3.18) and (3.19), the left side of (3.3) gets the following form:

$$\begin{aligned} u\frac{\partial G}{\partial x} + v\frac{\partial G}{\partial y} &= \frac{a^{\frac{5}{2}}xf'(\zeta)h(\zeta)}{\sqrt{v}} - \frac{a^{\frac{5}{2}}xf(\zeta)h'(\zeta)}{\sqrt{v}} \\ &= \frac{a^{\frac{5}{2}}x}{\sqrt{v}}\left[f'(\zeta)h(\zeta) - f(\zeta)h'(\zeta)\right]. \end{aligned} \tag{3.20}$$

The following approach has been used to transform the right side of (3.3) into the dimensionless form

$$\begin{aligned} \frac{\partial^2 G}{\partial^2 y} &= \frac{\partial}{\partial y}\left(\frac{a^2x}{v}h'\left(\sqrt{\frac{a}{v}}y\right)\right) \\ &= \frac{a^2x}{v}h''(\zeta)\left(\sqrt{\frac{a}{v}}y\right) \\ &= \frac{a^{\frac{5}{2}}x}{v^{\frac{3}{2}}}h''(\zeta). \end{aligned} \tag{3.21}$$

$$\frac{\partial u}{\partial y} = \frac{a^{\frac{3}{2}}x}{\sqrt{v}}f''(\zeta).$$

$$\gamma^* = \left(\mu + \frac{k}{2}\right) j = \mu\left(1 + \frac{k}{2\mu} j\right) j = \mu\left(1 + \frac{K}{2}\right) j. \tag{3.22}$$

$$\begin{aligned}
\frac{\gamma^*}{\rho\ j}\frac{\partial^2 G}{\partial^2 y} &= \frac{\mu\left(1+\frac{K}{2}\right) j}{\rho\ j}\frac{a^{\frac{5}{2}} x}{v^{\frac{3}{2}}} h''(\zeta) \\
&= \frac{a^{\frac{5}{2}} x}{\sqrt{v}}\left[\frac{\mu\left(1+\frac{K}{2}\right)}{\rho\ v} h''(\zeta)\right] \\
&= \frac{a^{\frac{5}{2}} x}{\sqrt{v}}\left[\frac{\mu\left(1+\frac{K}{2}\right)}{\mu} h''(\zeta)\right] \\
&= \frac{a^{\frac{5}{2}} x}{\sqrt{v}}\left[\left(1+\frac{K}{2}\right) h''(\zeta)\right].
\end{aligned} \tag{3.23}$$

$$\begin{aligned}
\frac{k}{\rho\ j}\left(2G + \frac{\partial u}{\partial y}\right) &= \frac{k}{\rho\ j}\left[2ax\sqrt{\frac{a}{v}} h(\zeta) + \frac{a^{\frac{3}{2}} x}{\sqrt{v}} f''(\zeta)\right] \\
&= a^{\frac{5}{2}}\frac{x}{\sqrt{v}}\left[\frac{k}{\rho\ j\ a}(2h(\zeta) + f''(\zeta))\right] \\
&= a^{\frac{5}{2}}\frac{x}{\sqrt{v}}\left[\frac{k}{\rho\ a\frac{v}{a}}(2h(\zeta) + f''(\eta))\right] \quad \left(\because j = \frac{v}{a}\right) \\
&= a^{\frac{5}{2}}\frac{x}{\sqrt{v}}\left[\frac{k}{\rho\ v}(2h(\zeta) + f''(\zeta))\right] \\
&= a^{\frac{5}{2}}\frac{x}{\sqrt{v}}\left[K(2h(\zeta) + f''(\zeta))\right].
\end{aligned} \tag{3.24}$$

Using (3.21)-(3.24), the dimensionless form of right side (3.3) is as follows:

$$\begin{aligned}
&\frac{\gamma^*}{\rho\ j}\frac{\partial^2 G}{\partial^2 y} - \frac{k}{\rho\ j}\left(2G + \frac{\partial u}{\partial y}\right) \\
&= \frac{a^{\frac{5}{2}} x}{\sqrt{v}}\left[\left(1+\frac{K}{2}\right) h''\right] - a^{\frac{5}{2}}\frac{x}{\sqrt{v}}\left[K\left(2h(\zeta) + f''(\zeta)\right)\right]
\end{aligned}$$

Hence the dimensionless form of (3.3) becomes:

$$\begin{aligned}
\frac{a^{\frac{5}{2}} x}{\sqrt{v}}[f'(\zeta)h(\zeta) - f(\zeta)h'(\zeta)] &= a^{\frac{5}{2}}\frac{x}{\sqrt{v}}\left(1+\frac{K}{2}\right) h''(\zeta) - a^{\frac{5}{2}}\frac{x}{\sqrt{v}}[K2h(\zeta) \\
&\quad + f''(\zeta)]. \\
\Rightarrow [f'(\zeta)h(\zeta) - f(\zeta)h'(\zeta)] &= \left(1+\frac{K}{2}\right) h''(\zeta) - K\left(2h(\zeta) + f''(\zeta)\right).
\end{aligned}$$

$$\Rightarrow \left(1+\frac{K}{2}\right)h''+fh'-f'h-K\left(2h+f''\right). \tag{3.25}$$

Now we include below the procedure for the conversion of (3.4) into the dimensionless form

$$\theta(\zeta)=\frac{T-T_\infty}{T_f-T_\infty}.$$

$$\Rightarrow\ T=\left(T_f-T_\infty\right)\theta(\zeta)+T_\infty. \tag{3.26}$$

$$\frac{\partial T}{\partial x}=0. \tag{3.27}$$

$$u\frac{\partial T}{\partial x}=0. \tag{3.28}$$

$$\frac{\partial T}{\partial y}=\sqrt{\frac{a}{v}}\left(T_f-T_\infty\right)\theta'(\zeta). \tag{3.29}$$

$$v\frac{\partial T}{\partial y}=-a\left(T_f-T_\infty\right)\theta'(\zeta)f(\zeta). \tag{3.30}$$

Using (3.26)-(3.30), the left side of (3.4) gets the following form:

$$\begin{aligned}u\frac{\partial T}{\partial x}+v\frac{\partial T}{\partial y}&=0-a\left(T_f-T_\infty\right)\theta'(\zeta)f(\zeta)\\&=-a\left(T_f-T_\infty\right)\theta'(\zeta)f(\zeta)\end{aligned} \tag{3.31}$$

To convert the right side of (3.4) into the dimensionless form, we proceed as follows

$$\frac{\partial^2 T}{\partial^2 y}=\frac{a}{v}\left(T_f-T_\infty\right)\theta''(\zeta).$$

$$\frac{k_1}{\rho\ C_p}\frac{\partial^2 T}{\partial^2 y}=\frac{k_1}{\rho\ C_p}\frac{a}{v}\left(T_f-T_\infty\right)\theta''(\zeta). \tag{3.32}$$

$$\begin{aligned}\frac{\left(\mu\ B_0-E_0\right)^2\sigma}{\rho\ C_p}&=\frac{\left(\mu^2B_0^2+E_0^2-2E_0\mu\ B_0\right)\sigma}{\rho\ C_p}\\&=\frac{\left(a^2x^2\left(f'(\eta)\right)^2B_0^2+E_0^2-2E_0axf'(\zeta)B_0\right)\sigma}{\rho\ C_p}\quad(u=axf'(\zeta))\\&=(ax)^2\ B_0^2\frac{\left(\left(f'(\eta)\right)^2+\frac{E_0^2}{(ax)^2B_0^2}-\frac{2E_0}{(ax)B_0}f'(\zeta)\right)\sigma}{\rho\ C_p}\qquad(u=ax)\\&=u_w^2B_0^2\sigma\frac{\left(\left(f'(\zeta)\right)^2+E^2-2Ef'(\eta)\right)}{\rho\ C_p}.\left(E=\frac{E_0}{(ax)\ B_0}\right)\end{aligned} \tag{3.33}$$

$$\left(\frac{\mu+k}{\rho\ C_p}\right)\left(\frac{\partial u}{\partial y}\right)^2 = \left(\frac{\mu+k}{\rho\ C_p}\right)\left(\frac{a^{\frac{3}{2}}x}{\sqrt{v}}\right)^2 (f''(\zeta))^2$$

$$= \left(\frac{\mu+k}{\rho\ v}\right)\left(\frac{a^3x^2}{C_p}\right)(f''(\zeta))^2$$

$$= \left(\frac{\mu+k}{\mu}\right)\left(\frac{(ax)^2\,a}{C_p}\right)(f''(\zeta))^2$$

$$= \left(\frac{\mu}{\mu}+\frac{k}{\mu}\right)\left(\frac{u_w^2 a}{C_p}\right)(f''(\zeta))^2 \quad (u_w = ax, \quad \mu = \rho\ v)$$

$$= (1+K)\left(\frac{u_w^2 a}{C_p}\right)(f''(\zeta))^2 \qquad \left(K = \frac{k}{\mu}\right)$$

$$= \left[(1+K)\left(\frac{u_w^2}{C_p\,(T_f - T_\infty)}\right)\left(\frac{v\rho\ C_p}{k_1}\right)\right](f''(\zeta))^2\left(\frac{ak_1}{v\rho\ C_p}\right)$$

$$(T_f - T_\infty)$$

$$= \left[(1+K)\,E_c P_r\,(f''(\zeta))^2\right]\left(\frac{ak_1}{v\rho\ C_p}\right)(T_f - T_\infty)\,. \tag{3.34}$$

$$\phi(\zeta) = \frac{(C - C_\infty)}{(C_f - C_\infty)}$$

$$\Rightarrow C = \phi(\zeta)\,(C_f - C_\infty) + C_\infty \tag{3.35}$$

$$\frac{\partial C}{\partial y} = \sqrt{\frac{a}{v}}\,(C_f - C_\infty)\,\phi'(\zeta) \tag{3.36}$$

$$\tau\ D_B \frac{\partial T}{\partial y}\frac{\partial C}{\partial y} = \tau\ D_B\left(\sqrt{\frac{a}{v}}\,(T_f - T_\infty)\,\theta'(\zeta)\right)\left(\sqrt{\frac{a}{v}}\,(C_f - C_\infty)\,\phi'(\zeta)\right)$$

$$= \left[\frac{\tau}{v} D_B\,(C_f - C_\infty)\,\theta'(\zeta)\phi'(\zeta)\right] a\,(T_f - T_\infty)$$

$$= N_b\theta'(\zeta)\phi'(\zeta) a\,(T_f - T_\infty)\,. \quad \left(N_b = \frac{\tau}{v} D_B\,(C_f - C_\infty)\right) \tag{3.37}$$

$$\tau\ \frac{D_T}{T_\infty}\left(\frac{\partial T}{\partial y}\right)^2 = \tau\ \frac{D_T}{T_\infty}\left(\sqrt{\frac{a}{v}}\,(T_f - T_\infty)\,\theta'(\zeta)\right)^2$$

$$= \frac{\tau}{T_\infty}\frac{D_T}{v}\,(T_f - T_\infty)\,(\theta'(\zeta))^2\,a\,(T_f - T_\infty)$$

$$= N_t\,(\theta'(\zeta))^2\ \ a\,(T_f - T_\infty)\,. \quad \left(N_t = \frac{D_t\tau}{T_\infty\ v}\,(T_f - T_\infty)\right) \tag{3.38}$$

$$\theta(\zeta) = \frac{T - T_\infty}{T_f - T_\infty}$$

$$\Rightarrow T = (T_f - T_\infty)\,\theta(\zeta) + T_\infty = T_\infty\left(\frac{T_f}{T_\infty} - 1\right)\theta(\zeta) + T_\infty$$

$$\Rightarrow\ T = T_\infty\,((\theta_w - 1)\,\theta(\zeta) + 1) \tag{3.39}$$

$$\frac{\partial T}{\partial y} = T_\infty\left((\theta_w - 1)\,\theta'(\zeta)\sqrt{\frac{a}{v}}\right)$$

$$q_r = -\frac{4\sigma^*}{3k^*}\frac{\partial T^4}{\partial y}$$

$$
\begin{aligned}
&= -\frac{16\sigma^*}{3k^*}T^3\frac{\partial T}{\partial y} \\
&= -\frac{16\sigma^* T_\infty^3}{3k^*}\left[(\theta_w-1)\,\theta(\zeta)+1\right]^3\frac{\partial T}{\partial y}. \\
\frac{1}{\rho\ C_p}\frac{\partial q_r}{\partial y} &= -\frac{16\sigma^* T_\infty^3}{3k^*\rho\ C_p}\left[\left((\theta_w-1)\,\theta(\zeta)+1\right)^3\frac{\partial^2 T}{\partial y^2}\right] \\
&\quad -\frac{16\sigma^* T_\infty^3}{3k^*\rho\ C_p}\left[\frac{\partial T}{\partial y}3\left((\theta_w-1)\,\theta(\zeta)+1\right)^2(\theta_w-1)\frac{\partial \theta}{\partial y}\right] \\
&= -\frac{16\sigma^* T_\infty^3}{3k^*\rho\ C_p}\left[\left((\theta_w-1)\,\theta(\zeta)+1\right)^3\frac{a}{v}\left(T_f-T_\infty\right)\theta''(\zeta)\right] \\
&\quad -\frac{16\sigma^* T_\infty^3}{3k^*\rho\ C_p}\left[\frac{\partial T}{\partial y}3\left((\theta_w-1)\,\theta(\zeta)+1\right)^2(\theta_w-1)\right] \\
&\quad \left[\theta'(\zeta)\sqrt{\frac{a}{v}}\left(T_f-T_\infty\right)\frac{1}{\left(T_f-T_\infty\right)}\sqrt{\frac{a}{v}}\left(T_f-T_\infty\right)\theta'(\zeta)\right] \\
&= -\frac{16\sigma^* T_\infty^3}{3k^*k_1}\frac{k_1 a}{\rho\ C_p v}\left[\left((\theta_w-1)\,\theta(\zeta)+1\right)^3\theta''(\zeta)\right] \\
&\quad -\frac{16\sigma^* T_\infty^3}{3k^*k_1}\frac{k_1 a}{\rho\ C_p v}\left[3\left((\theta_w-1)\,\theta(\zeta)+1\right)^2(\theta_w-1)\,\theta'^2(\zeta)\left(T_f-T_\infty\right)\right] \\
&= -\frac{4R}{3Pr}a\left(T_f-T_\infty\right)\left[\left((\theta_w-1)\,\theta(\zeta)+1\right)^3\theta''(\zeta)\right] \\
&\quad -\frac{4R}{3Pr}a\left(T_f-T_\infty\right)\left[3\left((\theta_w-1)\,\theta(\zeta)+1\right)^2(\theta_w-1)\,\theta'^2(\zeta)\right] \\
&= -\frac{4R}{3Pr}\frac{v\rho\ C_p}{k_1}\frac{k_1}{v\rho\ C_P}a\left(T_f-T_\infty\right)\left[\left((\theta_w-1)\,\theta(\zeta)+1\right)^3\theta''(\zeta)\right] \\
&\quad -\frac{4R}{3Pr}\frac{v\rho\ C_p}{k_1}\frac{k_1}{v\rho\ C_P}a\left(T_f-T_\infty\right)\left[3\left((\theta_w-1)\,\theta(\zeta)+1\right)^2(\theta_w-1)\,\theta'^2(\zeta)\right] \\
&= -\frac{4R}{3Pr}Pr\frac{k_1}{v\rho\ C_P}a\left(T_f-T_\infty\right)\left[\left((\theta_w-1)\,\theta(\zeta)+1\right)^3\theta''(\zeta)\right] \\
&\quad -\frac{4R}{3Pr}Pr\frac{k_1}{v\rho\ C_P}a\left(T_f-T_\infty\right)\left[3\left((\theta_w-1)\,\theta(\zeta)+1\right)^2(\theta_w-1)\,\theta'^2(\zeta)\right] \\
&= -\frac{4R}{3}\frac{k_1}{v\rho\ C_P}a\left(T_f-T_\infty\right)\left[\left((\theta_w-1)\,\theta(\zeta)+1\right)^3\theta''(\zeta)\right] \\
&\quad -\frac{4R}{3}\frac{k_1}{v\rho\ C_P}a\left(T_f-T_\infty\right)\left[3\left((\theta_w-1)\,\theta(\zeta)+1\right)^2(\theta_w-1)\,\theta'^2(\zeta)\right].
\end{aligned}
\tag{3.40}
$$

Using (3.32) to (3.40), the dimensionless form of right side (3.4) is as follows

$$
\frac{k_1}{\rho\ C_p}\left(\frac{\partial^2 T}{\partial y^2}\right)+\frac{\left(\mu\ B_0-E_0\right)^2\sigma}{\rho\ C_p}+\frac{1}{\rho\ C_p}\frac{16\sigma^*}{3k^*}T_\infty^*\frac{\partial T}{\partial y}+\left(\frac{\mu+k}{\rho\ C_p}\right)\left(\frac{\partial u}{\partial y}\right)^2
$$

$$
\begin{aligned}
&+\tau\left[D_B\frac{\partial T}{\partial y}\frac{\partial C}{\partial y}+\frac{D_T}{T_\infty}\left(\frac{\partial T}{\partial y}\right)^2\right.\\
&=\frac{k_1}{\rho\ C_p}\frac{a}{v}\left(T_f-T_\infty\right)\theta''(\zeta)+u_w^2\ B_0^2\ \sigma\frac{\left(\left(f'(\zeta)\right)^2+E^2-2Ef'(\zeta)\right)}{\rho\ C_p}\\
&\quad+\left[(1+K)\,E_cP_r\left(f''(\zeta)\right)^2\right]\left(\frac{ak_1}{\rho\ C_p}\right)\left(T_f-T_\infty\right)\\
&\quad+\left[N_b\theta'(\zeta)\phi'(\zeta)\right]\left(T_f-T_\infty\right)a+\left[N_t\left(\theta'(\zeta)\right)^2\right]a\left(T_f-T_\infty\right)\\
&\quad+\frac{4R}{3}\frac{k_1}{v\rho\ C_P}a\left(T_f-T_\infty\right)\left[\left(\left(\theta_w-1\right)\theta(\zeta)+1\right)^3\theta''(\zeta)\right]\\
&\quad+\frac{4R}{3}\frac{k_1}{v\rho\ C_P}a\left(T_f-T_\infty\right)\left[3\left(\left(\theta_w-1\right)\theta(\zeta)+1\right)^2\left(\theta_w-1\right)\theta'^2(\zeta)\right].\\
&=a\left(T_f-T_\infty\right)\left[\frac{k_1}{\mu\ C_p}\theta''(\zeta)+E_cM^2\left(\left(f'(\zeta)\right)^2+E^2-2Ef'(\zeta)\right)\right]\\
&\quad+\left[(1+K)\,E_cP_r\left(f''(\zeta)\right)^2\right]\left(\frac{ak_1}{\rho\ C_p}\right)\left(T_f-T_\infty\right)\\
&\quad+\left[N_b\theta'(\zeta)\phi'(\eta)+\left[N_t\left(\theta'(\zeta)\right)^2\right]a\left(T_f-T_\infty\right)\right]\left(T_f-T_\infty\right)a\\
&\quad+\frac{4R}{3}\frac{k_1}{v\rho\ C_P}a\left(T_f-T_\infty\right)\left[\left(\left(\theta_w-1\right)\theta(\zeta)+1\right)^3\theta''(\zeta)\right]\\
&\quad+\frac{4R}{3}\frac{k_1}{v\rho\ C_P}a\left(T_f-T_\infty\right)\left[3\left(\left(\theta_w-1\right)\theta(\zeta)+1\right)^2\left(\theta_w-1\right)\theta'^2(\zeta)\right].\\
&=\frac{ak_1}{\mu\ C_p}\left(T_f-T_\infty\right)\left[\theta''(\zeta)+\frac{\mu\ C_p}{k_1}E_cM^2\left(\left(f'(\zeta)\right)^2+E^2-2Ef'(\zeta)\right)\right]\\
&\quad+\left[(1+K)\,E_cP_r\left(f''(\zeta)\right)^2\right]\left(\frac{ak_1}{\rho\ C_p}\right)\left(T_f-T_\infty\right)\\
&\quad+\left[N_b\theta'(\zeta)\phi'(\zeta)+N_t\left(\theta'(\zeta)\right)^2\right]a\left(T_f-T_\infty\right)\left(\frac{v\rho\ C_p}{k_1}\right)\left(\frac{k_1}{v\rho\ C_p}\right)\left(T_f-T_\infty\right)a\\
&\quad+\frac{4R}{3}\frac{k_1}{v\rho\ C_P}a\left(T_f-T_\infty\right)\left[\left(\left(\theta_w-1\right)\theta(\zeta)+1\right)^3\theta''(\zeta)\right]\\
&\quad+\frac{4R}{3}\frac{k_1}{v\rho\ C_P}a\left(T_f-T_\infty\right)\left[3\left(\left(\theta_w-1\right)\theta(\zeta)+1\right)^2\left(\theta_w-1\right)\theta'^2(\zeta)\right].\\
&=\frac{ak_1}{\mu\ C_p}\left(T_f-T_\infty\right)\left[\theta''(\zeta)+P_rE_cM^2\left(\left(f'(\zeta)\right)^2+E^2-2Ef'(\zeta)\right)\right]\\
&\quad+\left[(1+K)\,E_cP_r\left(f''(\zeta)\right)^2\right]\left(\frac{ak_1}{\rho\ C_p}\right)\left(T_f-T_\infty\right)\\
&\quad+\left[N_b\theta'(\zeta)\phi'(\zeta)+N_t\left(\theta'(\zeta)\right)^2\right]a\left(T_f-T_\infty\right)P_r\left(\frac{k_1}{\mu\ C_P}\right)\left(T_f-T_\infty\right)a\\
&\quad+\frac{4R}{3}\frac{k_1}{v\rho\ C_P}a\left(T_f-T_\infty\right)\left[\left(\left(\theta_w-1\right)\theta(\zeta)+1\right)^3\theta''(\zeta)\right]\\
&\quad+\frac{4R}{3}\frac{k_1}{v\rho\ C_P}a\left(T_f-T_\infty\right)\left[3\left(\left(\theta_w-1\right)\theta(\zeta)+1\right)^2\left(\theta_w-1\right)\theta'^2(\zeta)\right].
\end{aligned}
$$

$$
\begin{aligned}
&= \frac{ak_1}{\mu\ C_P}\left(T_f - T_\infty\right)\left[\theta''(\zeta) + \frac{\mu\ C_p}{k_1}E_c\ M^2\left(\left(f'(\zeta)\right)^2 + E^2 - 2Ef'(\zeta)\right)\right] \\
&\quad + \frac{ak_1}{\mu\ C_p}\left(T_f - T_\infty\right)\left[N_b\theta'(\zeta)\phi'(\zeta) + N_t\left(\theta'(\zeta)\right)^2\right]P_r \\
&\quad + \left(\frac{k_1}{\mu\ C_p}\right)a\left(T_f - T_\infty\right)\left[\left(1+K\right)E_cP_r\left(f''(\zeta)\right)^2\right] \\
&\quad + \frac{4R}{3}\frac{k_1}{v\rho\ C_P}a\left(T_f - T_\infty\right)\left[\left(\left(\theta_w - 1\right)\theta(\zeta) + 1\right)^3\theta''(\zeta)\right] \\
&\quad + \frac{4R}{3}\frac{k_1}{v\rho\ C_P}a\left(T_f - T_\infty\right)\left[3\left(\left(\theta_w - 1\right)\theta(\zeta) + 1\right)^2\left(\theta_w - 1\right)\theta'^2(\zeta)\right]. \qquad (3.41)
\end{aligned}
$$

Hence the dimensionless form of (3.4) becomes:

$$
\begin{aligned}
u\frac{\partial T}{\partial x} + v\frac{\partial T}{\partial y} &= \frac{k_1}{\rho\ C_p}\left(\frac{\partial^2 T}{\partial y^2}\right) + \frac{\left(\mu\ B_0 - E_0\right)^2\sigma}{\rho\ C_p} + \frac{1}{\rho\ C_p}\frac{16\sigma^*}{3k^*}T_\infty^*\frac{\partial T}{\partial y} \\
&\quad + \left(\frac{\mu + k}{\rho\ C_p}\right)\left(\frac{\partial u}{\partial y}\right)^2 + \tau\left[D_B\frac{\partial T}{\partial y}\frac{\partial C}{\partial y} + \frac{D_T}{T_\infty}\left(\frac{\partial T}{\partial y}\right)^2\right].
\end{aligned}
$$

$$
\begin{aligned}
\Rightarrow\ & -a\left(T_f - T_\infty\right)\theta'(\zeta)f(\zeta) \\
&= \frac{ak_1}{\mu\ C_p}\left(T_f - T_\infty\right)\left[\theta''(\zeta) + \frac{\mu\ C_p}{k_1}E_cM^2\left(\left(f'(\zeta)\right)^2 + E^2 - 2Ef'(\zeta)\right)\right] \\
&\quad + \frac{ak_1}{\mu\ C_p}\left(T_f - T_\infty\right)\left[N_b\theta'(\zeta)\phi'(\zeta) + N_t\left(\theta'(\zeta)\right)^2\right]P_r \\
&\quad + \left(\frac{k_1}{\mu\ C_p}\right)a\left(T_f - T_\infty\right)\left[\left(1+K\right)E_cP_r\left(f''(\zeta)\right)^2\right] \\
&\quad + \frac{4R}{3}\frac{k_1}{v\rho\ C_P}a\left(T_f - T_\infty\right)\left[\left(\left(\theta_w - 1\right)\theta(\zeta) + 1\right)^3\theta''(\zeta)\right] \\
&\quad + \frac{4R}{3}\frac{k_1}{v\rho\ C_P}a\left(T_f - T_\infty\right)\left[3\left(\left(\theta_w - 1\right)\theta(\zeta) + 1\right)^2\left(\theta_w - 1\right)\theta'^2(\zeta)\right].
\end{aligned}
$$

$$
\begin{aligned}
\Rightarrow\ & -\frac{\mu\ C_p}{k_1}\theta'(\zeta)f(\zeta) \\
&= \left[\theta''(\zeta) + P_rE_cM^2\left(\left(f'(\zeta)\right)^2 + E^2 - 2Ef'(\zeta)\right)\right] \\
&\quad + \left[N_b\theta'(\zeta)\phi'(\zeta) + N_t\left(\theta'(\zeta)\right)^2\right]P_r \\
&\quad + \left[\left(1+K\right)E_cP_r\left(f''(\eta)\right)^2\right] + \frac{4R}{3}\left[\left(\left(\theta_w - 1\right)\theta(\eta) + 1\right)^3\theta''(\zeta)\right] \\
&\quad + \frac{4R}{3}\left[3\left(\left(\theta_w - 1\right)\theta(\zeta) + 1\right)^2\left(\theta_w - 1\right)\theta'^2(\zeta)\right].
\end{aligned}
$$

$$
\begin{aligned}
\Rightarrow\ & -P_r\theta'(\zeta)f(\zeta) \\
&= \left[\theta''(\zeta) + P_rE_cM^2\left(\left(f'(\zeta)\right)^2 + E^2 - 2Ef'(\zeta)\right)\right] \\
&\quad + \left[N_b\theta'(\zeta)\phi'(\zeta) + N_t\left(\theta'(\zeta)\right)^2\right]P_r
\end{aligned}
$$

$$
\begin{aligned}
&+\left[(1+K)\,E_cP_r\,(f''(\zeta))^2\right]+\frac{4R}{3}\left[((\theta_w-1)\,\theta(\zeta)+1)^3\,\theta''(\zeta)\right]\\
&+\frac{4R}{3}\left[3\,((\theta_w-1)\,\theta(\zeta)+1)^2\,(\theta_w-1)\,\theta'^2(\zeta)\right].\\
\Rightarrow\ & P_r\theta'(\zeta)f(\zeta)+\left[\theta''(\zeta)+P_rE_cM^2\left((f'(\zeta))^2+E^2-2Ef'(\zeta)\right)\right]\\
&+\left[N_b\theta'(\zeta)\phi'(\zeta)+N_t\,(\theta'(\zeta))^2\right]P_r\\
&+\left[(1+K)\,E_cP_r\,(f''(\eta))^2\right]+\frac{4R}{3}\left[((\theta_w-1)\,\theta(\zeta)+1)^3\,\theta''(\zeta)\right]\\
&+\frac{4R}{3}\left[3\,((\theta_w-1)\,\theta(\zeta)+1)^2\,(\theta_w-1)\,\theta'^2(\zeta)\right]=0.\\
\Rightarrow\ & \theta''(\zeta)\left[1+\frac{4R}{3}\,((\theta_w-1)\,\theta(\zeta)+1)^3\right]\\
&+P_r\theta'(\zeta)f(\eta)+P_rE_cM^2\left((f'(\zeta))^2+E^2-2Ef'(\zeta)\right)\\
&+4R\,((\theta_w-1)\,\theta(\zeta)+1)^2\,(\theta_w-1)\,\theta'^2(\zeta)+(1+K)\,E_cP_r\,(f''(\zeta))^2\\
&+P_r\left[N_b\theta'(\zeta)\phi'(\zeta)+N_t\theta'^2(\zeta)\right]=0. \qquad (3.42)
\end{aligned}
$$

Now we conclude the procedure for conversion of (4.5) into the dimensionless form

$$\frac{\partial C}{\partial x}=0. \qquad (3.43)$$

$$u\frac{\partial C}{\partial x}=axf'(\zeta)(0)=0. \qquad (3.44)$$

$$
\begin{aligned}
v\frac{\partial C}{\partial y}&=-\sqrt{av}f(\zeta)\left(\sqrt{\frac{a}{v}}\right)(C_f-C_\infty)\,\phi'(\zeta).\\
&=-a\,(C_f-C_\infty)\,[f(\zeta)\phi'(\zeta)]\,. \qquad (3.45)
\end{aligned}
$$

Using (3.44) and (3.45), the left side of ((3.5)) gets the following form:

$$
\begin{aligned}
u\frac{\partial C}{\partial x}+v\frac{\partial C}{\partial y}&=0-a\,(C_f-C_\infty)\,[f(\zeta)\phi'(\zeta)]\\
&=-a\,(C_f-C_\infty)\,[f(\zeta)\phi'(\zeta)]\,. \qquad (3.46)
\end{aligned}
$$

To convert the right side of (3.5) into dimensionless form we proceed as follows

$$\frac{\partial^2 C}{\partial y^2}=\frac{a}{v}\,(C_f-C_\infty)\,\phi''(\zeta). \qquad (3.47)$$

$$\frac{\partial^2 T}{\partial y^2}=\frac{a}{v}\,(T_f-T_\infty)\,\theta''(\zeta). \qquad (3.48)$$

$$D_B \frac{\partial^2 C}{\partial y^2} = D_B \frac{a}{v} (C_f - C_\infty) \phi''(\zeta). \tag{3.49}$$

$$D_T \frac{\partial^2 T}{\partial y^2} = D_T \frac{a}{v} (T_f - T_\infty) \theta''(\zeta). \tag{3.50}$$

$$N_t = \frac{(\rho\ c)_p\ D_T}{(\rho\ c)_f\ v\ T_\infty} (T_f - T_\infty). \tag{3.51}$$

$$N_b = \frac{(\rho\ c)_p\ D_B}{(\rho\ c)_f\ v} (C_f - C_\infty). \tag{3.52}$$

Using (3.47)-(3.52), the dimensionless form of right side of (3.5) is as follows:

$$\begin{aligned}
&D_B \frac{\partial^2 C}{\partial y^2} + \frac{D_T}{T_\infty} \frac{\partial^2 T}{\partial y^2} \\
&= D_B \frac{a}{v} (C_f - C_\infty) \phi''(\zeta) + \frac{D_T}{T_\infty} \frac{a}{v} (T_f - T_\infty) \theta''(\zeta) \\
&= D_B \frac{a}{v} (C_f - C_\infty) \left[\phi''(\zeta) + \frac{D_T}{T_\infty} \frac{(T_f - T_\infty)}{D_B (C_f - C_\infty)} \theta''(\zeta) \right] \\
&= D_B \frac{a}{v} (C_f - C_\infty) \left[\phi''(\zeta) + \frac{D_T}{T_\infty} \frac{(T_f - T_\infty) (\rho\ c)_p (\rho\ c)_f}{D_B (C_f - C_\infty) (\rho\ c)_p (\rho\ c)_f} \theta''(\zeta) \right] \\
&= D_B \frac{a}{v} (C_f - C_\infty) \left[\phi''(\zeta) + \frac{(\rho\ c)_p\ D_T}{(\rho\ c)_f\ v\ T_\infty} (T_f - T_\infty) \frac{1}{\frac{(\rho\ c)_p\ D_B (C_f - C_\infty)}{(\rho\ c)_f\ v}} \theta''(\zeta) \right] \\
&= D_B \frac{a}{v} (C_f - C_\infty) \left[\phi''(\zeta) + \frac{N_t}{N_b} \theta''(\zeta) \right].
\end{aligned} \tag{3.53}$$

Therefore the dimensionless form of (3.5) becomes:

$$\begin{aligned}
& u \frac{\partial C}{\partial x} + v \frac{\partial C}{\partial y} = D_B \frac{\partial^2 C}{\partial y^2} + \frac{D_T}{T_\infty} \frac{\partial^2 T}{\partial y^2} \\
\Rightarrow\ & - a (C_f - C_\infty) [f(\zeta) \phi'(\zeta)] = D_B \frac{a}{v} (C_f - C_\infty) \left[\phi''(\zeta) + \frac{N_t}{N_b} \theta''(\zeta) \right] \\
\Rightarrow\ & [f(\zeta) \phi'(\zeta)] = D_B \frac{1}{v} \left[\phi''(\zeta) + \frac{N_t}{N_b} \theta''(\zeta) \right] \\
\Rightarrow\ & - \frac{v}{D_B} [f(\zeta) \phi'(\zeta)] = \left[\phi''(\zeta) + \frac{N_t}{N_b} \theta''(\zeta) \right] \\
\Rightarrow\ & - \frac{v}{\alpha} \frac{\alpha}{D_B} [f(\zeta) \phi'(\zeta)] = \left[\phi''(\zeta) + \frac{N_t}{N_b} \theta''(\zeta) \right] \qquad \left(L_e = \frac{\alpha}{D_B} \right)
\end{aligned}$$

$$\Rightarrow \; - P_r L_e \left[f(\zeta) \phi'(\zeta) \right] = \left[\phi''(\zeta) + \frac{N_t}{N_b} \theta''(\zeta) \right] \qquad \left(P_r = \frac{v}{\alpha} \right)$$

$$\Rightarrow \phi'' + P_r L_e f(\zeta) \phi'(\zeta) + \frac{N_t}{N_b} \theta'' = 0. \tag{3.54}$$

Rewriting the converted ODEs together

$$(1+K) f''' + f f'' - f'^2 + K h'(\zeta) - M^2 f' + M^2 E = 0, \tag{3.55}$$

$$\left(1 + \frac{K}{2} \right) h'' + f h' - f' h' - K \left(2h + f'' \right) = 0, \tag{3.56}$$

$$\begin{aligned} \theta'' \left[1 + \frac{4}{3} R \left((\theta_w - 1) \theta + 1 \right)^3 \right] + P_r f \theta' + M^2 E_c P_r \left[f'^2 + E^2 - 2 E f' \right] \\ + 4R \left((\theta_w - 1) \theta + 1 \right)^2 \left((\theta_w - 1) \theta'^2 \right) + (1+K) E_c P_r f''^2 \\ + P_r \left(N_b \theta' \phi' + N_t \theta'^2 \right) = 0, \end{aligned} \tag{3.57}$$

$$\phi''(\zeta) + P_r L_e f \phi' + \frac{N_t}{N_b} \theta'' = 0. \tag{3.58}$$

Conversion of the boundary conditions:

$$v = v_w, \qquad at \;\; y = 0.$$

$$\Rightarrow \; - \sqrt{av} f(\zeta) = v_w \qquad at \;\; \zeta = 0.$$

$$\Rightarrow \; f(\zeta) = - \frac{v_w}{\sqrt{av}} \qquad at \;\; \zeta = 0.$$

$$\Rightarrow \; f(\zeta) = - \left(av \right)^{\frac{-1}{2}} v_w \qquad at \;\; \zeta = 0.$$

$$\Rightarrow \; f(\zeta) = f_w. \qquad \left(f_w = - \left(av \right)^{\frac{-1}{2}} v_w \right) \qquad at \;\; \zeta = 0.$$

$$G = -n \frac{\partial u}{\partial y} \qquad at \;\; y = 0.$$

$$\Rightarrow \; ax \sqrt{\frac{a}{v}} h(\zeta) = - n \frac{a^{\frac{3}{2}}}{\sqrt{v}} x f''(\zeta) \qquad at \;\; \zeta = 0.$$

$$\Rightarrow \; h(\zeta) = -n f''(\zeta). \qquad at \;\; \zeta = 0.$$

$$u = ax + \alpha^* \left[(\mu + k) \frac{\partial u}{\partial y} + kG \right] \qquad at \;\; y = 0.$$

$$\Rightarrow \; a x f'(\zeta) = ax + \alpha^* \left[(\mu + k) \frac{a^{\frac{3}{2}}}{\sqrt{v}} x f''(\zeta) + kax \sqrt{\frac{a}{v}} h(\zeta) \right] \qquad at \;\; \zeta = 0.$$

$$\Rightarrow \; f'(\zeta) = 1 + \alpha^* \left[(\mu + k) \sqrt{\frac{a}{v}} f''(\zeta) + k \sqrt{\frac{a}{v}} h(\zeta) \right] \qquad at \;\; \zeta = 0.$$

$$\Rightarrow\ f'(\zeta)=1+\alpha^{*}\mu\ \sqrt{\frac{a}{v}}f''(\zeta)+\alpha^{*}k\sqrt{\frac{a}{v}}f''(\zeta)+\alpha^{*}k\sqrt{\frac{a}{v}}h(\zeta)\quad at\ \ \zeta=0.$$

$$\Rightarrow\ f'(\zeta)=1+\alpha\ f''(\zeta)+\alpha\ Kf''(\zeta)+\alpha\ Kh(\zeta)\ \ \left(K=\frac{k}{\mu},\alpha=\alpha^{*}\mu\sqrt{\frac{a}{v}}\right)$$

$$\Rightarrow\ f'(\zeta)=1+\alpha\,(1+K)\,f''(\zeta)-\alpha\ Knf''(\zeta)\qquad (h(\zeta)=-nf''(\zeta))$$

$$\Rightarrow\ f'(\zeta)=1+\alpha\,(1+K-Kn)\,f''(\zeta)\qquad at\ \ \zeta=0.$$

$$\Rightarrow\ f'(\zeta)=1+\alpha\,(1+K\,(1-n))\,f''(\zeta).\qquad at\ \ \zeta=0.$$

$$h_{ft}\,[T_f-T]=-k\frac{\partial T}{\partial y}\qquad at\ \ y=0.$$

$$\Rightarrow\ h_{ft}\,[T_f-T]=-k\left[\theta'(\zeta)\sqrt{\frac{a}{v}}\,(T_f-T_\infty)\right]\qquad at\ \ \zeta=0.$$

$$\Rightarrow\ \theta'(\zeta)=-\frac{h_{ft}\,(T_f-T)}{k\sqrt{\frac{a}{v}}\,(T_f-T_\infty)}\qquad at\ \ \zeta=0.$$

$$\Rightarrow\ \theta'(\zeta)=-\frac{h_{ft}}{k}\sqrt{\frac{\nu}{a}}\frac{[T_f-\theta(\zeta)\,(T_f-T_\infty)-T_\infty]}{T_f-T_\infty}\qquad at\ \ \zeta=0.$$

$$\Rightarrow\ \theta'(\zeta)=-\frac{h_{ft}}{k}\sqrt{\frac{\nu}{a}}\left[\frac{T_f-T_\infty}{T_f-T_\infty}-\theta(\zeta)\frac{T_f-T_\infty}{T_f-T_\infty}\right]\qquad at\ \ \zeta=0.$$

$$\Rightarrow\ \theta'(\zeta)=-\frac{h_{ft}}{k}\sqrt{\frac{\nu}{a}}\,(1-\theta(\zeta))\qquad at\ \ \zeta=0.$$

$$\Rightarrow\ \theta'(\zeta)=-\gamma_1\,(1-\theta(\zeta))\,.\qquad \left(\gamma_1=\frac{h_{ft}}{k}\sqrt{\frac{\nu}{a}}\right)\qquad at\ \ \zeta=0.$$

$$\Rightarrow\ u\to 0,\qquad as\ \ y=\infty.$$

$$\Rightarrow\ axf'(\infty)=0\qquad at\ \ \zeta=\infty.$$

$$\Rightarrow\ f'(\infty)=0.\qquad at\ \ \zeta=\infty.$$

$$\Rightarrow\ N\to 0,\qquad as\ \ y\to\infty.$$

$$\Rightarrow\ ax\sqrt{\frac{a}{v}}h(\zeta)=0\qquad at\ \ \zeta=\infty.$$

$$\Rightarrow\ h(\infty)=0.\qquad at\ \ \zeta=\infty.$$

$$\Rightarrow\ T\to\ T_\infty\qquad as\ \ y\to\infty$$

$$\Rightarrow\ \theta(\infty)=0\qquad at\ \ \zeta=\infty.$$

$$-\,D_B\frac{\partial C}{\partial y}=h_{fc}\,(C_f-C)\qquad at\ \ y=0.$$

$$\Rightarrow\ h_{fc}\,[C_f-C]=-D_B\left[\phi'(\zeta)\sqrt{\frac{a}{\nu}}\,(C_f-C_\infty)\right]\qquad at\ \ \zeta=0.$$

$$\Rightarrow\ \phi'(\zeta)=-\frac{h_{fc}\,(C_f-C)}{D_B\sqrt{\frac{a}{\nu}}\,(C_f-C_\infty)}\qquad at\ \ \zeta=0.$$

$$\Rightarrow \ \phi'(\zeta) = -\frac{h_{fc}}{D_B}\sqrt{\frac{\nu}{a}}\frac{(C_f - C)}{(C_f - T_\infty)} \qquad at \ \ \zeta = 0.$$

$$\Rightarrow \ \phi'(\zeta) = -\frac{h_{fc}}{D_B}\sqrt{\frac{\nu}{a}}\frac{[C_f - \phi(\zeta)\,(C_f - C_\infty) - C_\infty]}{(C_f - C_\infty)} \qquad at \ \ \zeta = 0.$$

$$\Rightarrow \ \phi'(\zeta) = -\frac{h_{fc}}{D_B}\sqrt{\frac{\nu}{a}}\left[\frac{C_f - C_\infty}{C_f - C_\infty} - \phi(\zeta)\frac{C_f - C_\infty}{C_f - C_\infty}\right] \qquad at \ \ \zeta = 0.$$

$$\Rightarrow \ \phi'(\zeta) = -\frac{h_{fc}}{D_B}\sqrt{\frac{\nu}{a}}\,(1 - \phi(\zeta)) \qquad at \ \ \zeta = 0.$$

$$\Rightarrow \ \phi'(\zeta) = -\gamma_2\,(1 - \phi(\zeta))\,. \qquad \left(\gamma_2 = \frac{h_{fc}}{D_B}\sqrt{\frac{\nu}{a}}\right) \qquad at \ \ \zeta = 0.$$

Boundary conditions are as follows:

$$\left.\begin{aligned} &f(0) = f_w, \quad f'(0) = 1 + \alpha\,(1 + K\,(1 - n))\,f''(0), \\ &h(0) = -nf''(0), \quad \theta'(0) = -\gamma_1\,(1 - \theta(0))\,, \\ &\phi'(0) = -\gamma_2\,(1 - \phi(0))\,, \quad at \ \ y = 0, \\ &f'(y) \Rightarrow 0, \ h(y) \Rightarrow 0, \ \theta(y) \Rightarrow 0, \ \phi(y) \Rightarrow 0, \ as \ y \to \ \infty. \end{aligned}\right\} \tag{3.59}$$

The local skin friction is given as

$$Cf_x = \frac{2\tau_w}{\rho\,(ax)^2}. \tag{3.60}$$

Shear stress at the surface is defined as

$$\tau_w = \left[(\mu + k)\,\frac{\partial u}{\partial y} + kN\right]_{y=0}. \tag{3.61}$$

Converting τ_w into dimensionless form as follows:

$$\tau_w = ax\sqrt{\frac{a}{v}}\mu\ f''(0)\,[1 + (1 - n)\,K]\,. \tag{3.62}$$

To get the dimensionless form of Cf_x, the following procedure is worked out.

$$
\begin{aligned}
Cf_x &= \frac{2\tau_w}{\rho\,(ax)^2} \\
&= \frac{2ax\sqrt{\frac{a}{v}}\mu\ f''(0)\,[1+(1-n)\,K]}{\rho\,(ax)^2} \\
&= \frac{2\sqrt{\frac{a}{v}}\mu\ f''(0)\,[1+(1-n)\,K]}{\rho\,(ax)}.
\end{aligned}
$$

Multiplying both sides by $\frac{1}{2}\rho\,(ax)\,\sqrt{\frac{v}{a}}\frac{1}{\mu}$,

$$
\begin{aligned}
&\frac{1}{2}Cf_x\,(ax)\,\sqrt{\frac{v}{a}}\frac{\rho}{\mu} = f''(0)\,[1+(1-n)\,K] \\
\Rightarrow\ &\frac{1}{2}Cf_x\,(ax)\,\sqrt{\frac{v}{a}}\frac{1}{v} = f''(0)\,[1+(1-n)\,K] \qquad \left(v=\frac{\mu}{\rho},\quad \frac{1}{v}=\frac{\rho}{\mu}\right) \\
\Rightarrow\ &\frac{1}{2}Cf_x\sqrt{\frac{a}{v}}x = f''(0)\,[1+(1-n)\,K] \\
\Rightarrow\ &\frac{1}{2}Cf_xRe_x^{\frac{1}{2}} = f''(0)\,[1+(1-n)\,K]
\end{aligned}
$$

Hence, the dimensionless form of the coefficient of skin friction is

$$
\frac{1}{2}Cf_xRe_x^{\frac{1}{2}} = f''(0)\,[1+(1-n)\,K]\,, \tag{3.63}
$$

where Re represent the Reynolds number defined as $Re = \sqrt{\frac{a}{v}}x$. The Nusselt number is given as

$$
Nu_x = \frac{xq_w}{K_f\,(T_f - T_\infty)}, \tag{3.64}
$$

where q_w are given by

$$
q_w = \left[-k_f\frac{\partial T}{\partial y} + q_r\right]_{y=0}. \tag{3.65}
$$

Converting q_w into dimensionless form, it gets the form:

$$
q_w = -k_f\sqrt{\frac{a}{v}}\,(T_f - T_\infty)\,\theta'(0)\left[1+\frac{4}{3}R\,((\theta_w-1)\,\theta(0)+1)^3\right]. \tag{3.66}
$$

To get the dimensionless form of Nu_x, the following procedure is worked out

$$\begin{aligned} Nu_x &= \frac{xq_w}{K_f\left(T_f - T_\infty\right)} \\ &= \frac{-xk_f\sqrt{\frac{a}{v}}\left(T_f - T_\infty\right)\theta'(0)\left[1+\frac{4}{3}R\left(\left(\theta_w-1\right)\theta(0)+1\right)^3\right]}{K_f\left(T_f - T_\infty\right)} \\ &= -x\sqrt{\frac{a}{v}}\left[1+\frac{4}{3}R\left(\left(\theta_w-1\right)\theta(0)+1\right)^3\right]\theta'(0). \end{aligned}$$

Multiplying both sides by $\frac{1}{x}\sqrt{\frac{v}{a}}$,

$$\begin{aligned} & Nu_x\frac{1}{x}\sqrt{\frac{v}{a}} = -\left[1+\frac{4}{3}R\left(\left(\theta_w-1\right)\theta(0)+1\right)^3\right]\theta'(0). \\ \Rightarrow\ & Nu_x Re_x^{\frac{-1}{2}} = -\left[1+\frac{4}{3}R\left(\left(\theta_w-1\right)\theta(0)+1\right)^3\right]\theta'(0). \end{aligned}$$

Hence, the dimensionless form of the Nusselt number is

$$Nu_x Re_x^{\frac{-1}{2}} = -\left[1+\frac{4}{3}R\left(\left(\theta_w-1\right)\theta(0)+1\right)^3\right]\theta'(0), \tag{3.67}$$

where Re represent the Reynolds number defined as $Re = \sqrt{\frac{a}{v}}x$.

The Sherwood number is given as

$$Sh_x = \frac{xq_w}{D_B\left(C_f - C_\infty\right)}. \tag{3.68}$$

where q_w are given by

$$q_m = \left[-D_B\frac{\partial C}{\partial y}\right]_{y=o}. \tag{3.69}$$

Converting q_m into dimensionless form, it gets the form:

$$q_m = -D_B\left[\left(C_f - C_\infty\right)\sqrt{\frac{a}{v}}\phi'(0)\right]. \tag{3.70}$$

To get the dimensionless form of Sh_x, the following procedure is worked out.

$$\begin{aligned} Sh_x &= \frac{xq_w}{D_B\left(C_f - C_\infty\right)} \\ &= \frac{xD_B\left[\left(C_f - C_\infty\right)\sqrt{\frac{a}{v}}\phi'(0)\right]}{D_B\left(C_f - C_\infty\right)} \\ &= -x\sqrt{\frac{a}{v}}\phi'(0). \end{aligned}$$

Multiplying both sides by $\frac{1}{x}\sqrt{\frac{v}{a}}$,

$$\begin{aligned} & Sh_x\frac{1}{x}\sqrt{\frac{v}{a}} = -\phi'(0). \\ \Rightarrow\ & Sh_x Re_x^{\frac{-1}{2}} = -\phi'(0). \end{aligned}$$

Hence, the dimensionless form of Sherwood number is

$$Sh_x Re_x^{\frac{-1}{2}} = -\phi'(0), \tag{3.71}$$

where Re represent the Reynolds number defined as $Re = \sqrt{\frac{a}{v}}x$.

3.4 Solution Methodology

For solving (3.55) and (3.56) with the associated boundary conditions (3.59), we use the shooting method. First of all, we need to convert these equations into a system of first order differential equations. Let us use the following notations.

$$\left.\begin{aligned} f = S_1, \quad f' = S_1' = S_2, \quad f'' = S_2' = S_3, \\ h = S_4, \quad h' = S_4' = S_5. \end{aligned}\right\} \tag{3.72}$$

The resulting IVP takes the form:

$$\left.\begin{aligned} S_1' = S_2, & \qquad S_1(0) = f_w, \\ S_2' = S_3, & \qquad S_2(0) = 1 + \alpha\left(1 + K\left(1 - n\right)\right)p, \end{aligned}\right\} \tag{3.73}$$

$$\left.\begin{aligned} S_3' &= \frac{S_2^2 - S_1 S_3 - K S_5 + M^2 S_2 - M^2 E}{1+K}, & S_3(0) &= p, \\ S_4' &= S_5, & S_4(0) &= -np, \\ S_5' &= \frac{2\left(S_2 S_4 + K\left(2S_4 + S_3\right) - S_1 S_5\right)}{2+K}. & S_5(0) &= q. \end{aligned}\right\} \tag{3.74}$$

In the above system of equations (3.74), the missing initial conditions p and q are to be chosen such that

$$\left(S_2(p,q)\right)_{\zeta=\zeta_\infty} = 0, \qquad \left(S_4(p,q)\right)_{\zeta=\zeta_\infty} = 0. \tag{3.75}$$

As the numerical computation can not be performed on an unbounded domain, therefore the domain of the above problem has been taken as $[0, \zeta_\infty]$ instead of $[0, \infty)$, where ζ_∞ is an appropriate initial positive real number. We use Newton's method to solve (3.75), through the following formula

$$\begin{bmatrix} p \\ q \end{bmatrix}_{n+1} = \begin{bmatrix} p \\ q \end{bmatrix}_{n} - \begin{bmatrix} \frac{\partial S_2(p,q)}{\partial p} & \frac{\partial S_2(p,q)}{\partial q} \\ \frac{\partial S_4(p,q)}{\partial p} & \frac{\partial S_4(p,q)}{\partial q} \end{bmatrix}_{n}^{-1} \cdot \begin{bmatrix} S_2 \\ S_4 \end{bmatrix}_{n}$$

Furthermore, the following notations will be useful for computing the entries of the Jacobian matrix

$$\begin{aligned} &\frac{\partial S_1}{\partial p} = S_6, \quad \frac{\partial S_2}{\partial p} = S_7, \quad \frac{\partial S_3}{\partial p} = S_8, \quad \frac{\partial S_4}{\partial p} = S_9, \quad \frac{\partial S_5}{\partial p} = S_{10}, \\ &\frac{\partial S_1}{\partial q} = S_{11}, \quad \frac{\partial S_2}{\partial q} = S_{12}, \quad \frac{\partial S_3}{\partial q} = S_{13}, \quad \frac{\partial S_4}{\partial q} = S_{14}, \quad \frac{\partial S_5}{\partial q} = S_{15}. \end{aligned}$$

Newton's iterative scheme will change the form after utilizing the above-mentioned notations as follows

$$\begin{bmatrix} p \\ q \end{bmatrix}_{n+1} = \begin{bmatrix} p \\ q \end{bmatrix}_{n} - \begin{bmatrix} S_7 & S_{12} \\ S_9 & S_{14} \end{bmatrix}_{n}^{-1} \cdot \begin{bmatrix} S_2 \\ S_4 \end{bmatrix}_{n}$$

Now differentiating the system of five first order ODEs with respect to p and q, we get another system of ODEs, as follows:

$$S_1' = S_2, \qquad S_1(0) = f_w,$$

$$
\begin{aligned}
S_2' &= S_3, & S_2(0) &= 1 + \alpha\left(1 + K\left(1 - n\right)\right)p,\\
S_3' &= \frac{S_2^2 - S_1S_3 - KS_5 + M^2S_2 - M^2E}{1+K}, & S_3(0) &= p,\\
S_4' &= S_5, & S_4(0) &= -np,\\
S_5' &= \frac{2\left(S_2S_4 + K\left(2S_4 + S_3\right) - S_1S_5\right)}{2+K}, & S_5(0) &= q,\\
S_6' &= S_7, & S_6(0) &= 0,\\
S_7' &= S_8, & S_7(0) &= 1 + \alpha\left(1 + K\left(1 - n\right)\right),\\
S_8' &= \frac{2S_2S_7 - S_1S_8 - S_3S_6 - KS_{10} + M^2S_7}{1+K}, & S_8(0) &= -n,\\
S_9' &= S_{10}, & S_9(0) &= 0,\\
S_{10}' &= \frac{2\left(S_2S_9 - S_4S_7 - S_1S_{10} - S_5S_6 + 2KS_9 + KS_8\right)}{2+K}, & S_{10}(0) &= 0,\\
S_{11}' &= S_{12}, & S_{11}(0) &= 0,\\
S_{12}' &= S_{13}, & S_{12}(0) &= 0,\\
S_{13}' &= \frac{2S_2S_{12} - S_1S_{13} - S_3S_{11} - KS_{15} + M^2S_{12}}{1+K}, & S_3(0) &= 0,\\
S_{14}' &= S_{15}, & S_{14}(0) &= 0,\\
S_{15}' &= \frac{2\left(S_2S_{14} - S_4S_{12} - S_1S_{15} - S_5S_{11} + K\left(2S_{14} + S_{13}\right)\right)}{2+K}. & S_{15}(0) &= 1.
\end{aligned}
\tag{3.76}
$$

The following criteria is the stopping condition for the shooting method:

$$max \mid \{|S_2(\zeta_\infty)|, |S_4(\zeta_\infty)|\} \mid < \epsilon,$$

where ϵ is a small positive real number. Throughout this work, ϵ has been taken as 10^{-10} unless otherwise mentioned. Also, for equations (3.57) and (3.58), the following notations have been used

$$
\begin{aligned}
&\theta(\zeta) = V_1, && \theta'(\zeta) = V_1' = V_2, && \theta''(\zeta) = V_1'' = V_2',\\
&\phi(\zeta) = V_3, && \phi'(\zeta) = V_3' = V_4, && \phi''(\zeta) = V_3'' = V_4'.\\
&B_1 = \theta_w - 1, && B_2 = 1 + B_1V_1,
\end{aligned}
$$

$$E_1 = \frac{1}{\left[1 + \frac{4}{3}RB_2^3\right]},$$

$$E_2 = M^2 E_c P_r \left(f'^2 + E^2 - 2Ef'\right) + (1+K)\left(f''^2\right) + 4RB_1B_2^2V_2^2 + PrV_2\left(f + N_bV_4 + N_tV_2\right),$$

$$E_3 = \frac{4RB_1B_2^2V_5}{(E_1)^2},$$

$$E_4 = 8RB_1B_2^2V_2V_6 + 8RB_1^2B_2V_2^2V_5 + P_rV_6\left(f + N_bV_4 + N_tV_2\right) + PrV_2\left(N_bV_8 + N_tV_6\right),$$

$$E_5 = \frac{4RB_1B_2^2V_9}{(E_1)^2},$$

$$E_6 = 8RB_1B_2^2V_2V_{10} + 8RB_1^2B_2V_2^2V_9 + P_rV_{10}\left(f + N_bV_4 + N_tV_2\right) + PrV_2\left(N_bV_{12} + N_tV_{10}\right).$$

As a result, the coupled ODEs are converted into the following system of first order ODEs

$$\left.\begin{aligned} V_1' &= V_2, & V_1(0) &= l,\\ V_2' &= E_1 * E_2, & V_2(0) &= -\gamma_1\left(1-l\right),\\ V_3' &= V_4, & V_3(0) &= m,\\ V_4' &= -L_eP_rfV_4 - (Nt/Nb) * (E1 * E2), & V_4(0) &= -\gamma_2\left(1-m\right). \end{aligned}\right\} \tag{3.77}$$

The above initial value problem has been solved by using the RK-4 method. The missing conditions l and m are choosen very carefully, so that the following conditions must hold

$$[V_1(l,m)]_{\zeta=\zeta_\infty} = 0, \qquad [V_3(l,m)]_{\zeta=\zeta_\infty} = 0. \tag{3.78}$$

To solve the above algebaric equations, we apply the Newton's method which has the following scheme

$$\begin{bmatrix} l \\ m \end{bmatrix}_{n+1} = \begin{bmatrix} l \\ m \end{bmatrix}_{n+1} - \begin{bmatrix} \frac{\partial V_1(l,m)}{\partial l} & \frac{\partial V_1(l,m)}{\partial m} \\ \frac{\partial V_3(l,m)}{\partial l} & \frac{\partial V_3(l,m)}{\partial m} \end{bmatrix}_n^{-1} \cdot \begin{bmatrix} V_1 \\ V_3 \end{bmatrix}_n$$

Now, introduce the following notations

$$\begin{aligned} &\frac{\partial V_1}{\partial l} = V_5, \quad \frac{\partial V_2}{\partial l} = V_6, \quad \frac{\partial V_3}{\partial l} = V_7, \quad \frac{\partial V_4}{\partial l} = V_8, \\ &\frac{\partial V_1}{\partial m} = V_9, \quad \frac{\partial V_2}{\partial m} = V_{10}, \quad \frac{\partial V_3}{\partial m} = V_{11}, \quad \frac{\partial V_4}{\partial m} = V_{12}. \end{aligned}$$

As a result of these new notations, the Newton's iterative scheme gets the form

$$\begin{bmatrix} l \\ m \end{bmatrix}_{n+1} = \begin{bmatrix} l \\ m \end{bmatrix}_n - \begin{bmatrix} V_5 & V_9 \\ V_7 & V_{11} \end{bmatrix}_n^{-1} \cdot \begin{bmatrix} V_1 \\ V_3 \end{bmatrix}_n$$

Now, we will get another system of eight 1st order ODEs after differentiating the above system of four ODEs of 1st order w.r.t to l and m

$$\begin{aligned} V_5' &= V_6, & V_5(0) &= 1, \\ V_6' &= E_1 * E_4 + E_3 * E_2, & V_6(0) &= \gamma_1, \\ V_7' &= V_8, & V_7(0) &= 0, \\ V_8' &= -L_e P_r f V_8 - (Nt/Nb) * (E1 * E4 + E3 * E2), & V_8(0) &= 0, \\ V_9' &= V_{10}, & V_9(0) &= 0, \\ V_{10}' &= E_1 * E_6 + E_5 * E_2, & V_{10}(0) &= 0, \\ V_{11}' &= V_{12}, & V_{11}(0) &= 1, \\ V_{12}' &= -L_e P_r f V_{12} - (Nt) * (E1 * E6 + E5 * E2). & V_{12}(0) &= \gamma_2. \end{aligned}$$

The stopping criteria for the Newton's method is set as:

$$max \mid \{|V_1(\zeta_\infty)|, |V_3(\zeta_\infty)|\} \mid < \epsilon,$$

where ϵ is a small positive real number.

3.5 Results and Discussion

The numerical results of the equations in the preceding sections will be discussed through the graphs and tables in this section. Various important parameters, such as the material parameter K, suction/injection parameter f_w, magnetic parameter M, Prandtl number Pr, radiation parameter R, Lewis number Le, Brownian motion parameter Nb, thermophoresis parameter Nt, thermal Biot number γ_1, and solutal Biot number γ_2, are taken into account when performing numerical calculations. These parameters have a direct influence on the distribution of velocity, temperature and concentration.

Table 3.1 describes the computed numerical results of C_f using different values of physical parameters given in the table. Skin friction C_f is decreased by raising the values of the material parameter K and suction parameter f_w. It is observed, the increase in Hartman number M and suction/injection parameter f_w enhance the local skin-friction coefficient, whereas the local skin friction coefficient shows a decreasing behavior for buoyancy ratio parameter n and the slip parameter α. In this table, I_f and I_h are the intervals from which the missing conditions f and h can be chosen.

Tables 3.2 and 3.3 discuss the effect of significant characteristics of the local Nusselt number $Nu(Re_x)^{-\frac{1}{2}}$ and Sherwood number $Sh(Re_x)^{-\frac{1}{2}}$. The local Nusselt number and Sherwood number fall by enlarging the Eckert number Ec, and the thermophoresis parameter Nt. The local Nusselt number and Sherwood number mount while enlarging the radiation parameter R, temperature ratio parameter θ_w, Prandtl number Pr and Lewis number Le. The effect of slip parameter α on the velocity profile $f'(\zeta)$ is presented in Figure 3.2.

Increasing the values of the slip parameter α reduces the velocity field and the boundary thickness as depicted in Figure 3.2. In this table, I_θ and I_ϕ are the intervals from which the missing conditions θ and ϕ can be chosen.

The impact of the suction parameter f_w on the velocity profile $f'(\zeta)$ is presented in Figure 3.3. For gradually increasing suction parameter f_w, the velocity profile

decreases and the boundary layer width grows. The impact of the material parameter K on the velocity profile $f'(\zeta)$ is presented in Figure 3.4. By increasing K, the velocity field reduces in the lower half of the surface whereas it enhances in the upper half. The impact of the material parameter K on the microrotation profile $h(\zeta)$ is displayed in Figure 3.5 whereas diminishing trend is noticed near the surface, where a declining trend is visible towards the surface and escalates away from the stretching sheet. As the material parameter is increased, the viscosity of the fluid falls.

Figure 3.6 and 3.7 depict the impact of Hartman number M on the velocity profile $f'(\zeta)$ and the temperature profile $\theta'(\zeta)$. It shows that the huge values of the magnetic parameter M cause an increase in both the velocity profile $f'(\zeta)$ and the temperature profile $\theta'(\zeta)$.

Figure 3.8 demonstrates the impact of the thermal Biot number γ_1 on the temperature profile $\theta'(\zeta)$. We notice that the enhanced values of the thermal Biot number γ_1 cause a higher energy. Figure 3.9 displays the influence of Eckert number Ec on the temperature profile $\theta'(\zeta)$. Temperature profile increases when the Eckert number is increased.

Figure 3.10 represents the impact of the temperature ratio parameter θ_w on the temperature profile. Temperature rises when the temperature ratio parameter θ_w is increased, as shown in Figure.

Figure 3.11 depicts the effect of the Prandtl number Pr on the temperature profile $\theta'(\zeta)$. The temperature of the fluid decreases as the Prandtl number increases due to a thinner boundary layer thickness and reduced thermal diffusivity.

Figure 3.12 depicts the effect of the thermophoresis parameter Nt on the temperature profile $\theta'(\zeta)$. For the increasing values of the thermophoresis parameter, it is obvious that the thermal boundary layer thickness and temperature are increased. Figure 3.13 shows that as the thermal radiation parameter R is increased, the boundary layer thickness and temperature increase. In the presence of radiation, the working fluid absorbs more heat, which improves the temperature profile.

Figure 3.14 depicts the effect of increasing Lewis number Le values on the concentration profile $\phi(\zeta)$. Because the Lewis number is the ratio of the kinematic viscosity of the nanofluid to the Brownian diffusion coefficient, increasing the Lewis number leads to an increase in the viscosity of the fluid, which resists fluid motion and hence reduces the concentration of nanoparticles.

In Figure 3.15, we see that the thermophoresis parameter Nt has an increasing impact on the concentration profile $\phi(\zeta)$ and solutal boundary layer thickness. The thermophoresis parameter and the thermal diffusion coefficient are directly related. For bigger values of the thermophoresis parameter Nt, more nanoparticle diffusion occurs, and thus the concentration of the nanofluid is increased.

Figure 3.16 depicts how an increase in the Prandtl number Pr causes a reduction in the concentration profile $\phi(\zeta)$. As the Prandtl number increases, the thermal diusivity decreases, resulting in the low range temperature seen in Figure 3.16.

The effect of Brownian motion parameter Nb on the concentration profile $\phi(\zeta)$ is presented in Figure 3.17. Increasing the values of the Brownian motion parameter reduces the concentration profile.

Figure 3.18 shows the effect of solutal Biot number γ_2 on the concentration profile $\phi(\zeta)$. The concentration profiles are greatly improved for higher solutal Biot number values.

Rising values of both Nb and Nt, as seen in Figure 3.19, reduce the rate of heat transmission on the surface. Figure 3.19 depicts the relationship between the thermophoresis parameter and Brownian motion parameter on Sherwood number, indicating that mass transfer rate increases for Nb and reduces for Nt.

TABLE 3.1: Results of $(Re_x)^{\frac{1}{2}}\frac{1}{2}C_f$ for various parameters

K	M	n	f_w	α	$(Re_x)^{\frac{1}{2}}\frac{1}{2}C_f$	I_f	I_h
0.2					-0.37183	[-0.3,-0.1]	[0,5]
0.3					-0.37483	[-0.3,-0.1]	[0,5]
0.4					-0.37769	[-0.3,-0.1]	[0,5]
0.2					-0.37093	[-0.3,-0.1]	[0,5]
	0.3				-0.37052	[-0.3,-0.1]	[0,5]
	0.4				-0.37112	[-0.3,-0.1]	[0,5]
	0.1	0.6			-0.37073	[-0.3,-0.1]	[0,5]
		0.7			-0.36959	[-0.3,-0.1]	[0,5]
		0.8			-0.36842	[-0.3,-0.1]	[0,5]
			0.2		-0.38154	[-0.3,-0.1]	[0,5]
			0.3		-0.39134	[-0.3,-0.1]	[0,5]
			0.4		-0.40120	[-0.3,-0.1]	[0,5]
			0.1	1.5	-0.35621	[-0.3,-0.1]	[0,5]
				1.6	-0.34191	[-0.3,-0.1]	[0,5]
				1.7	-0.33785	[-0.3,-0.1]	[0,5]

TABLE 3.2: Results of $Nu(Re_x)^{-\frac{1}{2}}$ *and* $Sh(Re_x)^{-\frac{1}{2}}$ when $K = 0.2$, $E = 0.2$, $f_w = 0.1$, $\alpha = 1.4$, $n = 0.5$, $N_t = 0.2$, $L_e = 1.2$, $\gamma_1 = \gamma_2 = 0.1$

R	θ_w	P_r	E_c	N_b	$Nu(Re_x)^{-\frac{1}{2}}$	$Sh(Re_x)^{-\frac{1}{2}}$	I_θ	I_ϕ
0.3					0.11587	0.08736	[-0.3, 0.2]	[-0.3, 0.3]
0.4					0.12622	0.08739	[-0.2, 0.3]	[-0.4, 0.3]
0.5					0.13633	0.08741	[-0.2, 0.2]	[-0.4, 0.2]
0.2	1.4				0.10596	0.08734	[-0.3, 0.3]	[-0.3, 0.3]
	1.5				0.10665	0.08735	[-0.3, 0.3]	[-0.3, 0.3]
	1.6				0.10735	0.08737	[-0.3, 0.2]	[-0.2, 0.3]
	1.3	1.7			0.10597	0.08780	[-0.3, 0.1]	[-0.2, 0.3]
		1.8			0.10659	0.08821	[-0.2, 0.2]	[-0.2, 0.3]
		1.9	0.2		0.10716	0.08860	[-0.2, 0.2]	[-0.2, 0.3]
			0.3		0.10312	0.08741	[-0.2, 0.2]	[-0.5, 0.3]
			0.4		0.10097	0.08740	[-0.2, 0.2]	[-0.4, 0.4]
			0.1	1.3	0.09882	0.08754	[-0.3, 0.2]	[-0.2, 0.4]
				1.4	0.09872	0.08742	[-0.2, 0.3]	[-0.2, 0.3]
				1.5	0.09852	0.08740	[-0.2, 0.2]	[-0.3, 0.3]

TABLE 3.3: Results of $Nu(Re_x)^{-\frac{1}{2}}$ *and* $Sh(Re_x)^{-\frac{1}{2}}$ when $K = 0.2$, $E = 0.2$, $f_w = 0.1$, $\alpha = 1.4$, $n = 0.5$, $N_b = 0.2$, $P_r = 1.6$, $E_c = 0.1$

N_t	L_e	γ_1	γ_2	$Nu(Re_x)^{-\frac{1}{2}}$	$Sh(Re_x)^{-\frac{1}{2}}$	I_θ	I_ϕ
0.3				0.10503	0.08689	[-0.3, 0.2]	[-0.3, 0.3]
0.4				0.10478	0.08644	[-0.2, 0.3]	[-0.4, 0.3]
0.5				0.10453	0.08600	[-0.2, 0.2]	[-0.4, 0.2]
0.2	1.3			0.10533	0.08795	[-0.3, 0.3]	[-0.3, 0.3]
	1.4			0.10538	0.08850	[-0.3, 0.3]	[-0.3, 0.3]
	1.5			0.10543	0.08893	[-0.3, 0.2]	[-0.2, 0.3]
	1.2	0.2		0.17775	0.08669	[-0.3, 0.1]	[-0.2, 0.3]
		0.3		0.22928	0.08624	[-0.2, 0.2]	[-0.5, 0.3]
		0.4		0.26719	0.08592	[-0.2, 0.2]	[-0.4, 0.4]
		0.1	0.2	0.10358	0.15643	[-0.3, 0.2]	[-0.2, 0.4]
			0.3	0.10210	0.21246	[-0.2, 0.3]	[-0.2, 0.3]
			0.4	0.10082	0.21246	[-0.2, 0.2]	[-0.3, 0.3]

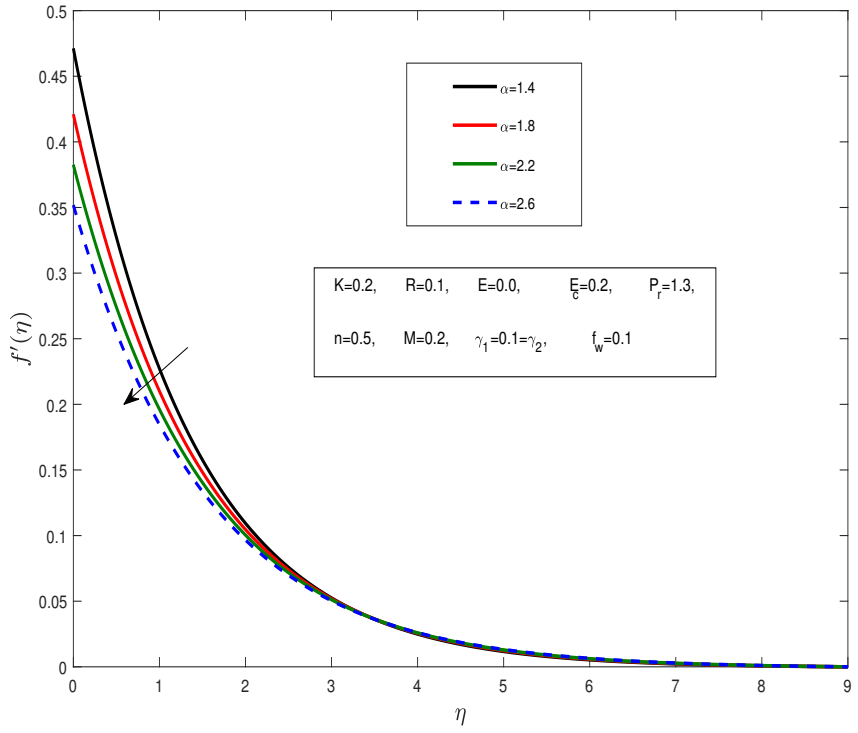

FIGURE 3.2: Influence of α on $f'(\zeta)$.

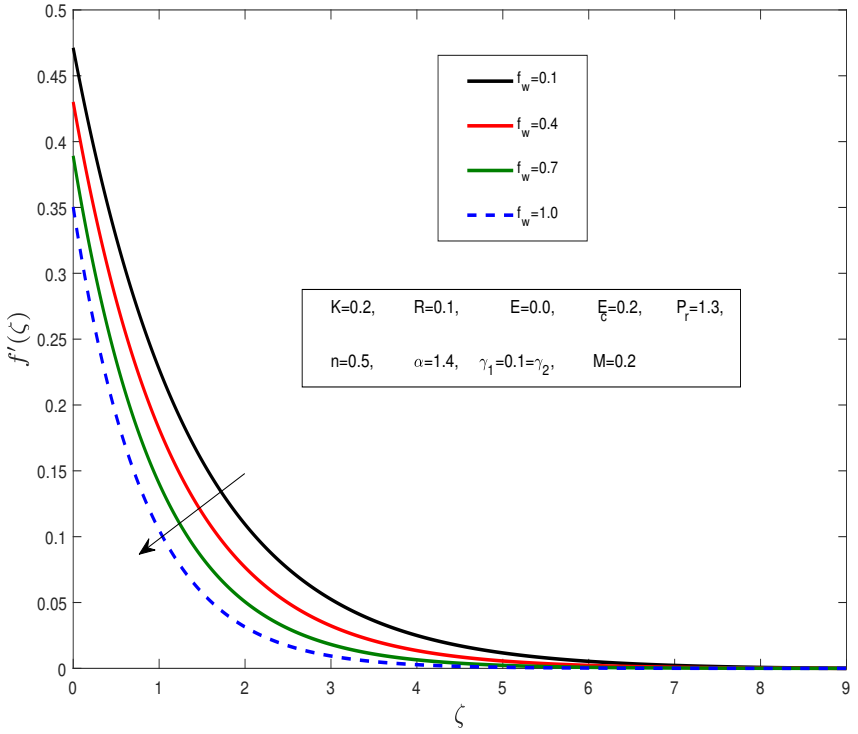

FIGURE 3.3: Influence of f_w on $f'(\zeta)$.

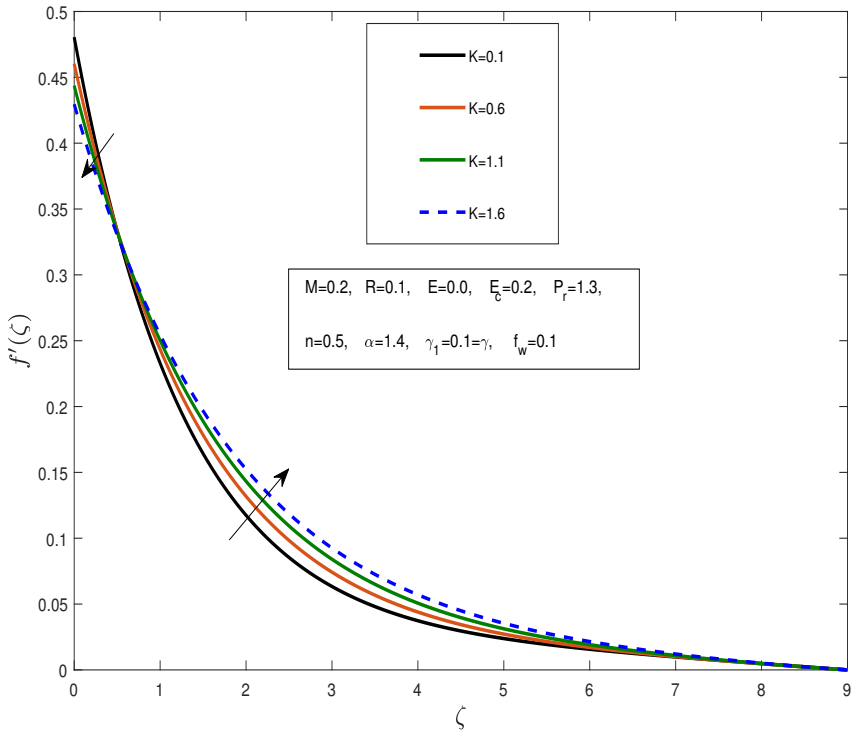

FIGURE 3.4: Influence of K on $f'(\zeta)$.

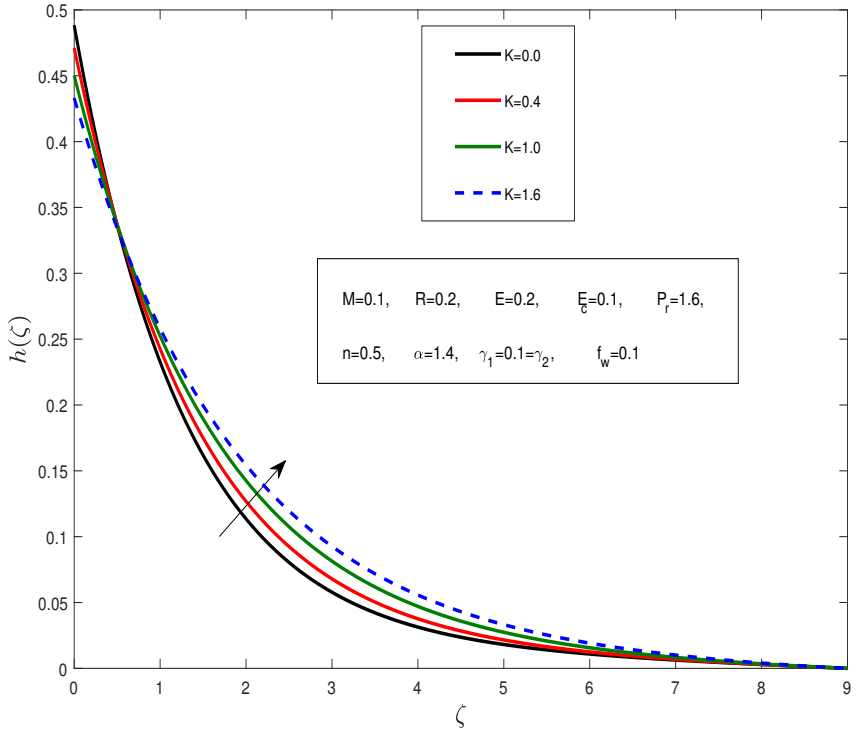

FIGURE 3.5: Influence of K on $h(\zeta)$.

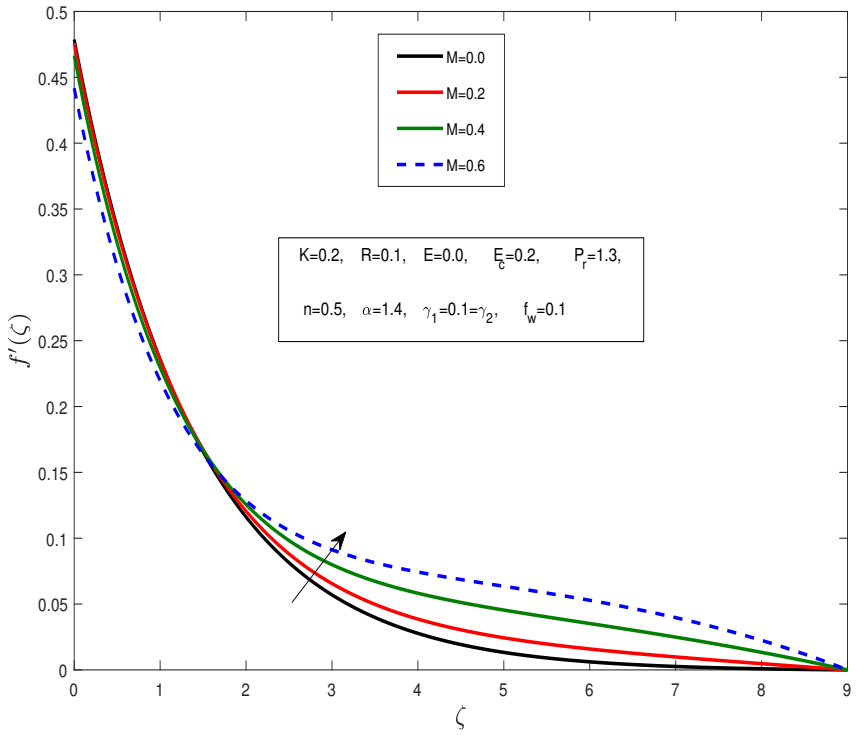

FIGURE 3.6: Influence of M on $f'(\zeta)$.

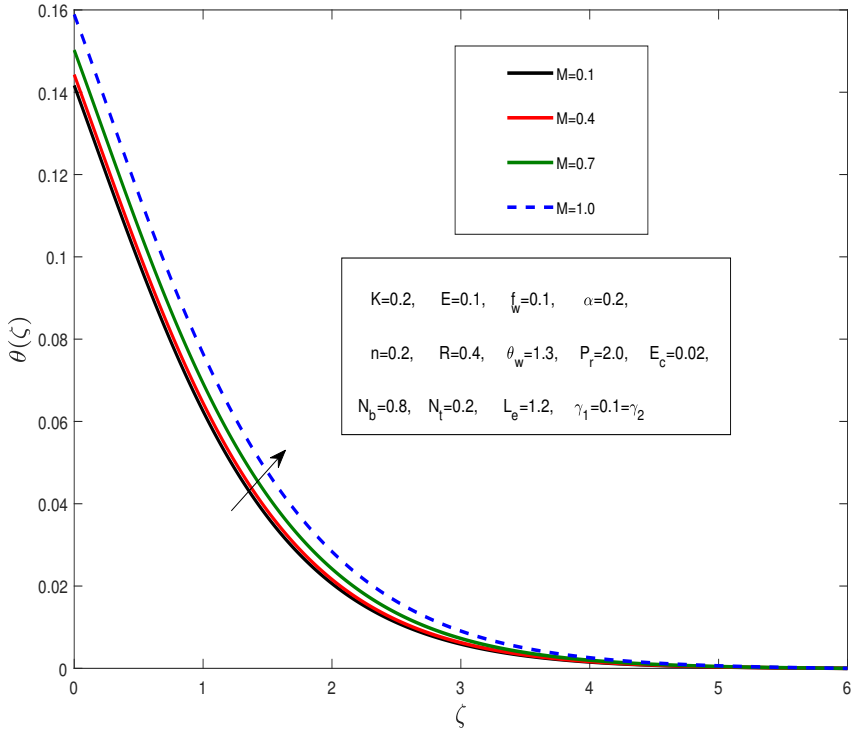

FIGURE 3.7: Influence of M on $\theta(\zeta)$.

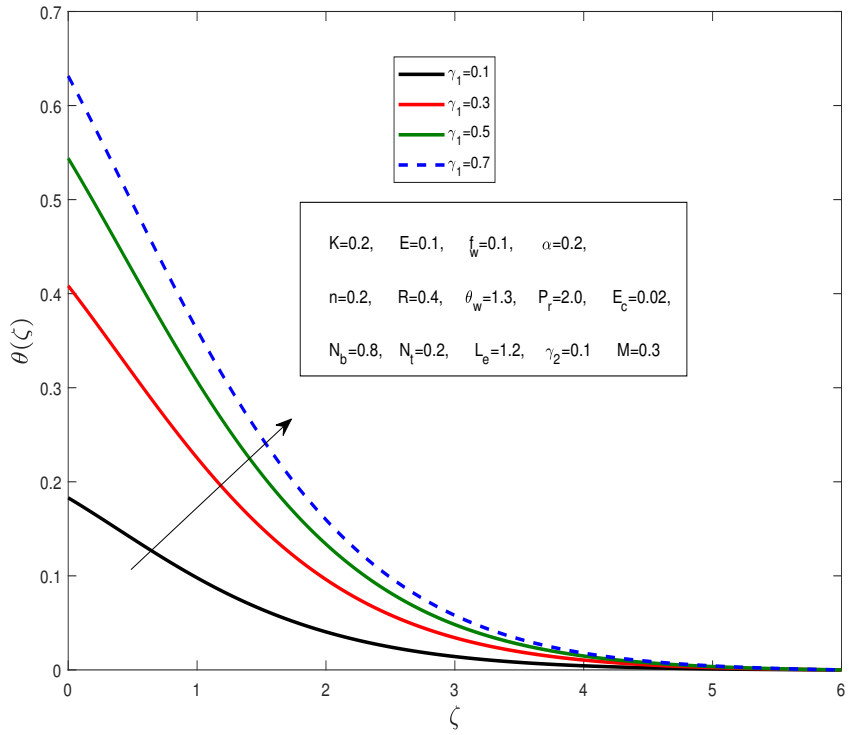

FIGURE 3.8: Influence of γ_1 on $\theta(\zeta)$.

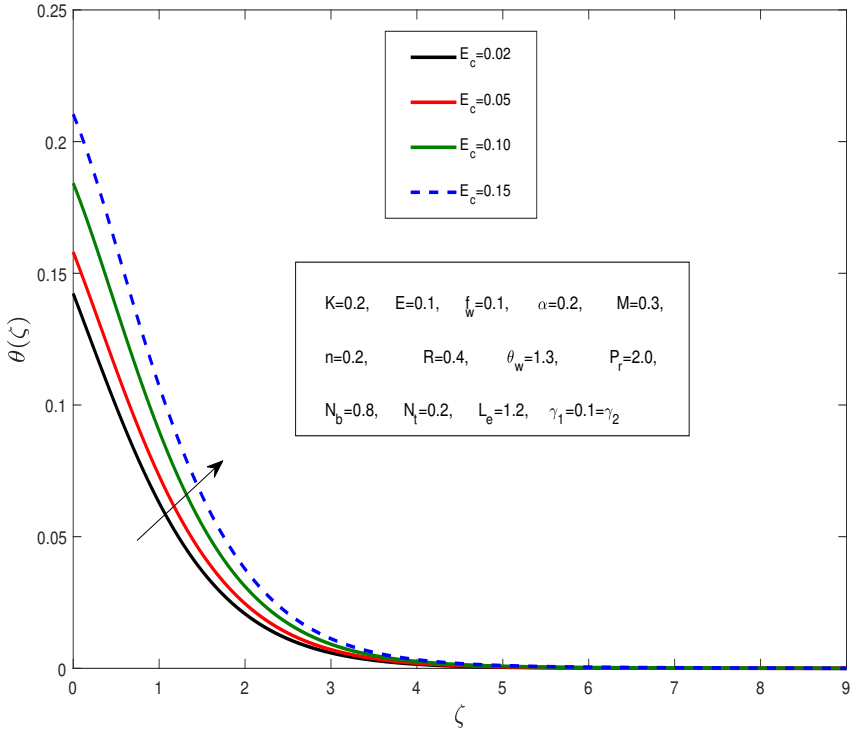

FIGURE 3.9: Influence of Ec on $\theta(\zeta)$.

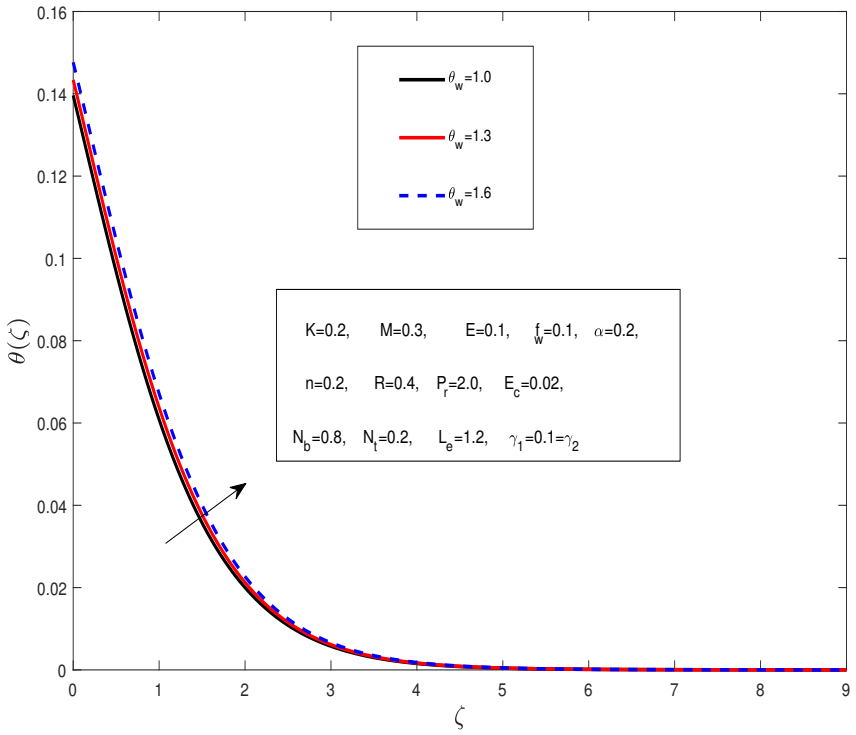

FIGURE 3.10: Influence of θ_w on $\theta(\zeta)$.

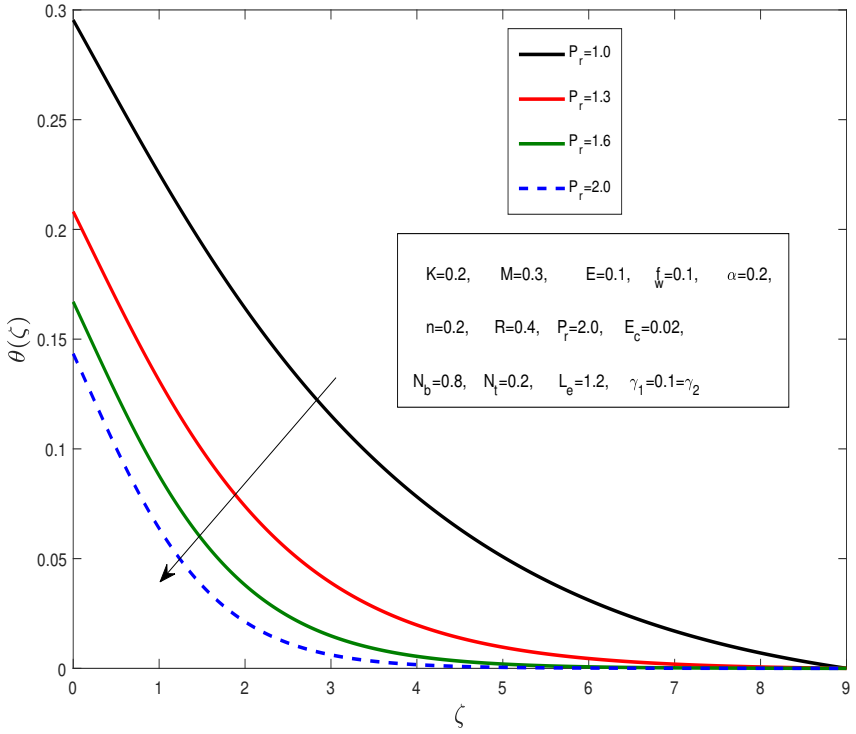

FIGURE 3.11: Influence of P_r on $\theta(\zeta)$.

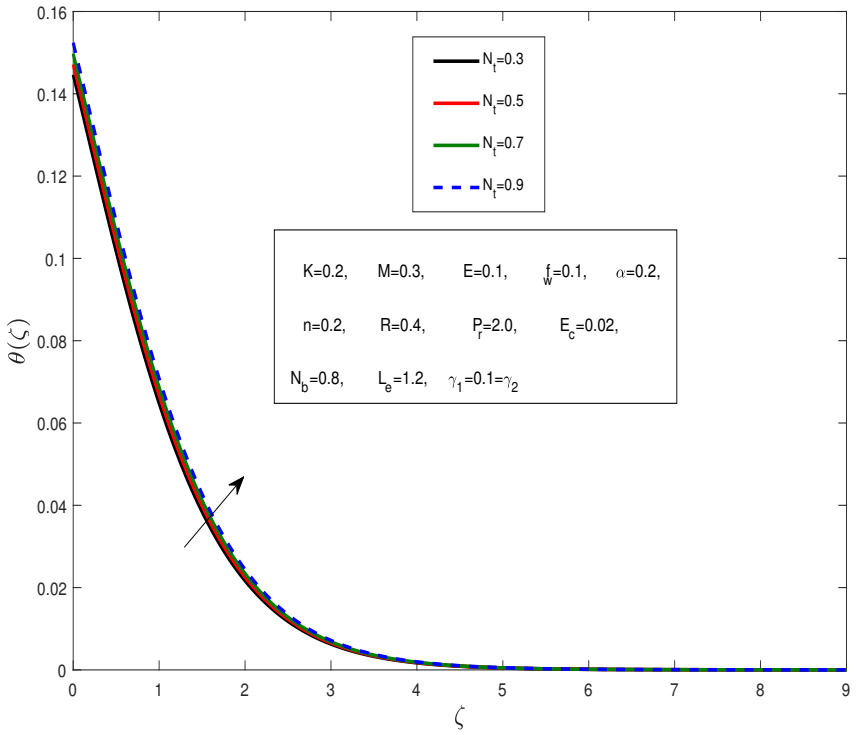

FIGURE 3.12: Influence of Nt on $\theta(\zeta)$.

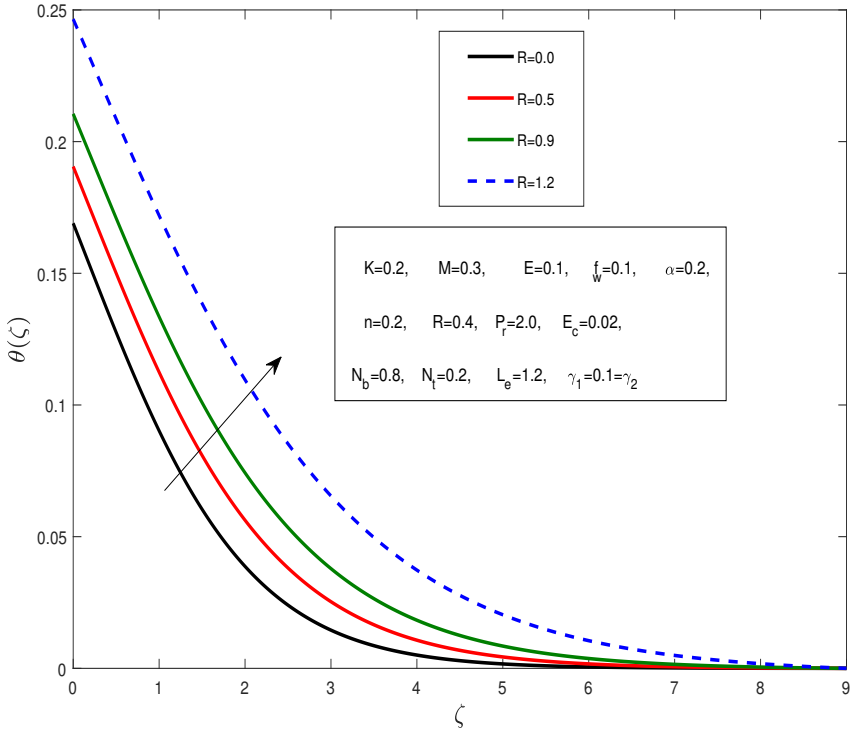

FIGURE 3.13: Influence of R on $\theta(\zeta)$.

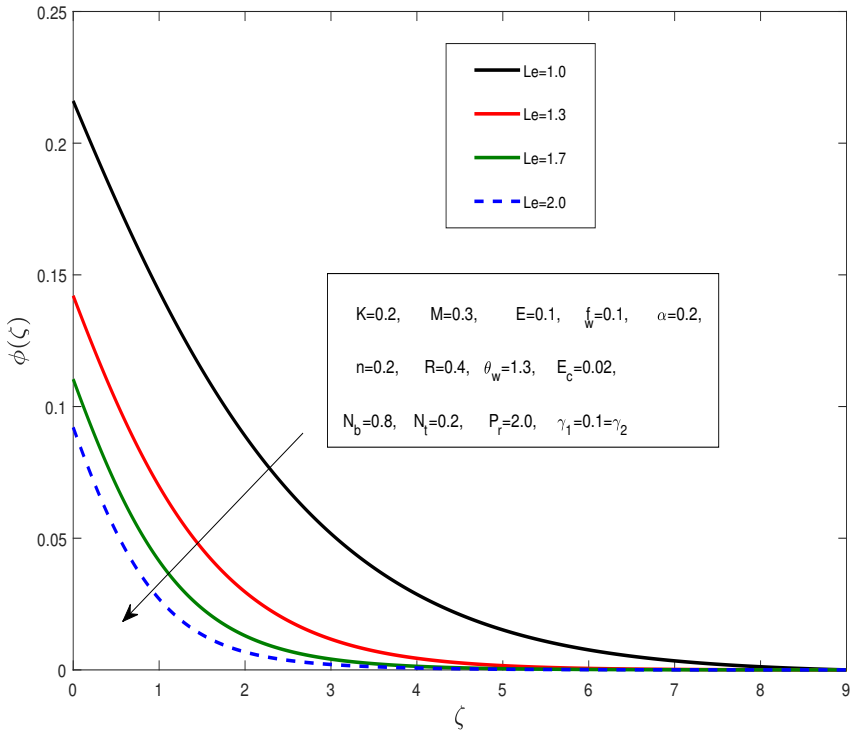

FIGURE 3.14: Influence of L_e on $\phi(\zeta)$.

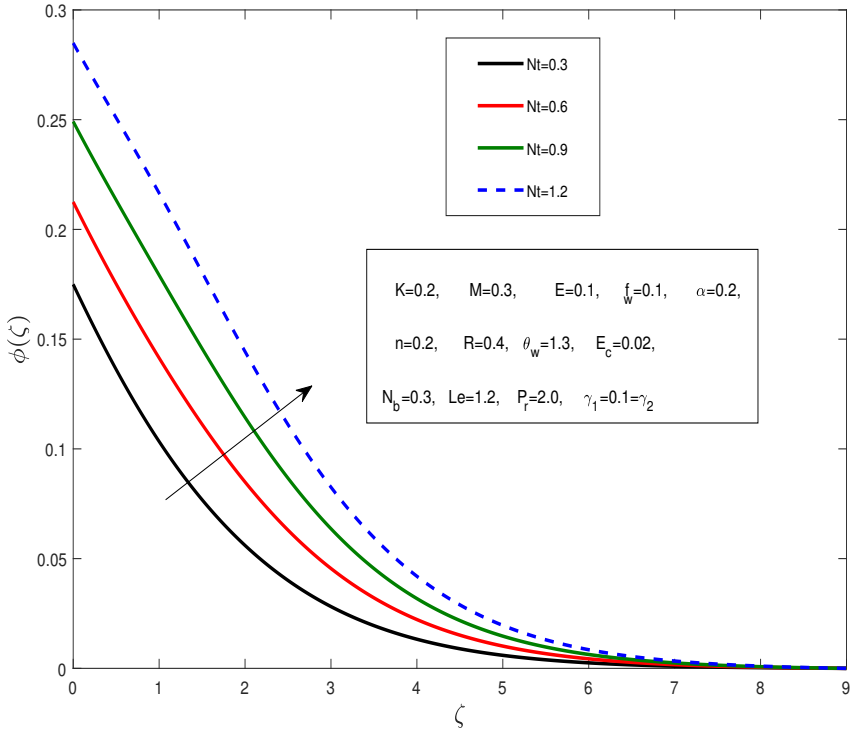

FIGURE 3.15: Influence of Nt on $\phi(\zeta)$.

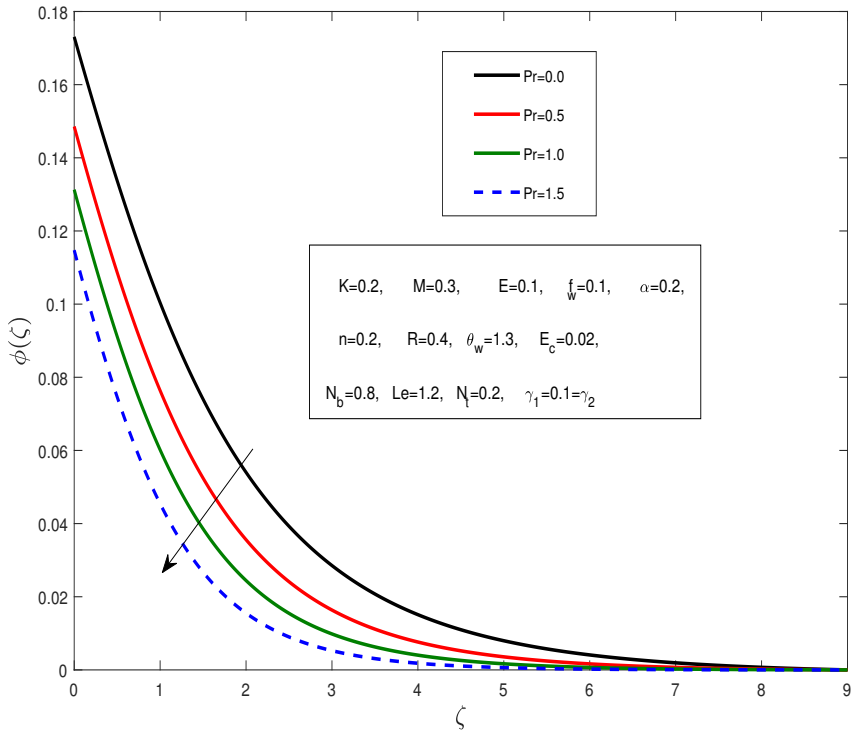

FIGURE 3.16: Influence of P_r on $\phi(\zeta)$.

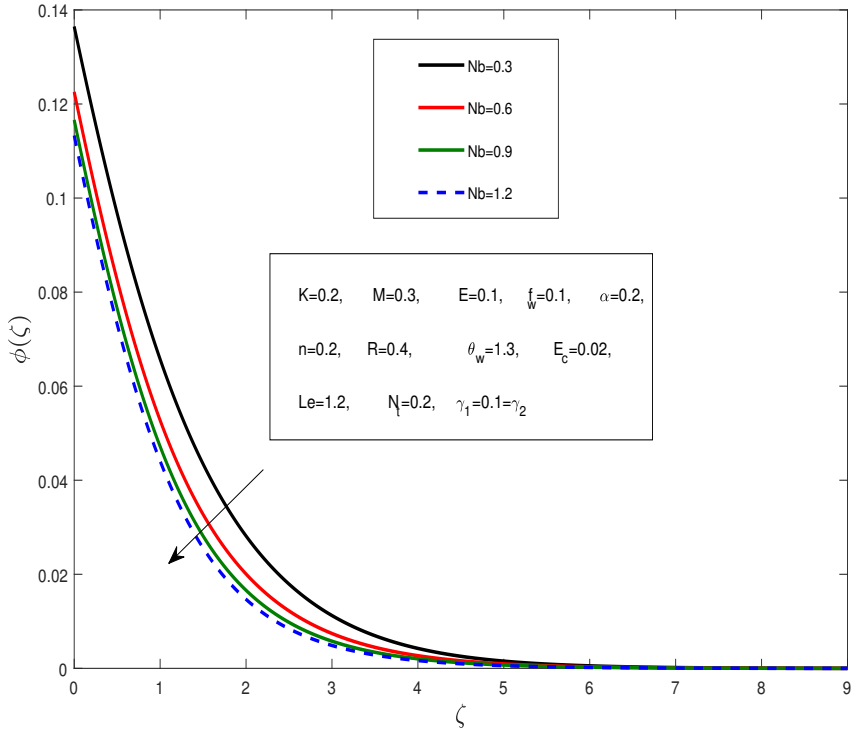

FIGURE 3.17: Influence of Nb on $\phi(\zeta)$.

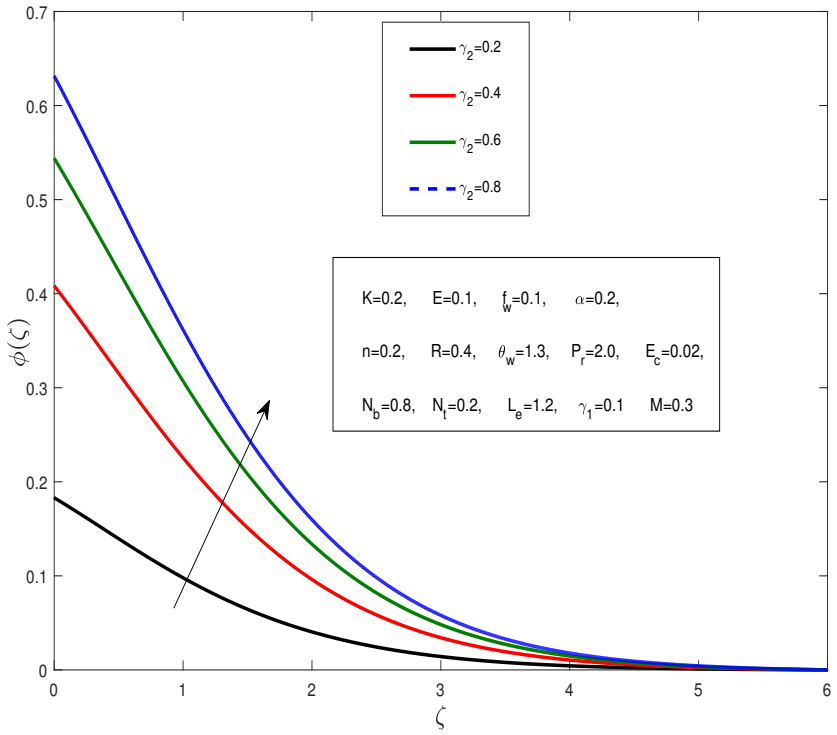

FIGURE 3.18: Influence of γ_2 on $\phi(\zeta)$.

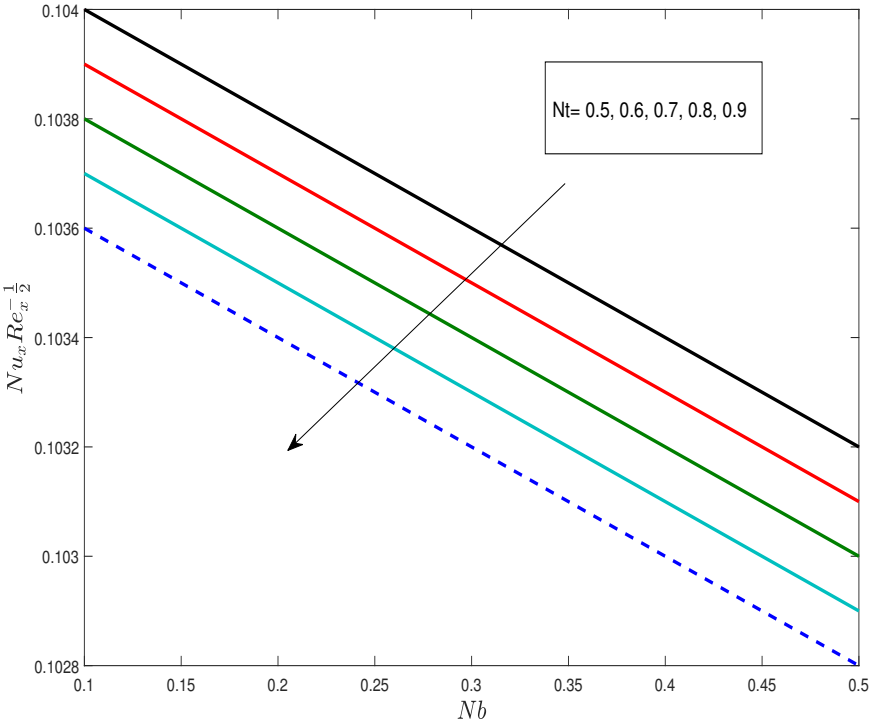

FIGURE 3.19: Influence of Nt *and* Nb on $Nu_x Re_x{}^{-\frac{1}{2}}$.

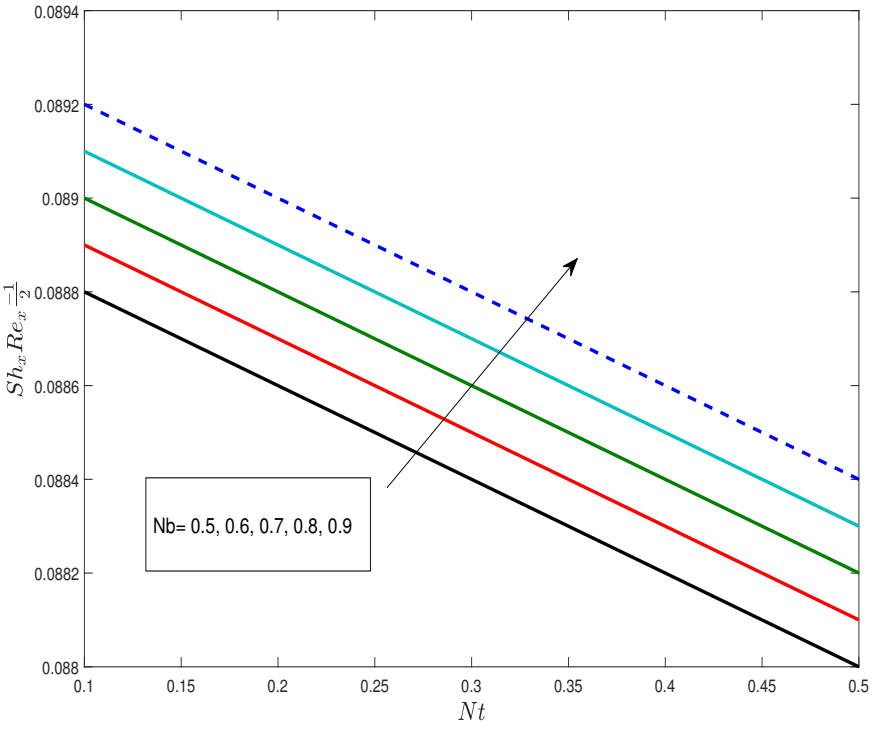

FIGURE 3.20: Influence of Nt *and* Nb on the $Sh_x Re_x{}^{-\frac{1}{2}}$.

Chapter 4

The Cattaneo-Christov double diffusion model analysis of EMHD micropolar fluid flow using nonlinear thermal radiation

4.1 Introduction

In this chapter, we extend the flow model discussed in Chapter 3 by including the impacts of Cattaneo-Christov double diffusion. The reduced system of ODEs after applying a proper similarity transform is solved numerically. Graphs and tables describe the behavior of physical quantities such as, Pr, Nb, Nt, Ec, Le, M, and R etc. Numerical values of skin friction coefficient, Nusselt number and Sherwood number have also been computed and discussed in this chapter. Tables and graphs are used to investigate the numerical results produced.

4.2 Problem Formulation

The set of equations describing the flow are as follows:

$$\frac{\partial u}{\partial x}+\frac{\partial v}{\partial y}=0, \tag{4.1}$$

$$u\frac{\partial u}{\partial x}+v\frac{\partial u}{\partial y}=\left(\frac{\mu+k}{\rho}\right)\frac{\partial^2 u}{\partial^2 y}+\frac{k}{\rho}\frac{\partial G}{\partial y}+\frac{\sigma}{\rho}\left(E_0B_0-B_0^2u\right), \tag{4.2}$$

$$u\frac{\partial G}{\partial x}+v\frac{\partial G}{\partial y}=\frac{\gamma^*}{\rho j}\frac{\partial^2 G}{\partial^2 y}-\frac{k}{\rho j}\left(2G+\frac{\partial u}{\partial y}\right), \tag{4.3}$$

$$\begin{aligned}u\frac{\partial T}{\partial x}+v\frac{\partial T}{\partial y}+\lambda_T\Bigg[&u\frac{\partial u}{\partial x}\frac{\partial T}{\partial x}+v\frac{\partial v}{\partial y}\frac{\partial T}{\partial y}+u\frac{\partial v}{\partial x}\frac{\partial T}{\partial y}+v\frac{\partial u}{\partial y}\frac{\partial T}{\partial x}+2uv\frac{\partial^2 T}{\partial x\partial y}\\&+u^2\frac{\partial^2 T}{\partial x^2}+v^2\frac{\partial^2 T}{\partial y^2}\Bigg]=\frac{k}{\rho C_p}\left(\frac{\partial^2 T}{\partial^2 y}\right)+\frac{(uB_0-E_0)^2\,\sigma}{\rho C_p}-\frac{1}{\rho C_p}\frac{\partial q_r}{\partial y},\\&+\left(\frac{\mu+k}{\rho C_p}\right)\left(\frac{\partial u}{\partial y}\right)^2+\tau\left[D_B\frac{\partial T}{\partial y}\frac{\partial C}{\partial y}+\frac{D_T}{T_\infty}\left(\frac{\partial T}{\partial y}\right)^2\right],\end{aligned} \tag{4.4}$$

$$\begin{aligned}u\frac{\partial C}{\partial x}+v\frac{\partial C}{\partial y}+\lambda_C\Bigg[&u\frac{\partial u}{\partial x}\frac{\partial C}{\partial x}+v\frac{\partial v}{\partial y}\frac{\partial C}{\partial y}+u\frac{\partial v}{\partial x}\frac{\partial C}{\partial y}+v\frac{\partial u}{\partial y}\frac{\partial C}{\partial x}+2uv\frac{\partial^2 C}{\partial x\partial y}\\&+u^2\frac{\partial^2 C}{\partial x^2}+v^2\frac{\partial^2 C}{\partial y^2}\Bigg]=D_B\frac{\partial^2 C}{\partial^2 y}+\frac{D_T}{T_\infty}\frac{\partial^2 T}{\partial^2 y}.\end{aligned} \tag{4.5}$$

The aformentioned set of equations corresponding boundary conditions are

$$\left.\begin{aligned}&u=ax+\alpha^*\left[(\mu+k)\frac{\partial u}{\partial y}+kG\right],\quad v=v_w,\\&G=-\zeta\frac{\partial u}{\partial y},\quad -k\left(\frac{\partial T}{\partial y}\right)=h_{ft}\left(T_f-T\right),\\&-D_B\frac{\partial C}{\partial y}=h_{fc}\left(C_f-C\right)\qquad at\quad y=0,\\&u\to 0,\ G\to 0,\ T\to T_\infty,\ C\to C_\infty\ as\ y\to\infty.\end{aligned}\right\} \tag{4.6}$$

4.3 Conversion of the Model

In this section, we convert the system of equations (4.1)-(4.5) along with the boundary conditions (4.6) into a unitless form. The following similarity transformation is employed

$$\left.\begin{aligned}&\zeta=\sqrt{\frac{a}{v}},\quad G=ax\sqrt{\frac{a}{v}}h(\zeta),\quad u=axf'(\zeta),\quad v=-\sqrt{av}f(\zeta),\\&\theta(\zeta)=\frac{T-T_\infty}{T_f-T_\infty},\quad \phi(\zeta)=\frac{C-C_\infty}{C_f-C_\infty}.\end{aligned}\right\} \tag{4.7}$$

In the above discussions K, M, f_w, P_r, α, E, R, E_c, N_t, N_b and L_e are the material parameter, Hartman number, Suction/injection parameter, Prandtl number, slip parameter, electric parameter, radiation parameter, Eckert number, thermophoresis parameter, Brownian motion parameter and Lewis number respectively. These quantities are written as follows:

$$\left.\begin{aligned} &K=\frac{k}{\mu},\quad M^2=\frac{\sigma B_0^2}{\rho a},\quad f_w=-(av)^{\frac{-1}{2}}v_w,\quad P_r=\frac{\mu C_p}{k},\\ &\alpha=\alpha^*\mu\sqrt{\frac{a}{v}},\quad E=\frac{E_0}{\mu_w B_0},\quad R=\frac{4\sigma^* T_\infty^3}{k^* k_1},\quad E_c=\frac{u_w^2}{C_p\left(T_f-T_\infty\right)},\\ &N_t=\frac{\tau D_T}{vT_\infty}\left(T_f-T_\infty\right),\quad N_b=\frac{\tau}{v}D_B\left(C_f-C_\infty\right),\quad L_e=\frac{\alpha}{D_B},\\ &\gamma_2=\frac{h_{fc}}{D_B}\sqrt{\frac{v}{a}},\quad \gamma_1=\frac{h_{ft}}{k}\sqrt{\frac{v}{a}},\quad Re_x^2=\frac{ax}{v},\quad \theta_w=\frac{T_f}{T_\infty}. \end{aligned}\right\}$$

The complete process for converting equation (4.1)-(4.3), is the same as presented in Chapter 3. The entire procedure for converting (4.4) into the dimensionless form has been discussed below

$$\frac{\partial T}{\partial x}=0. \tag{4.8}$$

$$u\frac{\partial u}{\partial x}+v\frac{\partial u}{\partial y}=a^2x\left[\left(f'(\zeta)^2\right)-f(\zeta)f''(\zeta)\right]. \tag{4.9}$$

Multiplying (4.8) and (4.9), we get

$$\left(u\frac{\partial u}{\partial x}+v\frac{\partial u}{\partial y}\right)\frac{\partial T}{\partial x}=0. \tag{4.10}$$

$$u\frac{\partial v}{\partial x}+v\frac{\partial v}{\partial y}=a^{\frac{3}{2}}v^{\frac{1}{2}}f(\zeta)f'(\zeta) \tag{4.11}$$

.

$$\frac{\partial T}{\partial y}=\left(T_f-T_\infty\right)\sqrt{\frac{a}{v}}\theta'(\zeta). \tag{4.12}$$

Multiplying (4.11) and (4.12), we get

$$\left(u\frac{\partial v}{\partial x}+v\frac{\partial v}{\partial y}\right)\frac{\partial T}{\partial y}=a^2\left(T_f-T_\infty\right)(\zeta)f'(\zeta)\theta'(\zeta). \tag{4.13}$$

$$u^2\frac{\partial^2 T}{\partial x^2}=0. \tag{4.14}$$

$$v^2\frac{\partial^2 T}{\partial y^2} = a^2\left(T_f - T_\infty\right) f^2(\zeta)\theta''(\zeta). \tag{4.15}$$

$$2uv\frac{\partial}{\partial x}\left(\frac{\partial T}{\partial y}\right) = 2\left(axf'(\zeta)\right)\left(-\sqrt{av}f(\zeta)\right)\frac{\partial}{\partial x}\left(\left(T_f - T_\infty\right)\sqrt{\frac{a}{v}}\theta'(\zeta)\right)$$

$$2uv\frac{\partial}{\partial x}\left(\frac{\partial T}{\partial y}\right) = 0. \tag{4.16}$$

By adding (4.10),(4.13),(4.14),(4.15),(4.16) we get

$$\begin{aligned}
&\lambda_1\left[\left(u\frac{\partial u}{\partial x}+v\frac{\partial u}{\partial y}\right)\frac{\partial T}{\partial x}+\left(u\frac{\partial v}{\partial x}+v\frac{\partial v}{\partial y}\right)\frac{\partial T}{\partial y}+u^2\frac{\partial^2 T}{\partial x^2}+v^2\frac{\partial^2 T}{\partial y^2}+2uv\frac{\partial^2 T}{\partial x\partial y}\right]\\
&=\lambda_1\left[a^2\left(T_f-T_\infty\right)f(\zeta)f'(\zeta)\theta'(\zeta)+a^2\left(T_f-T_\infty\right)f^2(\zeta)\theta''(\zeta)\right]\\
&=\lambda_1 a^2\left(T_f-T_\infty\right)\left[f(\zeta)f'(\zeta)\theta'(\zeta)+f^2(\zeta)\theta''(\zeta)\right]\\
&=\lambda_T\left[f(\zeta)f'(\zeta)\theta'(\zeta)+f^2(\zeta)\theta''(\zeta)\right].
\end{aligned} \tag{4.17}$$

By utilizing (4.17), the extended dimensionless form of the energy equation becomes:

$$\begin{aligned}
&\theta''(\zeta)\left[1+\frac{4R}{3}\left(\left(\theta_w-1\right)\theta(\zeta)+1\right)^3+\lambda_T\ f^2(\zeta)\right]\\
&\quad+P_r\theta'(\zeta)f(\zeta)+\lambda_T\theta'(\zeta)f(\zeta)f'(\zeta)+P_rE_cM^2\left(f'^2(\eta)+E^2-2Ef'(\zeta)\right)\\
&\quad+4R\left(\left(\theta_w-1\right)\theta(\zeta)+1\right)^2\left(\theta_w-1\right)\theta'^2(\zeta)+\left(1+K\right)E_cP_r\left(f''(\zeta)\right)^2\\
&\quad+P_r\left[N_b\theta'(\zeta)\phi'(\eta)+N_t\theta'^2(\zeta)\right]=0.\\
\Rightarrow\ &\theta''(\zeta)\left[1+\frac{4R}{3}\left(\left(\theta_w-1\right)\theta(\zeta)+1\right)^3+\lambda_T\ f^2(\zeta)\right]\\
&\quad+\theta'(\zeta)\left[P_rf(\zeta)+\lambda_Tf(\zeta)f'(\zeta)+4R\left(\left(\theta_w-1\right)\theta(\zeta)+1\right)^2\left(\theta_w-1\right)\theta'(\zeta)\right]\\
&\quad+P_rE_cM^2\left(f'^2(\zeta)+E^2-2Ef'(\zeta)\right)+\left(1+K\right)E_cP_r\left(f''(\zeta)\right)^2\\
&\quad+P_r\left[N_b\theta'(\zeta)\phi'(\zeta)+N_t\theta'^2(\zeta)\right]=0.
\end{aligned} \tag{4.18}$$

$$\begin{aligned}
\theta''(\zeta)=&\frac{-1}{\left[1+\frac{4R}{3}\left(\left(\theta_w-1\right)\theta(\zeta)+1\right)^3+\lambda_T\ f^2(\zeta)\right]}\theta'(\zeta)\Big[P_rf(\zeta)+\lambda_Tf(\zeta)f'(\zeta)\\
&+4R\left(\left(\theta_w-1\right)\theta(\zeta)+1\right)^2\left(\theta_w-1\right)\theta'(\zeta)\Big]+P_rE_cM^2\left(f'^2(\zeta)+E^2\right.
\end{aligned}$$

$$-2Ef'(\zeta)+(1+K)\,E_cP_r\,(f''(\zeta))^2+P_r\left[N_b\theta'(\zeta)\phi'(\zeta)+N_t\theta'^2(\zeta)\right]=0. \tag{4.19}$$

As we have Cattaneo-Christov diffusion model in (4.4), that's why the new parameter arises which is given below:

$$\lambda_t=a^2\,(T_f-T_\infty)\,\lambda_1,$$

where λ_t is Cattaneo-Christov temperature parameter.

The entire procedure for converting (4.5) into the dimensionless form has been discussed below

$$\frac{\partial C}{\partial x}=0. \tag{4.20}$$

$$u\frac{\partial u}{\partial x}+v\frac{\partial u}{\partial y}=a^2x\left[\left(f'(\zeta)^2\right)-f(\zeta)f''(\zeta)\right]. \tag{4.21}$$

Multiplying (4.20) and (4.21), we get

$$\left(u\frac{\partial v}{\partial x}+v\frac{\partial v}{\partial y}\right)\frac{\partial C}{\partial x}=0. \tag{4.22}$$

$$\frac{\partial C}{\partial y}=\sqrt{\frac{a}{v}}\,(C_f-C_\infty)\,\phi''(\zeta). \tag{4.23}$$

$$u\frac{\partial v}{\partial x}+v\frac{\partial v}{\partial y}=a^{\frac{3}{2}}v^{\frac{1}{2}}f(\zeta)f'(\zeta). \tag{4.24}$$

Multiplying (4.23) and (4.24), we get

$$\left(u\frac{\partial v}{\partial x}+v\frac{\partial v}{\partial y}\right)\frac{\partial C}{\partial y}=a^2\,(C_f-C_\infty)\,f(\zeta)f'(\zeta)\phi'(\zeta). \tag{4.25}$$

$$u^2\frac{\partial^2 C}{\partial x^2}=0. \tag{4.26}$$

$$v^2\frac{\partial^2 C}{\partial y^2}=a^2\,(C_f-C_\infty)\,f^2(\zeta)\phi''(\zeta). \tag{4.27}$$

$$2uv\frac{\partial}{\partial x}\left(\frac{\partial C}{\partial y}\right)=2\,(axf'(\eta))\left(-\sqrt{av}f(\zeta)\right)\frac{\partial}{\partial x}\left((C_f-C_\infty)\sqrt{\frac{a}{v}}\phi''(\zeta)\right)$$

$$2uv\frac{\partial^2 C}{\partial x\partial y}=0. \tag{4.28}$$

By adding (4.22),(4.25),(4.26),(4.27),(4.28) we get

$$\lambda_2\Bigg[\left(u\frac{\partial u}{\partial x}+v\frac{\partial u}{\partial y}\right)\frac{\partial C}{\partial x}+\left(u\frac{\partial v}{\partial x}+v\frac{\partial v}{\partial y}\right)\frac{\partial C}{\partial y}+u^2\frac{\partial^2 C}{\partial x^2}+v^2\frac{\partial^2 C}{\partial y^2}+2uv\frac{\partial^2 C}{\partial x\partial y}\Bigg].$$
$$=\lambda_2\Big[a^2\left(C_f-_\infty\right)f(\zeta)f'(\zeta)\phi'(\zeta)+a^2\left(C_f-C_\infty\right)f^2(\zeta)\phi''(\zeta)\Big]$$
$$=\lambda_2 a^2\left(C_f-C_\infty\right)\Big[f(\zeta)f'(\zeta)\phi'(\zeta)+f^2(\zeta)\phi''(\zeta)\Big]$$
$$=\lambda_C\Big[f(\zeta)f'(\zeta)\phi'(\zeta)+f^2(\zeta)\phi''(\zeta)\Big]. \tag{4.29}$$

By utilizing (4.29), the extended dimensionless form becomes

$$\phi''(\zeta)\left(1+\lambda_C f^2(\zeta)\right)+\phi'(\zeta)\left(\lambda_C f(\zeta)f'(\zeta)\right)+P_rL_ef+\frac{N_t}{N_b}\theta''=0.$$
$$\Rightarrow\phi''(\zeta)=\frac{-1}{\left(1+\lambda_C f^2(\zeta)\right)}\Big[\phi'(\zeta)\left(\lambda_C f(\zeta)f'(\zeta)\right)+P_rL_ef+\frac{N_t}{N_b}\theta''\Big]. \tag{4.30}$$

As, we have used Cattaneo-Christtov diffusion model in (4.5) that's why the new parameter arises which is gievn below:

$$\lambda_C=a\left(C_f-C_\infty\right)\lambda_2,$$

where λ_c is Cattaneo-Christov temperature parameter.

The dimentionless form of the proposed flow model is:

$$f'''=\frac{1}{(1+K)}\left[f'^2-ff''+M^2f'-Kh'-M^2E\right], \tag{4.31}$$
$$\theta''(\eta)=\frac{-1}{\left[1+\frac{4R}{3}\left(\left(\theta_w-1\right)\theta(\zeta)+1\right)^3+\lambda_T\ f^2(\zeta)\right]}\theta'(\zeta)\Big[P_rf(\zeta)$$
$$+\lambda_Tf(\zeta)f'(\zeta)+4R\left(\left(\theta_w-1\right)\theta(\zeta)+1\right)^2\left(\theta_w-1\right)\theta'(\zeta)\Big]+P_rE_cM^2$$
$$\left(f'^2(\zeta)+E^2-2Ef'(\zeta)\right)(1+K)E_cP_r\left(f''(\zeta)\right)^2+P_r\left[N_b\theta'(\zeta)\phi'(\zeta)\right.$$
$$\left.+N_t\theta'^2(\zeta)=0,\right. \tag{4.32}$$
$$\phi''(\zeta)=\frac{-1}{\left(1+\lambda_C f^2(\zeta)\right)}\Big[\phi'(\zeta)\left(\lambda_C f(\zeta)f'(\zeta)\right)+P_rL_ef+\frac{N_t}{N_b}\theta''\Big]. \tag{4.33}$$

Now,

The dimensionless boundary conditions are as follows:

$$\left.\begin{aligned} &f(0) = f_w,\ f'(0) = 1 + \alpha\left(1 + K\left(1 - n\right)\right) f''(0),\ h(0) = -nf''(0), \\ &\phi'(0) = -\gamma_2\left(1 - \phi(0)\right),\ \theta'(0) = -\gamma_1\left(1 - \theta(0)\right), \quad at\ \ y = 0 \\ &f'(y) \to\ 0, h(y) \to\ 0, \phi(y) \to\ 0, \theta(y) \to\ 0,\ as\ y \to\ \infty. \end{aligned}\right\} \tag{4.34}$$

The complete discussion in order to get the expression for dimensionless form of skin friction coefficient, Nusselt number and Sherwood number has been discussed in chapter 3.

4.4 Solution Methodology

For solving (4.34) and (4.33) with the associated boundary conditions (3.42), we use the shooting method. First of all, we need to convert these equations into a system of first order differential equations.

Let us use the following notations.

$$\theta(\zeta) = W_1, \qquad \theta'(\zeta) = W_1' = W_2, \qquad \theta''(\zeta) = W_1'' = W_2',$$
$$\phi(\zeta) = W_3, \qquad \phi'(\eta) = W_3' = W_4, \qquad \phi''(\zeta) = W_3'' = W_4'.$$
$$A_1 = \theta_w - 1, \qquad A_2 = 1 + A_1 W_1,$$
$$Z_1 = \frac{1}{\left[1 + \lambda_t f^2 + \frac{4}{3} R A_2^3\right]},$$
$$Z_2 = M^2 E_c P_r \left(f'^2 + E^2 - 2Ef'\right) + \left(1 + K\right)\left(f''^2\right) + 4RA_1 A_2^2 W_2^2$$
$$+ Pr\left(f + \lambda_t f' f'' + N_b \phi' + N_t \theta'\right),$$
$$Z_3 = \frac{4RA_1 A_2^2 W_5}{(Z_1)^2},$$

$$Z_4 = 8RA_1 A_2^2 W_2 W_6 + 8RA_1^2 A_2 W_2^2 W_5 + P_r W_6\left(f + \lambda_t f' f''\right.$$

$$\left. + N_b W_4 + N_t W_2 + Pr W_2\left(N_b W_8 + N_t W_6\right).\right.$$

$$Z_5 = \frac{4RA_1A_2^2W_9}{(Z_1)^2},$$

$$Z_6 = 8RA_1A_2^2W_2W_{10} + 8RA_1^2A_2W_2^2W_9 + P_rW_{10}\left(f + \lambda_t f' f'' + N_bW_4 + N_tW_2\right) + PrW_2\left(N_bW_{12} + N_tW_{10}\right).$$

As a result, the coupled ODEs are converted into the following system of Ist order differential equation

$$\left.\begin{aligned} W_1' &= W_2, & W_1(0) &= s,\\ W_2' &= Z_1 * Z_2, & Z_2(0) &= -\gamma_1\left(1-s\right),\\ W_3' &= W_4, & W_3(0) &= t,\\ W_4' &= \frac{-1}{(1+\lambda_t f^2)}\Big[W_4\left(L_eP_rf + \lambda_t f' f''\right) & & \\ &\quad + (Nt/Nb) * (Z1 * Z2)\Big]. & W_4(0) &= -\gamma_2\left(1-t\right). \end{aligned}\right\} \tag{4.35}$$

The above initial value problem has been solved by using the RK-4 method. The missing conditions s and t are choosen very carefully, so that the following conditions must hold

$$(W_1(s,t))_{\zeta=\zeta_\infty} = 0, \qquad (W_3(s,t))_{\zeta=\zeta_\infty} = 0. \tag{4.36}$$

To solve the above algebaric equations, we apply the Newton's method which has the following scheme

$$\begin{bmatrix} s \\ t \end{bmatrix}_{n+1} = \begin{bmatrix} s \\ t \end{bmatrix}_{n} - \begin{bmatrix} \frac{\partial W_1(s,t)}{\partial s} & \frac{\partial W_1(s,t)}{\partial t} \\ \frac{\partial W_3(s,t)}{\partial s} & \frac{\partial W_3(s,t)}{\partial t} \end{bmatrix}_n^{-1} \cdot \begin{bmatrix} W_1 \\ W_3 \end{bmatrix}_n$$

Now, introduce the following notations

$$\frac{\partial W_1}{\partial s} = W_5, \quad \frac{\partial W_2}{\partial s} = W_6, \quad \frac{\partial W_3}{\partial s} = W_7, \quad \frac{\partial W_4}{\partial s} = W_8,$$
$$\frac{\partial W_1}{\partial t} = W_9, \quad \frac{\partial W_2}{\partial t} = W_{10}, \quad \frac{\partial W_3}{\partial t} = W_{11}, \quad \frac{\partial W_4}{\partial t} = W_{12}.$$

Now,

As a result of these new notations, the Newton's iterative scheme gets the form

$$\begin{bmatrix} s \\ t \end{bmatrix}_{n+1} = \begin{bmatrix} s \\ t \end{bmatrix}_{n} - \begin{bmatrix} W_5 & W_9 \\ W_7 & W_{11} \end{bmatrix}_{n}^{-1} \cdot \begin{bmatrix} W_1 \\ W_3 \end{bmatrix}_{n}$$

Now, we will get another system of eight 1st order ODE's after differentiaiting the above system of four ODE's of 1st order w.r.t to s and t

$$\begin{aligned}
&W_5' = W_6, && W_5(0) = 0,\\
&W_6' = Z_1 * Z_4 + Z_3 * Z_2, && W_6(0) = \gamma_1,\\
&W_7' = W_8, && W_7(0) = 0,\\
&W_8' = \frac{-1}{(1+\lambda_T f^2)}\Big[W_6\left(L_e P_r f + \lambda_t f' f''\right)\\
&\qquad + (Nt/Nb) * (Z_1 * Z_4 + Z_3 * Z_2)\Big], && W_8(0) = 0,\\
&W_9' = W_{10}, && W_9(0) = 0,\\
&W_{10}' = Z_1 * Z_6 + Z_5 * Z_2, && W_{10}(0) = 0,\\
&W_{11}' = W_{12}, && W_{11}(0) = 1,\\
&W_{12}' = \frac{-1}{(1+\lambda_T f^2)}\Big[W_{12}\left(L_e P_r f + \lambda_t f' f''\right)\\
&\qquad + (Nt/Nb) * (Z_1 * Z_4 + Z_3 * Z_2)\Big]. && W_{12}(0) = \gamma_2.
\end{aligned}$$

The stopping criteria for the Newton's method is set as:

$$\max \mid W_1(\zeta_\infty), W_3(\zeta_\infty) \mid < \epsilon.$$

where ϵ is a small positive real number.

4.5 Results and Discussion

The numerical results of the equations in the preceding sections will be discussed through the graphs and tables in this section. Various important parameters, such as the material parameter K, suction/injection parameter f_w, magnetic parameter M, Prandtl number Pr, radiation parameter R, Lewis number Le, Brownian motion parameter Nb, thermophoresis parameter Nt, Cattaneo-Christov temperature parameter λ_t, Cattaneo-Christov concentration parameter λ_c, thermal Biot number γ_1, and solutal Biot number γ_2, are taken into account when performing numerical calculations. These parameters have a direct influence on the distribution of velocity, temperature and concentration. Table 4.1 and 4.2 discuss the effect of significant characteristics of the local Nusselt number $Nu(Re_x)^{-\frac{1}{2}}$ and Sherwood number $Sh(Re_x)^{-\frac{1}{2}}$. The local Nusselt number and Sherwood number fall by enlarging the Eckert number Ec, and the thermophoresis parameter Nt. The local Nusselt number and Sherwood number mount while enlarging the radiation parameter R, temperature ratio parameter θ_w, Prandtl number Pr and Lewis number Le. In this table, I_θ and I_ϕ are the intervals from which the missing conditions θ and ϕ can be chosen.

The effect of slip parameter α on the temperature profile $\theta(\zeta)$ is presented in Figure 4.1. By rising the values of the slip parameter α, the temperature profile $\theta(\zeta)$ shows an increasing behaviour. The impact of the suction parameter f_w on the temperature profile $\theta(\zeta)$ is presented in Figure 4.2. By increasing the values of the suction parameter f_w, the temperature profile $\theta'(\zeta)$ is found to increase. The impact of the material parameter K on the temperature profile $\theta(\zeta)$ is presented in Figure 4.3. Increasing the values of the material parameter K reduces the temperature profile $\theta(\zeta)$. Figure 4.4 represents the impact of the Hartman number M on the temperature profile $\theta(\zeta)$. Temperature rises when the Hartman number M is increased, as shown in Figure.

Figure 4.5 displays the influence of Cattaneo-Christov temperature parameter λ_t on the temperature profile $\theta(\zeta)$. Temperature profile decreases when the Cattaneo-Christov temperature parameter λ_t is increased. Figure 4.6 depicts the effect of

the thermophoresis parameter Nt on the temperature profile $\theta(\zeta)$. For the increasing values of the thermophoresis parameter, it is obvious that the thermal boundary layer thickness and temperature are increased. Figure 4.7 depicts the effect of the Prandtl number Pr on the temperature profile $\theta(\zeta)$. The temperature of the fluid decreases as the Prandtl number increases due to a thinner boundary layer thickness and reduced thermal diffusivity.

Figure 4.8 represents the impact of the Brownian motion parameter Nb on the temperature profile $\theta(\zeta)$. Temperature rises when the Brownian motion parameter Nb is increased, as shown in Figure. Figure 4.9 demonstrates the impact of the thermal Biot number γ_1 on the temperature profile $\theta(\zeta)$. We notice that the enhanced values of the thermal Biot number γ_1 cause a higher energy. Figure 4.10 depicts the effect of increasing Lewis number Le values on the concentration profile $\phi(\zeta)$. Because the Lewis number is the ratio of the kinematic viscosity oflorwhiteothe nanofluid to the Brownian diffusion coefficient, increasing the Lewis number leads to an increase in the viscosity of the fluid, which resists fluid motion and hence reduces the concentration of nanoparticles. Figure 4.11 depicts the effect of the thermophoresis parameter Nt on the temperature profile $\theta(\zeta)$.

Figure 4.12 displays the influence of Eckert number Ec on the concentration profile $\phi(\zeta)$. Concentration profile increases when the Eckert number is increased. Figure 4.13 displays the influence of Cattaneo-Christov concentration parameter λ_c on the temperature profile $\phi(\zeta)$. Temperature profile decreases when the Cattaneo-Christov concentration parameter λ_c is increased.

Figure 4.14 depicts how an increase in the Prandtl number Pr causes a reduction in the concentration profile $\phi(\zeta)$. As the Prandtl number increases, the thermal diusivity decreases, resulting in the low range temperature seen in Figure 4.14. The effect of Brownian motion parameter Nb on the concentration profile $\phi(\zeta)$ is presented in Figure 4.15. Increasing the values of the Brownian motion parameter reduces the concentration profile. Figure 4.16 shows the effect of solutal Biot number γ_2 on the concentration profile $\phi(\zeta)$. The concentration profiles are greatly improved for higher solutal Biot number values.

TABLE 4.1: Results of $Nu(Re_x)^{-\frac{1}{2}}$ *and* $Sh(Re_x)^{-\frac{1}{2}}$ when $K = 0.2$, $E = 0.2$, $M = 0.1$, $f_w = 0.1$, $\alpha = 1.4$, $n = 0.5$, $N_t = 0.2$, $L_e = 1.2$, $\gamma_1 = \gamma_2 = 0.1$

R	θ_w	P_r	E_c	N_b	λ_t	λ_c	$NuRe_x^{-\frac{1}{2}}$	$ShRe_x^{-\frac{1}{2}}$	I_θ	I_ϕ
0.3							0.11851	0.08672	[-0.3, 0.2]	[-0.3, 0.3]
0.4							0.11901	0.08673	[-0.3, 0.2]	[-0.3, 0.2]
0.5	1.3						0.11950	0.08674	[-0.3, 0.2]	[-0.4, 0.2]
0.1	1.4						0.12128	0.08675	[-0.2, 0.2]	[-0.5, 0.3]
	1.5						0.12264	0.08677	[-0.1, 0.2]	[-0.3, 0.3]
	1.6						0.12864	0.08878	[-0.3, 0.1]	[-0.2, 0.1]
		1.7					0.10762	0.08719	[-0.2, 0.1]	[-0.2, 0.1]
		1.8	0.1		0.1		0.10819	0.08764	[-0.2, 0.1]	[-0.2, 0.3]
		1.9	0.2		0.98		0.10906	0.08819	[-0.3, 0.2]	[-0.1, 0.3]
			0.3		0.96		0.10662	0.07833	[-0.1, 0.2]	[-0.1, 0.2]
			0.4	1.2	0.94	0.1	0.10653	0.06848	[-0.3, 0.4]	[-0.3, 0.2]
				1.3		0.98	0.10753	0.08615	[-0.5, 0.4]	[-0.3, 0.3]
				1.4		0.96	0.10766	0.08724	[-0.4, 0.3]	[-0.2, 0.2]
				1.5		0.94	0.10778	0.07812	[-0.3, 0.2]	[-0.2, 0.1]

TABLE 4.2: Results of $Nu(Re_x)^{-\frac{1}{2}}$ *and* $Sh(Re_x)^{-\frac{1}{2}}$ when $K = 0.2$, $E = 0.2$, $f_w = 0.1$, $\alpha = 1.4$, $n = 0.5$, $N_b = 0.2$, $P_r = 1.6$, $E_c = 0.1$

N_t	L_e	λ_t	λ_c	γ_1	γ_2	$NuRe_x^{-\frac{1}{2}}$	$ShRe_x^{-\frac{1}{2}}$	I_θ	I_ϕ
0.3						0.10759	0.07938	[-0.3, 0.2]	[-0.3, 0.3]
0.4						0.10741	0.07656	[-0.3, 0.2]	[-0.3, 0.2]
0.5						0.10723	0.07378	[-0.3, 0.2]	[-0.4, 0.2]
	1.3					0.10776	0.08319	[-0.2, 0.2]	[-0.5, 0.3]
	1.4					0.10777	0.08403	[-0.1, 0.2]	[-0.3, 0.3]
	1.5					0.10778	0.08477	[-0.3, 0.1]	[-0.2, 0.1]
		0.1		0.2		0.18917	0.07794	[-0.2, 0.1]	[-0.2, 0.1]
		0.98		0.3		0.25172	0.07485	[-0.3, 0.2]	[-0.1, 0.2]
		0.96		0.4		0.29073	0.07258	[-0.3, 0.4]	[-0.3, 0.2]
			0.98		0.2	0.10734	0.14703	[-0.5, 0.4]	[-0.3, 0.3]
			0.96		0.3	0.10736	0.19939	[-0.4, 0.3]	[-0.2, 0.2]
			0.94		0.4	0.10721	0.24259	[-0.3, 0.2]	[-0.2, 0.1]

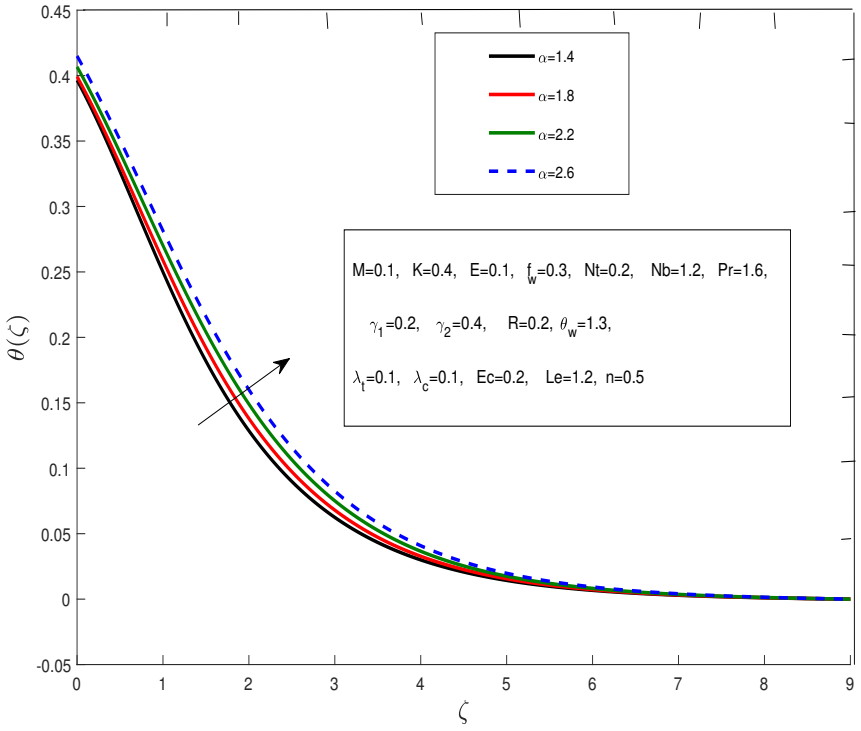

FIGURE 4.1: Impact of α on $\theta(\zeta)$.

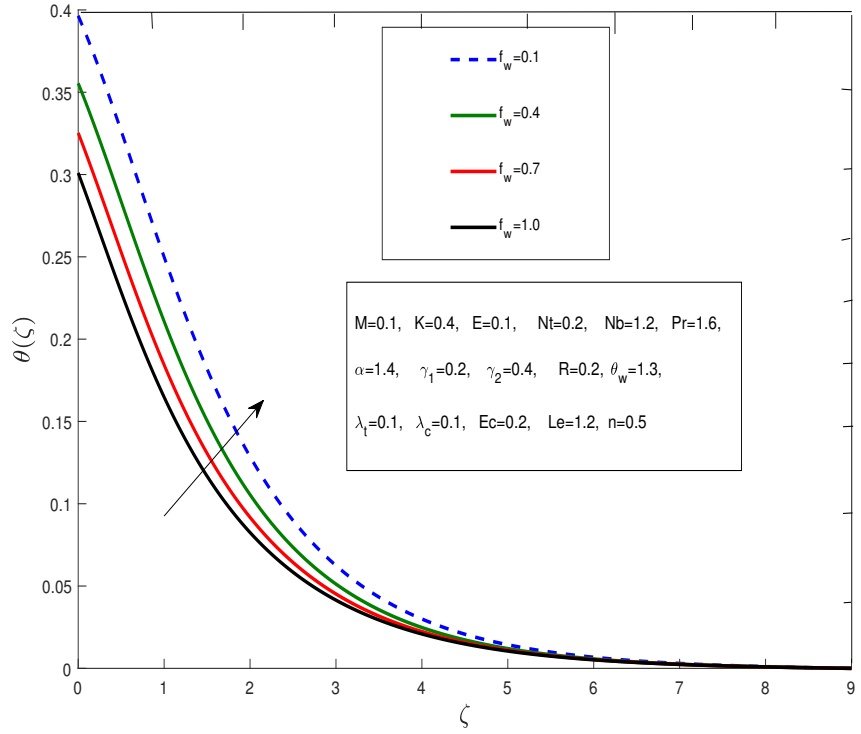

FIGURE 4.2: Impact of f_w on $\theta(\zeta)$.

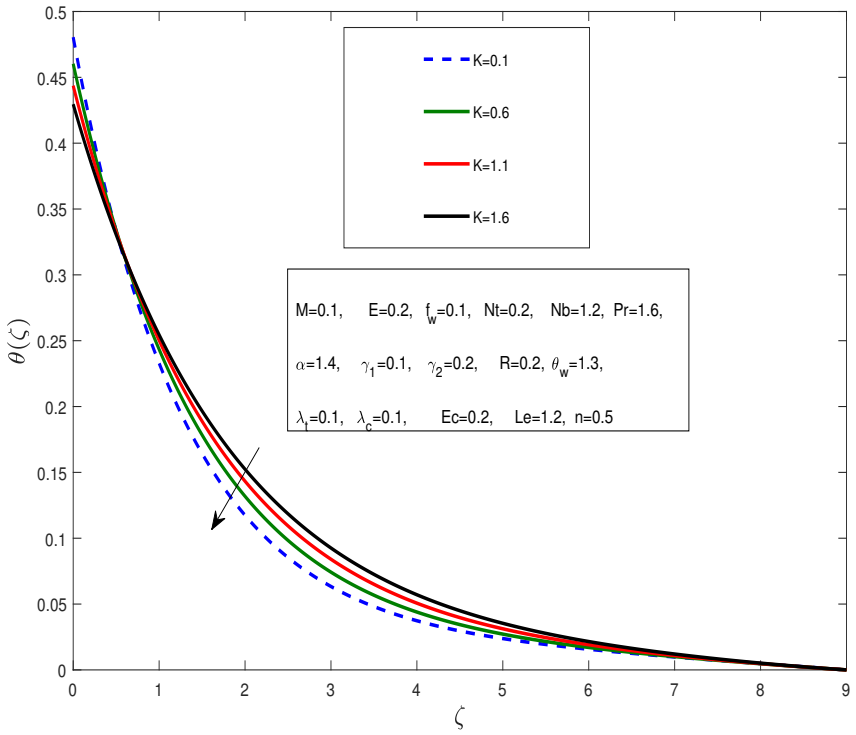

FIGURE 4.3: Impact of K on $\theta(\zeta)$.

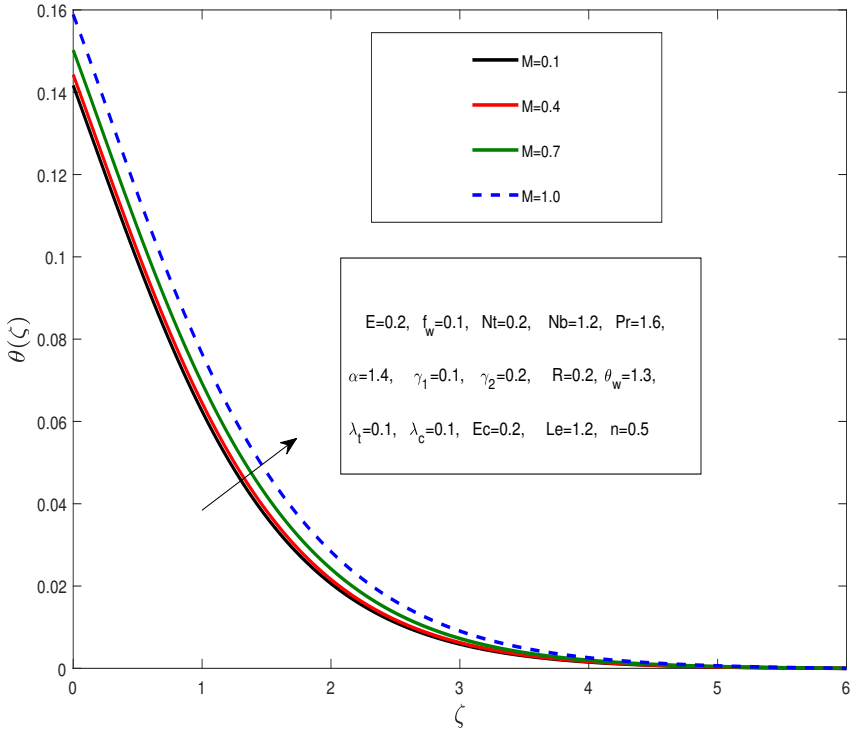

FIGURE 4.4: Impact of M on $\theta(\zeta)$.

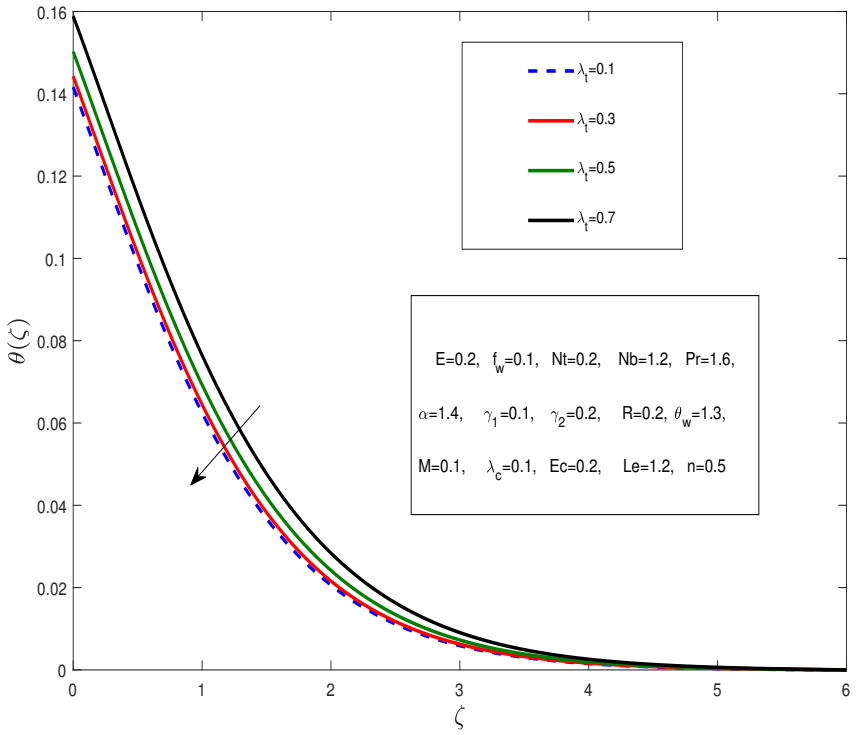

FIGURE 4.5: Impact of λ_t on $\theta(\zeta)$.

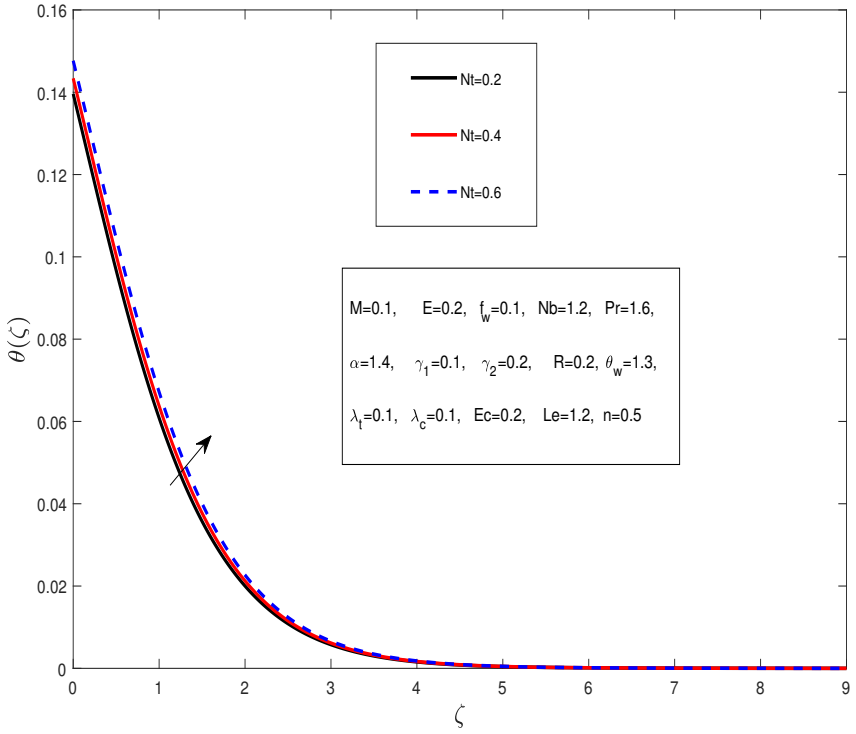

FIGURE 4.6: Impact of Nt on $\theta(\zeta)$.

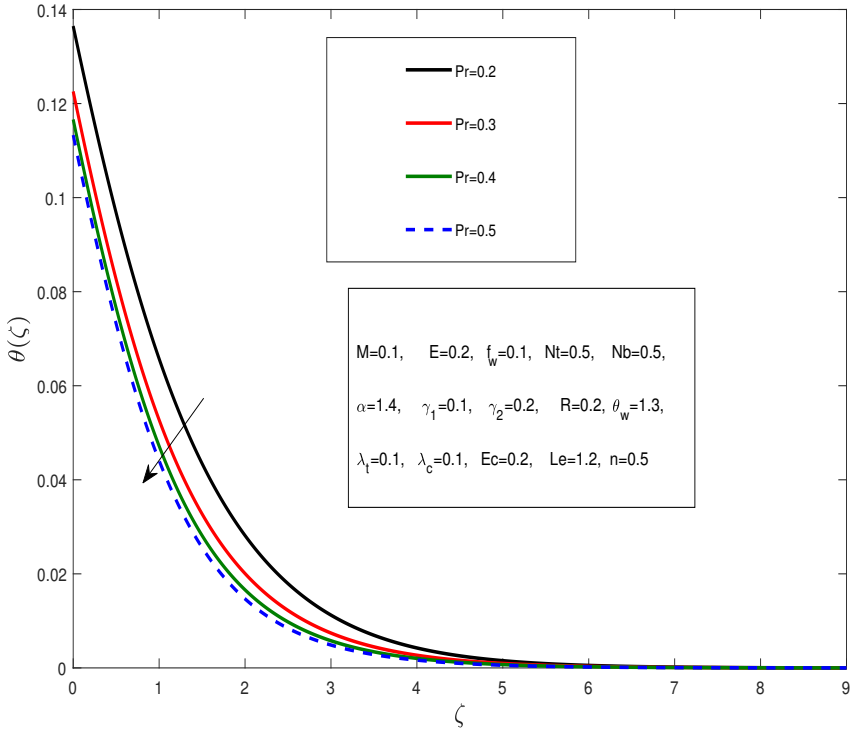

FIGURE 4.7: Impact of Pr on $\theta(\zeta)$.

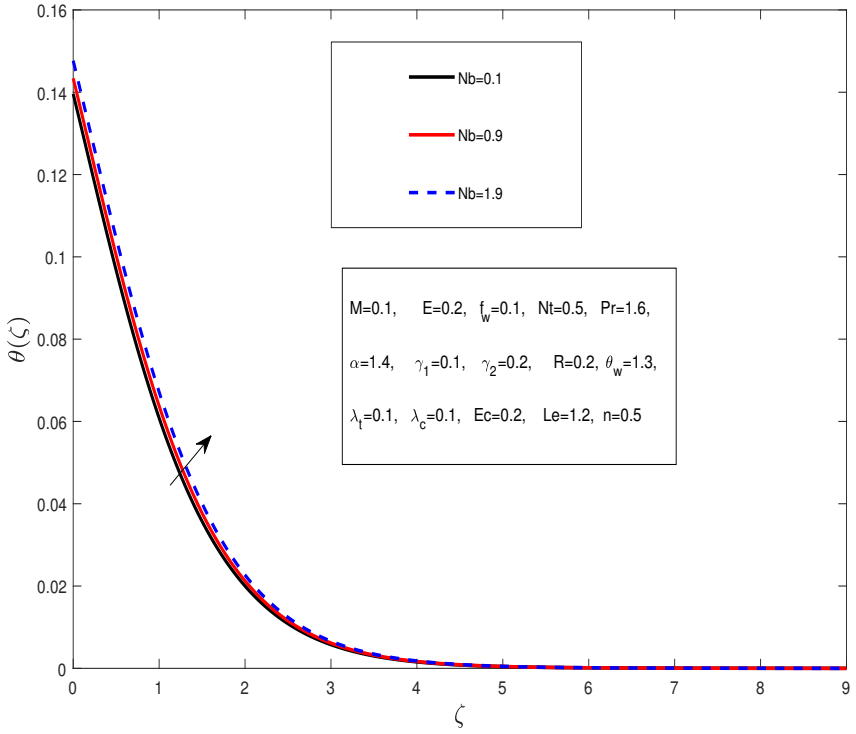

FIGURE 4.8: Impact of Nb on $\theta(\zeta)$.

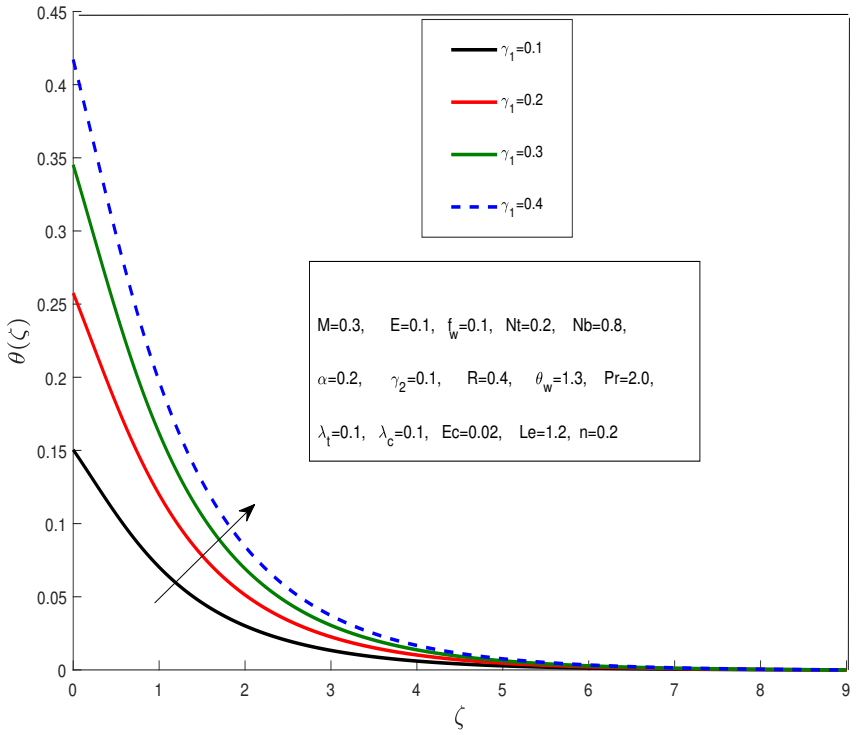

FIGURE 4.9: Impact of γ_1 on $\theta(\zeta)$.

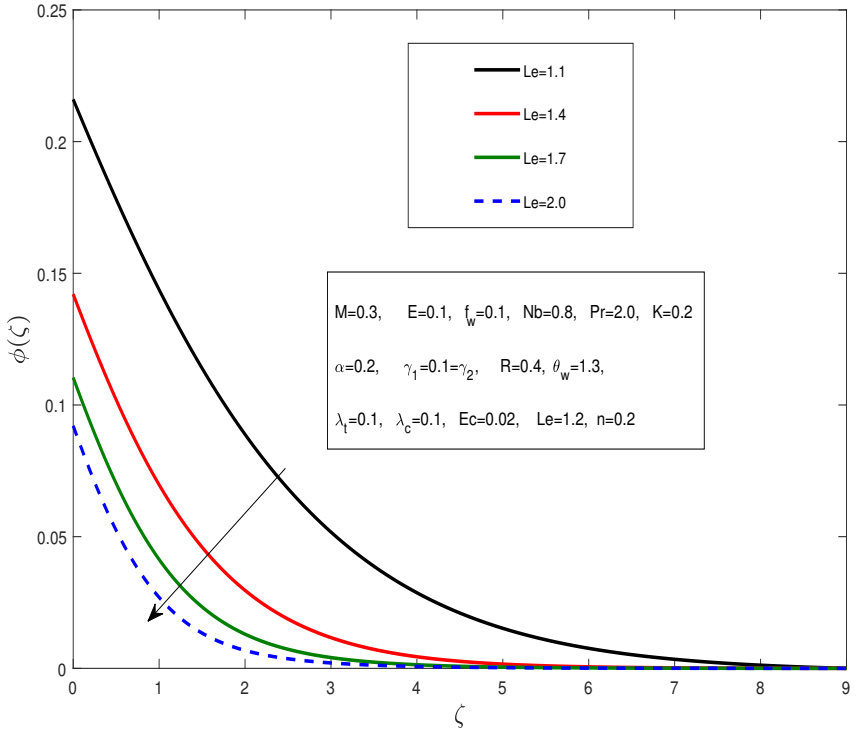

FIGURE 4.10: Impact of Le on $\phi(\zeta)$.

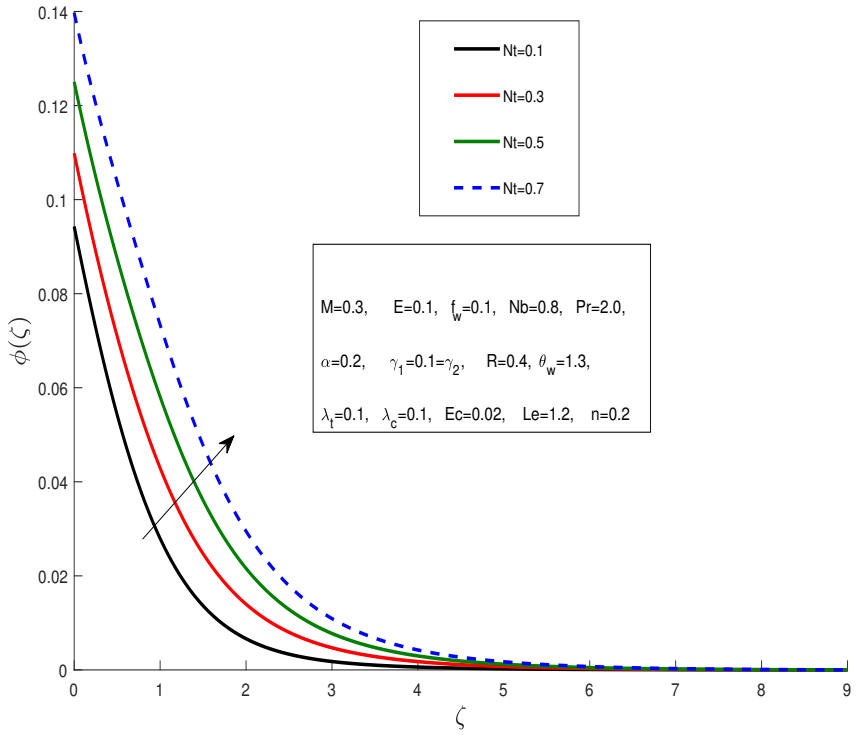

FIGURE 4.11: Impact of Nt on $\phi(\zeta)$.

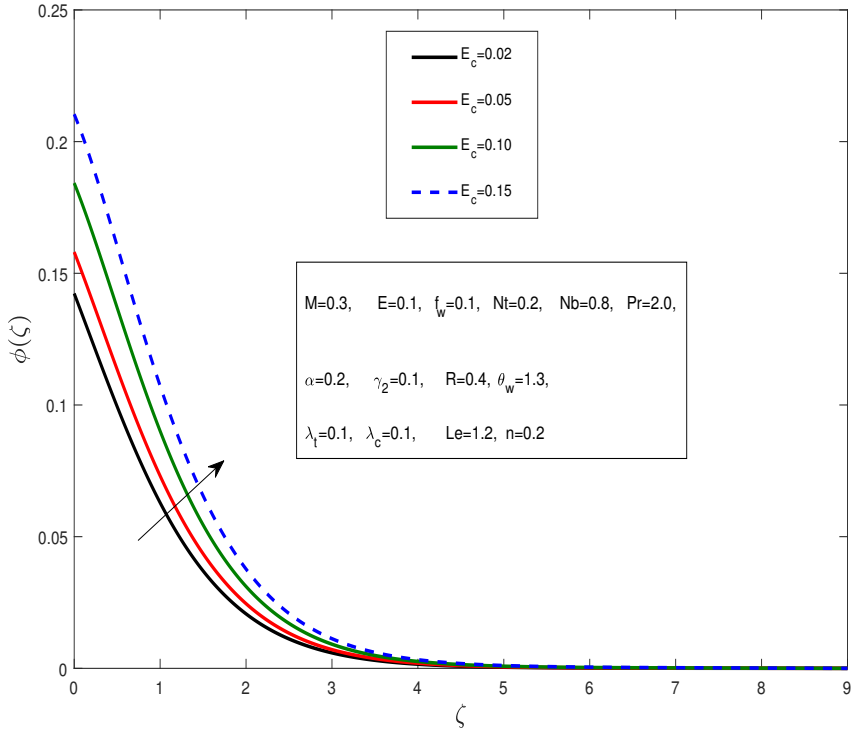

FIGURE 4.12: Impact of Ec on $\phi(\zeta)$.

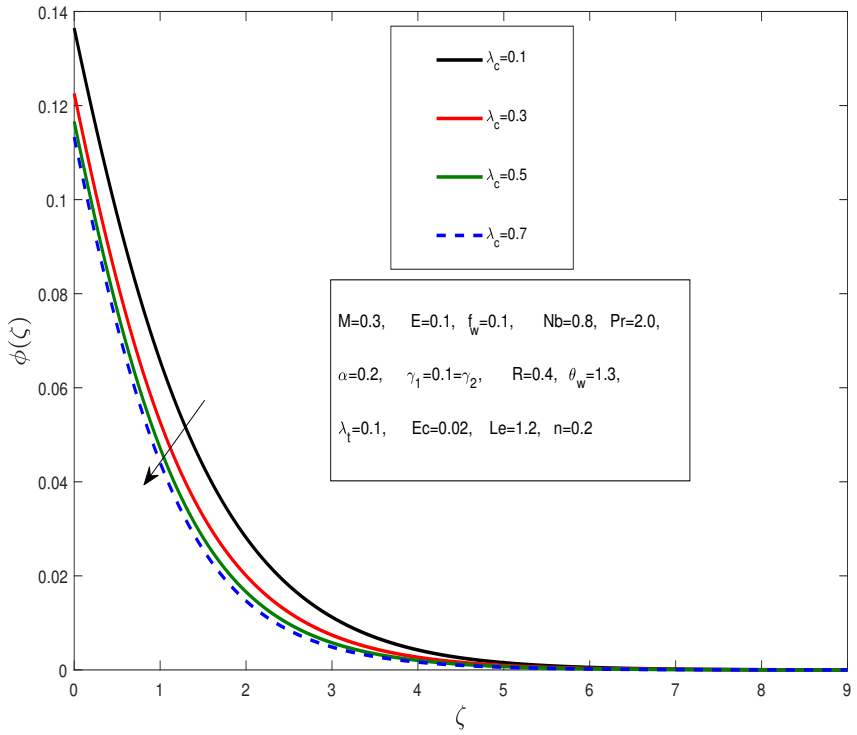

FIGURE 4.13: Impact of λ_c on $\phi(\zeta)$.

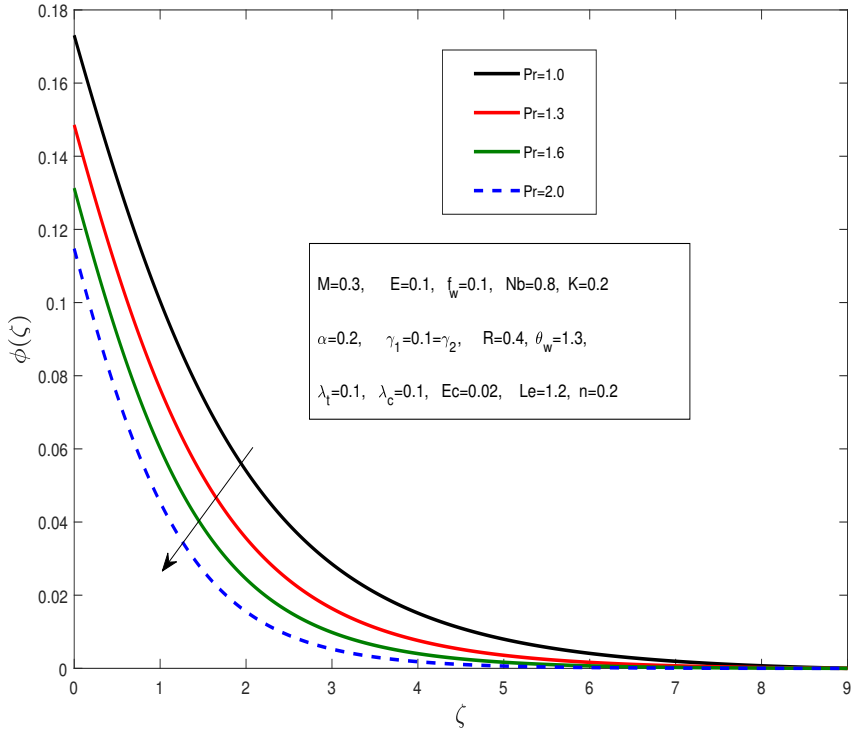

FIGURE 4.14: Impact of Pr on $\phi(\zeta)$.

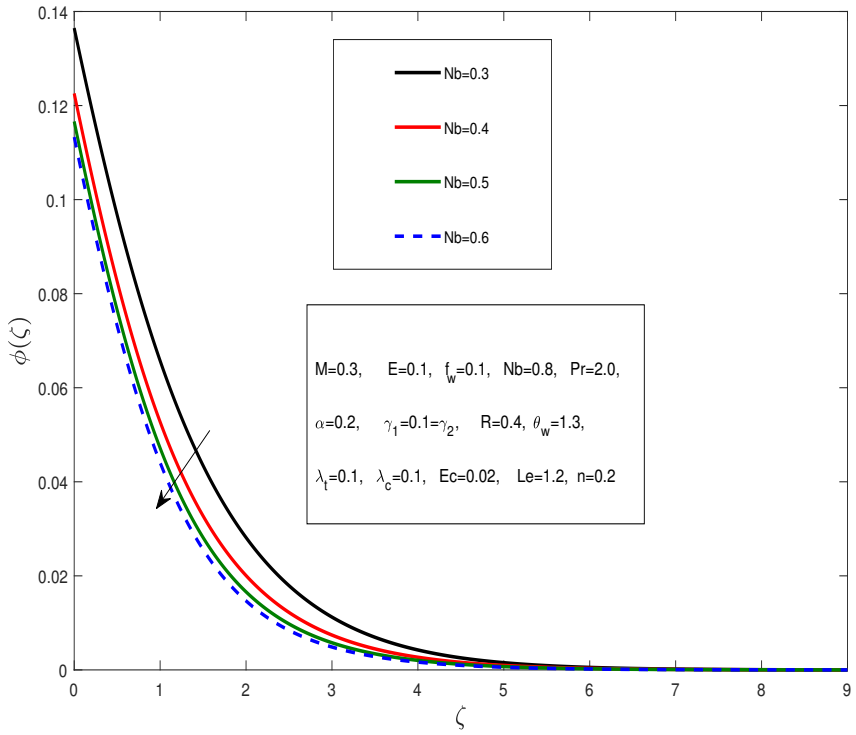

FIGURE 4.15: Impact of Nb on $\phi(\zeta)$.

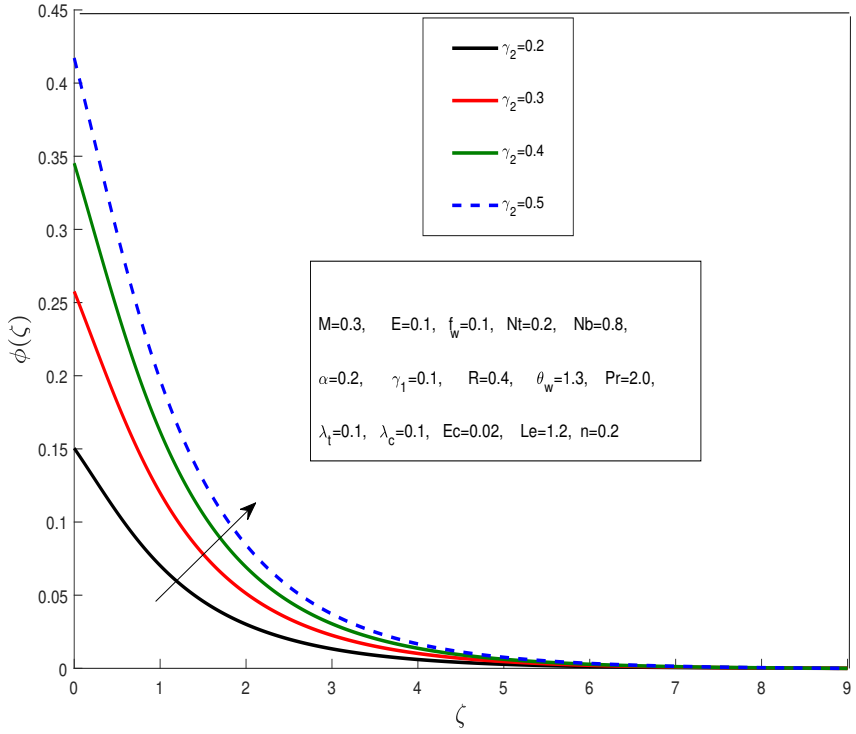

FIGURE 4.16: Impact of γ_2 on $\phi(\zeta)$.

Chapter 5

Conclusion

In this study, a review study of Hussain [30] is conducted and extended by considering the additional effects of Cattaneo-Christov double diffusion model with the assumptions of laminar, steady, incompressible, two dimensional, porous stretching sheet, viscous dissipation, nonlinear thermal radiation, Joule heating with convective boundary condition.

The obtained system of PDEs is transformed into a system of nonlinear and coupled ODEs by using a suitable similarity transformation. A numerical solution of the system of ODEs is obtained by employing the shooting method. The mathematical inferences are discussed for different physical parameters appearing in the solution influencing the flow and heat transform. The following noteworthy points can be drawn from the current investigation.

- The velocity profile decreases while the temperature profile increases as the value of α rises.
- The velocity profile decreases while the temperature profile increases as the value of f_w rises.
- As K increases, the velocity profile rises, while the temperature profile decreases.

- The velocity profile decreases while the temperature profile increases as the value of M rises.
- As the value of γ_1 rises, the velocity profile increases, whereas the temperature profile increases.
- The temperature profile increases as R increases in value.
- Rising values of both Nb and Nt reduces the rate of heat transfer on the surface.
- Mass transfer rate increases for the Nb and decreases for the Nt.
- As the E_c value increases, the velocity and temperature profiles are also increasing.
- The temperature profile falls as θ_w rises.
- As value of P_r rises, the energy profile and concentration profile both show a decreasing trend.
- With an increase in Nb, the concentration profile decreases and the energy profile increases.
- Le increases as the concentration profile decreases.
- With an increase in Nt, the energy profile and concentration profile both rise.
- When the Cattaneo-Christov temperature parameter λ_t is decreased, the nusselt number decreases and the sherwood number rises.
- The nusselt number increases as the Cattaneo-Christov diffusion parameter λ_c is decreased, whereas the sherwood number drops.

Bibliography

[1] A. C. Eringen, "Theory of micropolar fluids," *Journal of Mathematics and Mechanics*, pp. 1–18, 1966.

[2] A. C. Eringen, "Theory of thermomicrofluids," *Journal of Mathematical Analysis and Applications*, vol. 38, no. 2, pp. 480–496, 1972.

[3] J. J. Shu and J. S. Lee, "Fundamental solutions for micropolar fluids," *Journal of Engineering Mathematics*, vol. 61, no. 1, pp. 69–79, 2008.

[4] A. Rashad, S. Abbasbandy, and A. J. Chamkha, "Mixed convection flow of a micropolar fluid over a continuously moving vertical surface immersed in a thermally and solutally stratified medium with chemical reaction," *Journal of the Taiwan Institute of Chemical Engineers*, vol. 45, no. 5, pp. 2163–2169, 2014.

[5] F. Mabood, S. Ibrahim, M. Rashidi, M. Shadloo, and G. Lorenzini, "Non-uniform heat source/sink and soret effects on mhd non-darcian convective flow past a stretching sheet in a micropolar fluid with radiation," *International Journal of Heat and Mass Transfer*, vol. 93, pp. 674–682, 2016.

[6] A. Mirzaaghaian and D. Ganji, "Application of differential transformation method in micropolar fluid flow and heat transfer through permeable walls," *Alexandria Engineering Journal*, vol. 55, no. 3, pp. 2183–2191, 2016.

[7] M. Turkyilmazoglu, "Mixed convection flow of magnetohydrodynamic micropolar fluid due to a porous heated/cooled deformable plate: exact solutions," *International Journal of Heat and Mass Transfer*, vol. 106, pp. 127–134, 2017.

[8] M. Bilal, S. Hussain, and M. Sagheer, "Boundary layer flow of magneto-micropolar nanofluid flow with hall and ion-slip effects using variable thermal diffusivity," *Bulletin of the Polish Academy of Sciences. Technical Sciences*, vol. 65, no. 3, 2017.

[9] A. Eegunjobi and O. Makinde, "Irreversibility analysis of mhd buoyancy-driven variable viscosity liquid film along an inclined heated plate convective cooling," *Journal of Applied and Computational Mechanics*, vol. 5, no. 5, pp. 840–848, 2019.

[10] S. Atif, S. Hussain, and M. Sagheer, "Magnetohydrodynamic stratified bio-convective flow of micropolar nanofluid due to gyrotactic microorganisms," *AIP Advances*, vol. 9, no. 2, p. 025208, 2019.

[11] S. Ghadikolaei, K. Hosseinzadeh, D. Ganji, and B. Jafari, "Nonlinear thermal radiation effect on magneto casson nanofluid flow with joule heating effect over an inclined porous stretching sheet," *Case studies in thermal engineering*, vol. 12, pp. 176–187, 2018.

[12] J. Sui, P. Zhao, Z. Cheng, and M. Doi, "Influence of particulate thermophoresis on convection heat and mass transfer in a slip flow of a viscoelasticity-based micropolar fluid," *International Journal of Heat and Mass Transfer*, vol. 119, pp. 40–51, 2018.

[13] H. A. Nabwey and A. Mahdy, "Numerical approach of micropolar dust-particles natural convection fluid flow due to a permeable cone with nonlinear temperature," *Alexandria Engineering Journal*, vol. 60, no. 1, pp. 1739–1749, 2021.

[14] S. Choi, "Enhancing thermal conductivity of fluids with nano-particles," *ASME, FED*, vol. 231, pp. 99–105, 1995.

[15] J. Buongiorno, "Convective transport in nanofluids," *Journal of heat transfer*, vol. 128, no. 3, pp. 240–250, 2006.

[16] M. Ramzan and M. Bilal, "Time dependent mhd nano-second grade fluid flow induced by permeable vertical sheet with mixed convection and thermal radiation," *PloS one*, vol. 10, no. 5, p. e0124929, 2015.

[17] D. Pal, N. Roy, and K. Vajravelu, "Effects of thermal radiation and ohmic dissipation on mhd casson nanofluid flow over a vertical non-linear stretching surface using scaling group transformation," *International Journal of Mechanical Sciences*, vol. 114, pp. 257–267, 2016.

[18] M. Khan, M. Azam, and A. Alshomrani, "Effects of melting and heat generation/absorption on unsteady falkner-skan flow of carreau nanofluid over a wedge," *International Journal of Heat and Mass Transfer*, vol. 110, pp. 437–446, 2017.

[19] T. Hayat, T. Muhammad, S. A. Shehzad, and A. Alsaedi, "An analytical solution for magnetohydrodynamic oldroyd-b nanofluid flow induced by a stretching sheet with heat generation/absorption," *International Journal of Thermal Sciences*, vol. 111, pp. 274–288, 2017.

[20] M. Bilal, M. Sagheer, and S. Hussain, "Three dimensional mhd upper-convected maxwell nanofluid flow with nonlinear radiative heat flux," *Alexandria engineering journal*, vol. 57, no. 3, pp. 1917–1925, 2018.

[21] S. Saleem, S. Nadeem, M. Rashidi, and C. Raju, "An optimal analysis of radiated nanomaterial flow with viscous dissipation and heat source," *Microsystem Technologies*, vol. 25, no. 2, pp. 683–689, 2019.

[22] Y. Ma, R. Mohebbi, M. Rashidi, Z. Yang, and M. A. Sheremet, "Numerical study of mhd nanofluid natural convection in a baffled u-shaped enclosure," *International Journal of Heat and Mass Transfer*, vol. 130, pp. 123–134, 2019.

[23] M. M. Bhatti, M. A. Abbas, and M. M. Rashidi, "A robust numerical method for solving stagnation point flow over a permeable shrinking sheet under the influence of mhd," *Applied Mathematics and Computation*, vol. 316, pp. 381–389, 2018.

[24] S. d. Zhu, Y. m. Chu, and S. l. Qiu, "The homotopy perturbation method for discontinued problems arising in nanotechnology," *Computers & Mathematics with Applications*, vol. 58, no. 11-12, pp. 2398–2401, 2009.

[25] Y. Li and J. H. He, "Fabrication and characterization of zro nanofibers by critical bubble electrospinning for high-temperature- resistant adsorption and separation," *Adsorption Science & Technology*, vol. 37, no. 5-6, pp. 425–437, 2019.

[26] J. H. He, "Advances in bubble electrospinning," *Recent Patents on Nanotechnology*, vol. 13, no. 3, pp. 162–163, 2019.

[27] J. H. He, "A simple approach to one-dimensional convection-diffusion equation and its fractional modification for e reaction arising in rotating disk electrodes," *Journal of Electroanalytical Chemistry*, vol. 854, p. 113565, 2019.

[28] J. He and F. Ji, "Two-scale mathematics and fractional calculus for thermodynamics, therm," *Science*, vol. 23, no. 4, 2019.

[29] J. H. He, "A fractal variational theory for one-dimensional compressible flow in a microgravity space," *Fractals*, vol. 28, no. 02, p. 2050024, 2020.

[30] A. Hussain, "Magneto-micropolar nanofluid flow over a convectively heated sheet with non-linear radiation and viscous dissipation," 2018.

[31] R. W. Fox, A. McDonald, and P. Pitchard, "Introduction to fluid mechanics, 2004," 2006.

[32] R. Bansal, *A textbook of fluid mechanics*. Firewall Media, 2005.

[33] J. N. Reddy and D. K. Gartling, *The finite element method in heat transfer and fluid dynamics*. CRC press, 2010.

[34] P. A. Davidson and A. Thess, *Magnetohydrodynamics*, vol. 418. Springer Science & Business Media, 2002.

[35] M. Gad-el Hak, *Frontiers in experimental fluid mechanics*, vol. 46. Springer Science & Business Media, 2013.

[36] R. W. Lewis, P. Nithiarasu, and K. N. Seetharamu, *Fundamentals of the finite element method for heat and fluid flow.* John Wiley & Sons, 2004.

[37] J. Kunes, *Dimensionless physical quantities in science and engineering.* Elsevier, 2012.